CHARACTERIZING THE ROLE OF ADAPTOR PROTEINS IN ENDOCYTOSIS

by
Kyle Thomas Hoban

A dissertation submitted to Johns Hopkins University in conformity with the
requirements for the degree of Doctor of Philosophy

Baltimore, Maryland
October 2017

ABSTRACT

The plasma membrane (PM) is the barrier between the interior of a cell and the environment, and the composition of this membrane is continuously modified in response to fluctuating conditions. Endocytosis is the process by which portions of the PM and its components are trafficked into the cell, passing through a series of endosomal compartments that ultimately lead to the lysosome in mammalian cells; the lysosome's yeast organelle equivalent is known as the vacuole. Endocytosis at the PM can occur via multiple mechanisms. In the budding yeast *Saccharomyces cerevisiae*, the most well understood endocytic pathway is clathrin-mediated endocytosis (CME), and among the earliest players in CME initiation are endocytic adaptor proteins. These adaptors bind to lipids in the PM and proteins, known as cargos, that reside at or within this membrane, as well as other factors involved in CME. In this way, endocytic adaptors link the PM and its contents to the rest of the endocytic machinery. The selection of cargo for internalization is an important part of cellular responses to environmental change, often occurring via interaction of the adaptor with specific amino acid sequences within a cargo. The absence of endocytic adaptors can lead to abnormal phenotypes, such as the accumulation of cargo at the PM.

Though the cargo-sorting motifs recognized by some endocytic adaptors have been identified, the mechanism for others, including the muniscin family of adaptors, remains unknown. Additionally, the loss of certain adaptors may place increased importance on the functioning of other proteins in the cell. In this dissertation, we demonstrate that the muniscin adaptor in budding yeast, Syp1, selects cargo for endocytosis via an Asp-x-Tyr motif. We also present results of a visual screen that

identified two previously unknown Syp1 cargos, as well as data indicating that Syp1 can direct endocytosis through a clathrin-independent pathway, in addition to CME. We also present findings from a colony-sectoring screen demonstrating that the loss of Vps4, an ATPase necessary for the generation of multivesicular bodies, is lethal in an endocytosis adaptor mutant strain. Finally, we provide evidence that upregulation of endocytic recycling is responsible for this negative interaction.

Thesis Committee Members

Beverly Wendland, PhD (Thesis Advisor)

Valeria Culotta, PhD

Kyle Cunningham, PhD

Vince Hilser, PhD

Thesis Readers

Beverly Wendland, PhD

M. Andy Hoyt, PhD

ACKNOWLEDGMENTS

Thank you to my amazing friends from outside of school, especially those in Baltimore (Kyle Martin, Melissa Hendrix-Martin, Will Lederer, and Sarah Lederer), who helped keep me sane throughout my graduate studies. Your get-togethers, incredible senses of humor, and love of life and laughter helped pull me through some rough times, for which I am eternally grateful.

Thank you to my family: my brother Ryan, Grandmother "Em," Uncle Jack, and Aunt Alverda. Our family isn't large, but the support you have given me throughout this journey, along with "Bump" and Grandma Hoban before they left us, is immeasurable. You rooted for me the entire time, and it means more than you know. Thank you to Kevin's family as well. I know you've all pulled for me through the years, too, and it's a gift to have gained a second family that I love (and like!) as much as the first.

Thank you to my parents. No matter what I've done in life, you've provided guidance when I needed redirection and support when I was needed help continuing on difficult paths. You guided me as I grew up, accepted me when I came out of the closet in high school, and encouraged me not to quit graduate school when I wanted nothing more than to leave. Without you, I would not be the man or scientist I am today.

Finally, a special thank you to Kevin, my one-of-a-kind husband. It's not easy being with a graduate student. The long nights, early mornings, and stress-filled days through the months and years were exhausting for both of us. You moved to Baltimore with me and drove over an hour each way to work for four years so we could live together near the school. You gave me countless rides so I wouldn't have to walk in the cold or heat. Thank you for being there for me when I need it the most.

for Kevin

TABLE OF CONTENTS

LIST OF FIGURES & TABLES

CHAPTER 1

Open questions in the study of endocytic adaptor proteins

Abstract

Trafficking of material from the plasma membrane (PM) into the cell occurs via a process known as endocytosis. Once an endocytic vesicle has formed, the membrane, its components, and the lumenal contents are shuttled through a series endosomal compartments toward the vacuole, the yeast equivalent of the lysosome, for degradation. Multiple endocytic mechanisms act at the PM, and budding yeast possess two known forms, a clathrin-mediated pathway and a clathrin-independent route that requires the GTPase, Rho1. Initiation of clathrin-mediated endocytosis (CME) involves the recruitment of adaptor proteins, which bind to the PM and associated cargo proteins, selecting specific cargo for trafficking into the cell. The loss of endocytic adaptors can have deleterious effects on the cell, including the abnormal buildup of cargos at the PM. The mechanism by which a recently identified adaptor called Syp1 selects cargo proteins for internalization is unknown. Another currently unanswered question is whether genes that are non-essential in a wild-type background become necessary for cell viability in the absence of endocytic adaptors. Genetic screens have been used previously to answer similar questions and can help to address these inquiries as well.

Body

<u>Endocytosis at the plasma membrane</u>

Cellular processes require stable conditions, as many cellular components can only function or remain structurally intact within a narrow range of parameters. The environment in which a cell exists can change rapidly; pH, salinity, nutrient availability, osmolarity, temperature, etc., often swing wildly. Therefore, separating the cytoplasm from an unpredictable extracellular space, along with the ability to respond quickly to fluctuations in the surroundings of the cell, is absolutely essential for cell survival. The plasma membrane (PM) and proteins in the cytoplasm that remodel the PM allow for this cellular response. The PM is composed primarily of a phospholipid bilayer, a barrier that prevents the free movement of hydrophilic molecules into, or out of, the cell. This cell-surface membrane bilayer contains selective proteins such as permeases and transporters that allow only the passage of specific substances, such as ions or amino acids, across the PM. Therefore, the cell must be able to adjust the composition of specific transmembrane transporters within the PM in response to the availability of different nutrients in the environment. However, the state of the PM at one point in time may not be suitable after an environmental change, and the cell will need to make adjustments to the membrane composition to maintain viability.

One example of this pertains to the amino acid, methionine, and its high-affinity transporter in budding yeast, Mup1. When methionine is scarce, a yeast cell will increase the concentration of Mup1 at the PM to maximize methionine uptake; however, methionine is toxic if the intracellular concentration becomes too high (Isnard *et al.*, 1996). A sudden increase of methionine in the surroundings can leave the cell vulnerable

as a result of the elevated concentration of Mup1 at the PM, a response to prior unavailability of the amino acid. Therefore, cells possess a means to remove specific components of the PM, such as Mup1, while allowing others to remain, ensuring optimal growth and survival (Farrell *et al.*, 2015; Prosser *et al.*, 2016). This selective mechanism is known as endocytosis.

Endocytosis is the trafficking of PM and extracellular material to the cell interior. The endocytic pathway is composed of a series of endosomal compartments that ends at the lysosome, or vacuole in yeast. The literal translation of "endocytosis" from Latin means "into the cell." It is a type of active transport during which a small region of the PM is invaginated and subsequently cleaved from the rest of the outer membrane, forming an endocytic vesicle within the cytoplasmic compartment. Roth and Porter first discovered this process (Roth and Porter, 1964). The researchers were studying oocyte morphology of the mosquito, *Aedes aegypti*, shortly after a blood meal when they observed invaginations and pits in the PM of the cells by transmission electron microscopy. These features exhibited an electron-dense, extracellular coating, and nearby vesicles inside of the cell contained the same dense material. This led the scientists to postulate that oocytes take up proteins and other molecules from the surrounding yolk by internalizing regions of the PM at which they had concentrated, forming vesicles containing this material. What Roth and Porter had described formed the basis for endocytosis research in the following decades.

Accurate and efficient remodeling of the PM is necessary for cell viability. Endocytosis allows a cell to acquire essential nutrients that cannot be transported through the PM, modulate signaling pathways at specific times and locations, and control the

compositions of important channels and transporters within the PM. Endocytosis has also been implicated in a number of human diseases. For instance, non-enveloped viruses such as Hepatitis C and vaccinia viruses gain entry into the cell by coopting endocytic pathways for their internalization (Agnello *et al*., 1999; Sandvig and van Deurs, 2008). Proteins that mediate endocytosis have also been implicated in several neurological disorders, including Alzheimer's, Down syndrome, Parkinson's, and amyotrophic lateral sclerosis (Schreij *et al*., 2016); as well as cancers (Mosesson *et al*., 2008; Mellman and Yarden, 2013). This process can also be used as a mechanism for the delivery of therapeutics (Bareford and Swaan, 2007). Endocytosis has been demonstrated to be a key cellular mechanism and a promising target for medical treatments.

Several forms of endocytosis have been described in scientific literature since the process was first identified. The different pathways are broadly distinguished by whether a protein called clathrin, an important endocytic scaffold, is involved. The mechanism associated with clathrin is referred to as clathrin-mediated endocytosis (CME). Other pathways into the cell do not utilize clathrin and are, therefore, termed clathrin-independent endocytic (CIE) mechanisms. Many forms of CIE rely on the functioning of dynamin, which is also involved in CME, and small GTPases, such as the RhoA pathway; in contrast, the Rac CIE pathway relies on ruffling, in which large protrusions from the PM curve back toward the cell to form massive intracellular vesicles (Sandvig *et al*., 2008). The presence of multiple endocytic pathways in a cell increases the potential for specific and regulated cellular changes to compensate for altered environmental conditions.

The budding yeast, *Saccharomyces cerevisiae*, is an ideal model system and powerful biological tool with which to study endocytosis for several reasons, including the relatively short length of its cell cycle. Another advantage is that budding yeast can exist in haploid or diploid states, with haploid cells of opposite mating type being able to produce a diploid cell with two sets of chromosomes; diploid cells are able to sporulate and give rise to new haploid cells with one set of chromosomes. This capacity to change ploidy offers several opportunities for genetic manipulation. Yeast was the first eukaryote to have a fully sequenced genome and was also among the first eukaryotic organisms in which genome editing could be readily performed (McElver and Weber, 1992; Baudin *et al*., 1993; Lorenz *et al*., 1995; Longtine et al., 1998), and remained one of the few systems in which this was possible until the advent of the CRISPR, Cas9 method (Cong *et al*., 2013). Most importantly for the studies presented here, budding yeast possess two known endocytic mechanisms that are highly conserved in mammalian cells, CME and Rho1-dependent CIE.

Clathrin-mediated endocytosis

CME is the best understood form of endocytosis and is a complex process that involves approximately sixty different proteins that are sequentially recruited with a high degree of spatiotemporal specificity (Figure 1-1; Goode *et al*., 2015). During its initiation, adaptor proteins bind lipids and cargo proteins at the PM. Two of the earliest arriving yeast proteins to sites of CME are Syp1 and Ede1 (Gagny *et al*., 2000; Reider *et al*., 2009). The mammalian homologue of Ede1 is Eps15 (Benmerah *et al*., 1998; Carbone *et al*., 1997). Whether cargo concentration or adaptors themselves determine
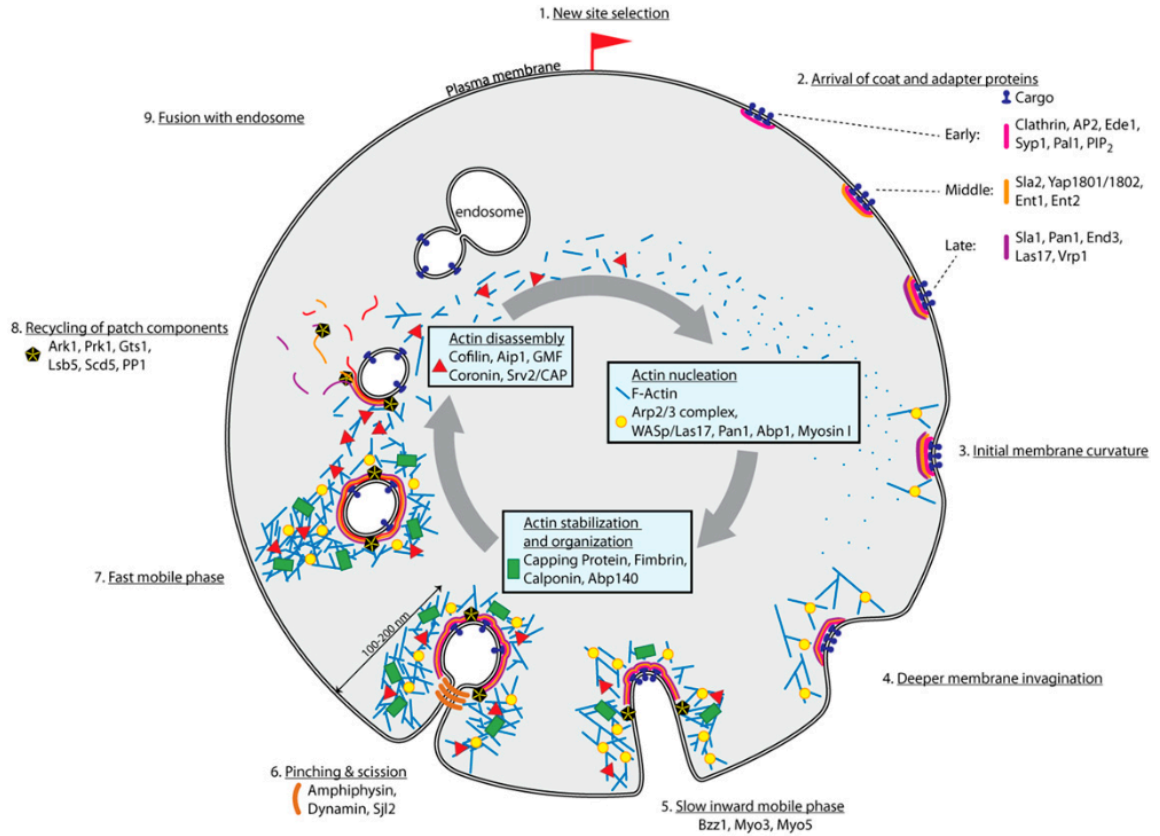
Figure 1-1. The phases of clathrin-mediated endocytosis. Diagram depicting the
initiation, invagination, scission, and uncoating of an endocytic vesicle that is delivered
to the early endosome (Goode *et al*., 2015).

where nascent CME events occur remains an open question in the field. Syp1 is among a group of early coat endocytic adaptor proteins, which bind to phospholipids and proteins within the PM and enable the association of later-arriving proteins to cortical patches (Reider and Wendland, 2011). Adaptors also recruit clathrin, a conserved heterohexameric protein that forms triskelions composed of three heavy and three light chain subunits (Ungewickell and Branton, 1981; Kirchhausen *et al.*, 1987). These triskelions oligomerize to form a lattice that contributes to curving the PM to form a membrane invagination that will eventually become a clathrin-coated vesicle (CCV) (McMahon and Boucrot, 2011). Other endocytic adaptors include Yap1801 and Yap1802, as well as the yeast epsins, Ent1 and Ent2 (Wendland *et al.*, 1999; Aguilar *et al.*, 2006; Maldonado-Báez *et al.*, 2008). Together with the proteins AP2 and Pal1, these factors make up the set of proteins associated with CME events known as the early coat (Keen, 1989; Carroll *et al.*, 2012).

After the early coat factors, constituents of the late coat are recruited to endocytic sites. Proteins of the late coat include Sla1, Pan1, and End3, and these three CME components physically interact to form a complex (Tang *et al.*, 1997, 2000). Each is highly important for the proper functioning of CME; for example, loss of End3 severely impedes endocytic efficiency (Chvatchko *et al.*, 1986; Bénédetti *et al.*, 1994), and cargo proteins accumulate nonspecifically at the PM. The actin regulators Vrp1 and Las17 are also part of the late coat, and the Las17 homologue in mammalian cells is WASp (Donnelly *et al.*, 1993; Naqvi *et al.*, 1998). At this point in the progression of CME, actin filaments (F-actin) are nucleated with the aid of the Arp2/3 complex, which polymerize to form branched structures that, along with many other factors, generate force to

invaginate the PM and produce a clathrin-coated pit (CCP) (Schwob and Martin, 1992; Schroer *et al*., 1994; Winter *et al*., 1997). The final stage of CME is scission of the CCP from the membrane. Factors involved in this process include the amphiphysins, Rvs161 and Rvs167, and yeast Dynamin (Munn *et al*., 1995; Lombardi and Riezman, 2001; Robinson *et al*., 1988; Yu and Cai, 2004). Once a CCV has been generated, the surrounding F-actin is disassembled. Finally, factors such as the Ark1 and Prk1 kinases promote the removal of coat proteins, including clathrin, from the vesicle, which can then be recycled for use by the cell in subsequent rounds of CME (Cope *et al*., 1999; Zeng and Cai, 1999). Determination of the order in which components of the endocytic machinery are recruited to cortical patches was aided by the use of two-color, live-cell fluorescence microscopy (Kaksonen *et al*. 2003, 2005). Researchers were able to accurately determine which of two labeled proteins arrive at sites of endocytosis first, allowing some of the complexity of the endocytic process to be dissected.

Clathrin-associated sorting proteins

Members of one family of endocytic adaptors associated with CME are referred to as clathrin-associated sorting proteins (CLASPs) because they bind clathrin directly during endocytic events. Epsins are one set of CLASP adaptors and are encoded by the genes *ENT1* and *ENT2* in budding yeast (Chen *et al*., 1998; Wendland *et al*., 1999). The Ent1 and Ent2 proteins are highly similar; both epsins contain similarly arranged features that are found commonly in adaptor proteins: ubiquitin-interacting motifs for the recognition of ubiquitinated cargos, NPF motifs that are bound by EH domain-containing factors in CME, and clathrin-binding motifs at the C-termini (Wendland *et al*., 1999;

9

Aguilar *et al.*, 2003, 2006). Finally, Ent1 and Ent2 each possess a single epsin N-terminal homology (ENTH) domain (Kay *et al.*, 1999).

The yeast epsins are an essential gene pair. The cell remains viable without one or the other; however, the loss of both proteins is lethal (Wendland *et al.*, 1999). Though budding yeast cannot survive in the complete absence of Ent1 and Ent2, the presence of a single copy of a gene fragment encoding the ENTH domain can support viability of the cells (Wendland *et al.*, 1999; Aguilar *et al.*, 2006). A site on the surface of the ENTH domain binds GTPase-activating proteins for Cdc42, a key regulator of polarity within cells (Adams *et al.*, 1990), and the ENTH domain has been shown to modulate Cdc42 signaling pathways (Aguilar *et al.*, 2006). It is this activity that is required for cell viability. Yap1801 and Yap1802 are additional yeast CLASPs, and their homologues in mammalian cells are AP180/PiCALM (Wendland and Emr, 1998; Wendland *et al.*, 1999). Aside from a slight difference in length, the Yap180s are also highly similar to one another, with each possessing an AP180 N-terminal homology (ANTH) domain (Ford *et al.*, 2001; Itoh *et al.*, 2001; De Camilli *et al.*, 2002; Stahelin *et al.*, 2003). In contrast to the ENTH domain of the epsins; consistent with this, the ANTH domain is not required for viability, and *YAP1801* and *YAP1802* are not an essential pair. Additionally, the Yap180 adaptors each have a similarly organized set of NPF motifs, along with a clathrin-binding motif, similar to the epsins (Wendland and Emr, 1998).

As the commonalities between the yeast epsins and Yap180 adaptors would suggest, these four endocytic proteins play overlapping roles in the functioning of endocytosis (Maldonado-Báez *et al.*, 2008). Though endocytosis generally proceeds unhindered in a *yap1801Δ yap1082Δ* or *ent1Δ ent2Δ* double mutant, aside from an

10

ENTH domain for viability in the case of an epsin mutants, the combined loss of all of these proteins from a cell leads to robust phenotypes associated with the interruption of endocytosis. These adaptor mutants grow more slowly than WT cells, are sensitive to higher temperatures, exhibit aberrant actin patch phenotypes, and nonspecifically accumulate cargo at the PM (Maldonado-Báez *et al*., 2008). Supporting the idea that these factors possess shared functions, reintroduction of a single gene expressing a full-length form of any of these four adaptor proteins is able to rescue the abnormal endocytosis phenotypes (Maldonado-Báez *et al*., 2008).

Though cells lacking these adaptors are less fit than WT yeast, the mutants are, nonetheless, viable. As such, this strain provides a sensitized genetic background, ideal for seeking out alleles that exhibit a negative genetic interaction with the loss of these adaptors. Negative interactions with the adaptor mutant background might reveal additional proteins involved in endocytosis or highlight processes that become more important when trafficking from the PM is inefficient. One study presented here aims to identify genes that make adaptor mutant cells inviable when disrupted, as well as to understand the cause of such connections.

Muniscins

Another class of endocytic adaptors is the muniscins. Syp1 is the sole muniscin in budding yeast, named for its ability to suppress phenotypes associated with a *pfy1Δ* strain: Suppressor of Yeast Profilin deletion (Marcoux *et al*., 2000). Syp1 is among the earliest arriving CME factors to nascent endocytic sites. The homologues of Syp1 in mammalian cells are FCHO1, FCHO2, and SGIP1, and all of these, including Syp1,

possess a central proline-rich domain (PRD), C-terminal µ homology domain (µHD), and, with the exception of SGIP1, N-terminal F-BAR domain (Reider *et al.*, 2009). Syp1 forms homodimers via the binding of two F-BAR domains (Reider *et al.*, 2009), and this interaction occurs through a conserved face of the domain (K. Hoban, unpublished). The F-BAR domain of Syp1 has been shown to tubulate membranes (Reider *et al.*, 2009), while the function of the PRD remains poorly understood. The µHD is the best characterized of the muniscin regions to date.

The µHD is named for its homology to a portion of the µ subunit of another endocytic adaptor, AP-2 (Reider *et al.*, 2009), and it can bind to specific cargo proteins at the PM and select them for trafficking into the cell. The only currently known Syp1 cargo is the cell wall integrity-sensor protein, Mid2 (Green *et al.*, 2003; Reider *et al.*, 2009). It was previously demonstrated that the overexpression of Syp1 causes Mid2-GFP, which localizes largely to the PM in WT cells, to be trafficked into the cell and directed to the vacuole (Reider *et al.*, 2009). However, the requirement of high-copy Syp1 for visualizing Mid2 internalization makes this cargo suboptimal for use in tests of Syp1-mediated cargo trafficking *in vivo*. The molecular mechanism by which Syp1 recognizes Mid2 also remains unknown; however, the way in which other adaptors have been shown to bind specific cargo proteins provides a blueprint for identifying the mechanism of Syp1-cargo interactions.

Adaptors frequently interact with cargos via short, specific peptide sequences within cytoplasmic domains of a target protein. One example of this is the clathrin adaptor, Sla1, which has been shown to bind NPFxD motifs (Howard *et al.*, 2002; Piao *et al.*, 2007). To confirm the importance of the motif for Sla1 cargo sorting, researchers

utilized, a truncated form of the **a**-type mating pheromone receptor, Ste2, which, unlike the WT protein, irregularly concentrates at the PM. An NPFSD sequence was then affixed to the cargo fragment, and the internalization of the Ste2 truncation was enhanced with the addition of this motif in a Sla1-dependent manner (Howard *et al*., 2002). In this dissertation, we utilize a phage display technique to help locate and identify the Syp1 cargo-sorting motif within Mid2. We also aim to identify additional cargos of this adaptor through a visual screen of protein localization in the presence and absence of Syp1. The discovery of a potential Syp1 sorting motif within any newly discovered cargo proteins would not only support findings suggesting the sequence is a cargo-sorting motif, but also provide a potentially superior alternative to Mid2 for testing the role of this motif *in vivo*.

Rho1-dependent clathrin-independent endocytosis

Despite the discovery of clathrin-independent endocytic (CIE) mechanisms in other eukaryotic cells, it was long thought that CME was the only type of endocytosis performed by budding yeast. Recently, this view changed as a result of a high-copy suppressor screen in a CME-deficient strain referred to as the adaptor mutant, which lacks the Yap180s and epsins, except for a single ENTH domain to maintain cell viability (Prosser *et al*., 2011). This study revealed that overexpression of proteins in the Mid2-initiated cell wall integrity pathway can rescue the sensitivity of the adaptor mutant to higher temperatures, as well as decrease the level of cargo proteins at the PM relative to those observed in WT cells. Results from the same report indicate that CME defects persist even when cargo trafficking is restored by upregulation of the cell wall integrity

pathway. These findings confirmed that a Rho1-dependent CIE mechanism exists in budding yeast.

In this CIE pathway, Mid2 signals for activation of Rho1 GTPase activity via the guanine-nucleotide exchange factors (GEFs), Rom1 and Rom2 (Ozaki *et al.*, 1996; Philip and Levin, 2001; Prosser *et al.*, 2011). Active Rho1 can then bind to its effector proteins (Delley and Hall, 1999). One of the five known Rho1 effectors is Bni1, a yeast formin protein that generates actin cables and is essential for the functioning of this endocytic pathway (Sagot *et al.*, 2002; Evangelista *et al.*, 2002; Prosser *et al.*, 2011). The homologue of the Rho1 GTPase in mammalian cells is RhoA. There are two mammalian endocytic mechanisms that require RhoA for their functioning: RhoA-dependent phagocytosis and RhoA-dependent CIE (Lamaze *et al.*, 2001; Werner *et al.*, 2001). Phagocytosis occurs when a cell takes up a large volume of material from its surroundings, during which the PM undergoes significant morphological changes to protrude and engulf an object in what becomes an internal vesicle called a phagosome. Mammalian RhoA-dependent phagocytosis is similar to yeast Rho1-dependent CIE in several ways: the RhoA pathway involves integrins, and Mid2 is integrin-like in primary sequence; both utilize GEFs, including RhoA GEFs, Vav1 and Vav3 (Werner *et al.*, 2001; Gakidis *et al.*, 2004); and each requires a formin for its functioning, mDia1 and mDia2 in the phagocytic mechanism (Colucci-Guyon *et al.*, 2005; Brandt *et al.*, 2007). RhoA-dependent endocytosis may also share similarities with yeast CIE, but the links are fewer and less clear (Prosser and Wendland, 2012).

Though much about the yeast Rho1-dependent CIE has been characterized, some aspects of the functioning of this pathway remain unknown. One such area is the

identification of candidate CIE adaptor proteins. A recent report revealed that α-arrestins, proteins associated with G protein-coupled receptor signaling regulation, are involved in cargo selection via the Rho1-dependent endocytic route (Prosser *et al*., 2015); however, it is likely that other adaptors for this CIE pathway remain undiscovered. Also, previous studies of Rho1-dependent CIE assessed internalization of the cargo protein, Ste3, the receptor for the **a**-mating type pheromone, but improved Ste3 internalization was only observed when components of CIE were overexpressed in a CME-deficient background (Prosser *et al*., 2011, 2015; Prosser and Wendland, 2012). It is possible that some protein cargos are more dependent upon CIE than the CME pathway; such cargo would be expected to exhibit internalization defects even when CME is functioning. Such a cargo would be useful in future studies of this clathrin-independent mechanism.

Downstream endocytic compartments

After an endocytic vesicle is formed, membrane and associated cargo proteins continue along the endocytic route within the cell. Clathrin-coated vesicles generated by CME are uncoated after being released from the PM (Goode *et al*., 2015). This allows the CME pathway proteins to be recycled for subsequent endocytic events, and the vesicle to be targeted to the early endosome. With the help of soluble *N*-ethylmaleimide–sensitive factor (NSF) attachment protein receptor (SNAREs) and other trafficking proteins, endocytic vesicles fuse with the early endosome. SNAREs are vital for such membrane fusion events. There are two broad types, vesicle-SNAREs (v-SNAREs) that are sorted into forming vesicles and target-SNAREs (t-SNAREs) that reside in the membranes of organelles to which vesicles will fuse, such as the early endosome and protrude into the

cytoplasm where they interact to form stable complexes (Burri and Lithgow, 2004).

Together, these classes of SNAREs aid in membrane fusion by undergoing a zippering

process in which the cytoplasmic domains of a t-SNARE complex and v-SNARE bind

(Ungermann *et al.*, 1998). Upon binding, the SNAREs attain the same orientation through

the formation of a *trans*-SNARE complex, bringing the membranes of the vesicle and

target compartment together for fusion. In this work, we investigate the trafficking of a v-

SNARE known as Snc1, the yeast homologue of mammalian synaptobrevin2/VAMP2

(Gerst *et al.*, 1992; Protopopov *et al.*, 1993).

Once at the early endosome, membrane and cargo can be directed to several

locations in the cell. For example, proteins designated for recycling are returned to the

PM. In endocytic recycling, vesicles are released from the early endosome in a process

similar to CME at the PM and targeted to recycling endosomes, which similarly generate

cargo-containing vesicles that then fuse with the PM (Grant and Donaldson, 2009). This

mechanism involves proteins such as the F-box protein, Rcy1 (Wiederkehr *et al.*, 2000).

Alternatively, vesicles budding from the early endosome may be trafficked to the Golgi

(Bonifacino and Rojas, 2006). However, cargo that are not selected for recycling to the

PM or transport to the Golgi are shuttled to compartments of the endocytic route that can

form intralumenal vesicles, known as multivesicular bodies (MVBs) (Felder *et al.*, 1990;

Gruenberg and Maxfield, 1995).

The formation of MVBs relies on the function of endosomal sorting complexes

required for transport (ESCRT), which work together to move membrane and cargos that

have been selected for degradation into the lumen of the MVB. Whereas endocytosis

creates vesicles that bud toward the cytoplasm, ESCRT complexes produce vesicles away

16

from the cytoplasm, despite the fact that proteins involved in both mechanisms are located in the cytoplasm itself. Ubiquitinated cargos are first recognized by components of the ESCRT-0 complex (Raiborg *et al.*, 2001, 2002; Ren *et al.*, 2009; Mayers *et al.*, 2011). This can occur as early as at the PM, aiding in the sorting of cargo into CCVs. Cargos are then passed to ESCRT-I complexes, followed by ESCRT-II (Teo *et al.*, 2006; Gill *et al.*, 2007). Unlike the earlier-acting complexes, ESCRT-III does not directly interact with cargo; instead, these proteins form large, multimeric structures that corral cargo to the center of ESCRT-III rings, while earlier complexes disperse for reutilization in initiating subsequent sites of ESCRT trafficking (Babst *et al.*, 2002; Ghazi-Tabatabai *et al.*, 2008; Hanson *et al.*, 2008). After the cargo-containing membrane at the center of these rings becomes invaginated, an ATPase associated with diverse cellular activities (AAA) called Vps4 disassembles the ESCRT-III complex, allowing for scission and release of a cargo-carrying vesicle into the lumen of the MVB (Robinson *et al.*, 1988; Rothman *et al.*, 1989; Babst *et al.*, 1997). Vps4 oligomerizes to form hexameric rings, and works in concert with other accessory proteins and regulatory factors such as Vta1, which promote Vps4 oligomerization and stimulate its ATPase activity (Yeo *et al.*, 2003).

Cargo proteins and membrane then move to late endosomes through the fusion of an MVB to either another MVB or to a preexisting late endosome (Huotari and Helenius, 2011). The final destination of endocytosed material destined for degradation is the vacuole, the budding yeast equivalent of the mammalian lysosome. The pH of the late endosome and vacuole lumens is much lower than the pH of the cytoplasm; the pH is between 4.5-5.5 within vacuoles under normal conditions, compared to approximately 6.5

17

in the cytoplasm (Klionsky *et al*., 1990). The increased acidity of these compartments aids in the degradation of the vesicles by lipases, permitting proteases access to protein domains that would otherwise be protected from such enzymes. The cell is then able to recycle the amino acids and other molecules released during these hydrolytic reactions. This highlights the importance of ESCRT complexes and the ability of the cell to form MVBs; without moving membrane and associated cargos into the lumen of these compartments, the cell is largely impeded from recycling membrane and non-extracellular protein domains via degradation mechanisms.

Genetic screens

Several ingenious approaches have been developed to address questions similar to those presented here. One such technique is known as a synthetic genetic array (SGA), which was originally developed to utilize the power of yeast genetics to perform high-throughput experiments that systematically identified negative genetic interactions (Tong *et al*., 2001). The approach employs a collection of budding yeast, all of the same mating type, in which a single gene has been deleted from each strain using the same selectable marker. A complete collection would, thus, include one mutant strain for each gene in *Saccharomyces cerevisiae* that is nonessential under standard conditions, of which there are approximately 4,800 (Winzeler *et al*., 1999). A query strain of the opposite mating type, in which the gene of interest has been replaced with a different selectable marker, can then be readily mated to each strain in the deletion collection. Subsequent sporulation and treatment to simultaneously select for the presence of both markers in haploid progeny ensures that only desired double mutant strains are obtained. We utilized the

SGA method of generating large numbers of yeast strains in a separate study, though not for identifying genetic interactions. Instead, we used the technique to quickly generate a large number of yeast strains in an attempt to identify potential cargos of the adaptor protein, Syp1. By easily incorporating a deletion of *SYP1* into a collection of strains expressing a green fluorescent protein (GFP) chimera, in which each strain has a different protein fused with GFP (Huh *et al.*, 2003), we can look for changes in protein localization in the absence of Syp1. A difference in cellular location would implicate a protein as being a cargo of this adaptor (Figure 1-2).

In the report first describing this SGA approach, the double mutants were then tested for the ability to grow (Tong *et al.*, 2001). Strains that did not grow represented synthetic lethal interactions, giving the SGA its name. Synthetic lethality describes a negative genetic interaction in which neither of two genes is essential, but the deletion of both in combination causes inviability. In a study presented here, we look for negative interactions between genes using a different assay, one utilizing a colony color-sectoring approach similar to one previously developed (Bender and Pringle, 1991). The assay takes advantage of the fact that an a*de2Δ* strain, in which adenine biosynthesis is disrupted, accumulates a red pigment; cells with this genotype turn red, along with the colonies they form (Roman, 1956; Dorfman, 1969; Jones and Fink, 1982). In a screen to identify negative genetic interactions with the adaptor mutant background, we utilized an additional deletion of the gene encoding Ade8, which acts upstream of Ade2 and prevents red pigmentation of the *ade2* mutant cells. A "cover plasmid" containing *ENT1* and *ADE8* was transformed into the adaptor mutant, cells in which *ENT1*, *ENT2*, *YAP1801*, and *YAP1802* have been deleted, excluding a single epsin ENTH domain. The cells were
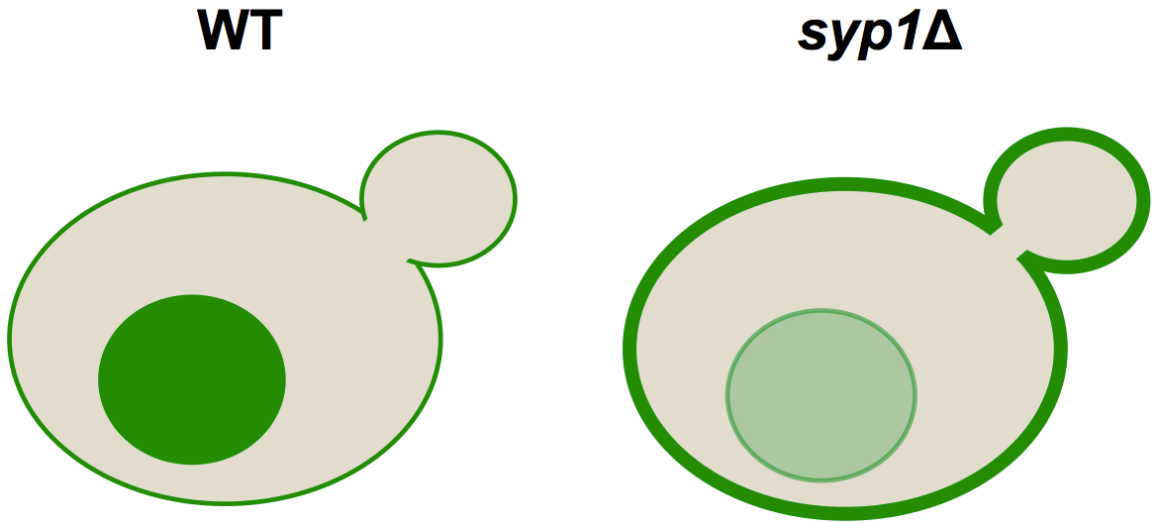
Figure 1-2. Model of altered localization of a Syp1 cargo (green) in a *syp1Δ* strain. A Syp1 cargo that localizes predominantly to the vacuole within a WT cell accumulates at the PM in the absence of Syp1.

then mutagenized with ethyl methanesulfonate (EMS) to introduce genomic point mutations (Lawley and Martin et al., 1975; Green *et al*., 2003). Any strain in which no synthetic lethal mutation has been generated will be able to lose the cover plasmid during cell division. Since cells that randomly lose this plasmid will be white in color, the colonies generated in this case will be both red and white, *i.e.* "sectored" colonies, representing daughters of cells that have and have not retained the plasmid, respectively. However, if synthetic lethal mutations do occur, the colonies formed will remain completely red and non-sectored (Figure 1-3). In Chapter 3, we discuss the finding that a negative genetic interaction exists between the adaptor mutants and Vps4, the AAA required for ESCRT-III disassembly and formation of MVBs.

As mentioned, another goal of the work described here was to identify the sorting motif within cargo proteins that is recognized by the Syp1 μHD. Experiments aiming to isolate the region of the only known Syp1 cargo, Mid2, bound by the μHD narrowed the location of the sorting sequence to a fragment of the cargo from residues 251 to 316. In an unbiased, parallel approach to identify potential Syp1 cargo-sorting motifs, we utilized a phage display technique to identify short peptides bound by the μHD. In this method, a library of filamentous phages expressing coat proteins of different sequences are generated and tested for binding to a target (Smith, 1985), the Syp1 μHD in this case. This is accomplished by inserting DNA encoding random peptide sequences into the gene expressing a coat protein of a phage, such as M13, for which the major coat protein is pVIII. Once the library is generated, phages are produced by infecting and isolating phage from bacteria. Phages with candidate binding motifs are then amplified during multiple rounds of binding to the target, with subsequent washing to remove unbound
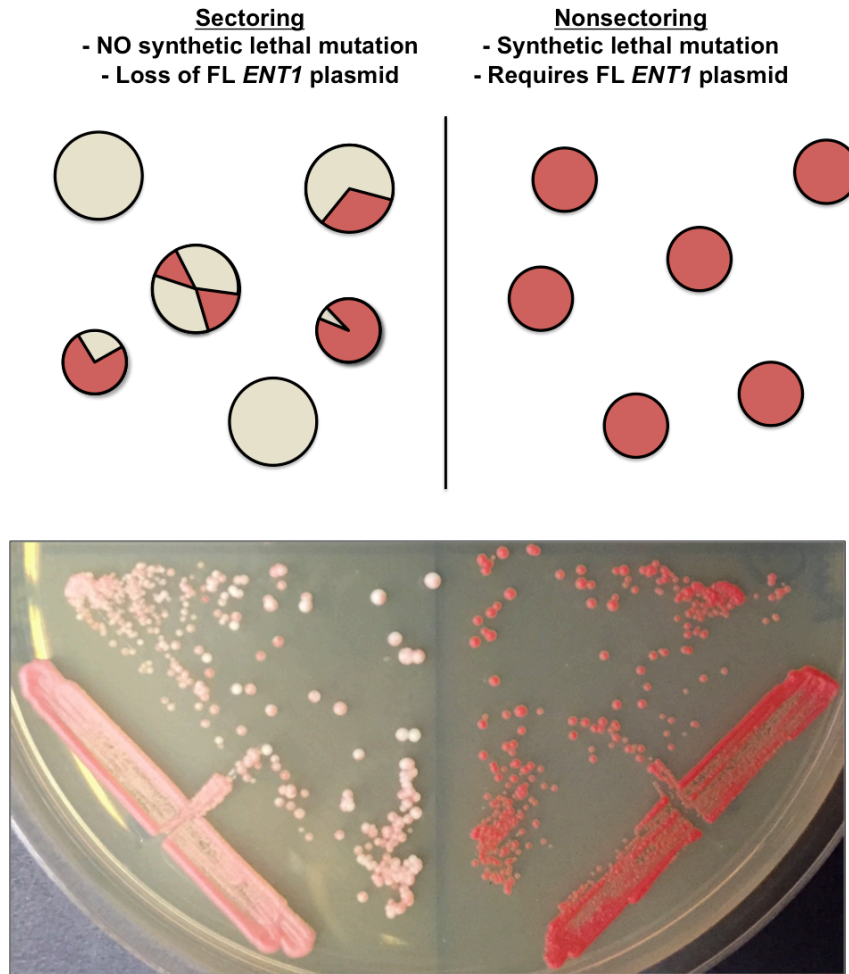
Figure 1-3. Colony-sectoring assay. (A) Diagram of colony-sectoring assay. (B) Cartoon

and experimental example of sectoring and nonsectoring colonies.

phages (Tonikian *et al.*, 2007). Finally, the genes for the coat proteins expressed by the

most abundant phage particles are sequenced. The following report demonstrates the

effectiveness of this approach, which provided clues that lead to the identification of a

Syp1 cargo-sorting motif.

References

Adams AE1, Johnson DI, Longnecker RM, Sloat BF, Pringle JR (1990) CDC42 and CDC43, two additional genes involved in budding and the establishment of cell polarity in the yeast Saccharomyces cerevisiae. *J Cell Biol* **111:** 131-42

Agnello V, Abel G, Elfahal M, Knight GB, Zhang QX (1999) Hepatitis C virus and other flaviviridae viruses enter cells via low density lipoprotein receptor. *Proc Natl Acad Sci* **96:** 12766-71

Aguilar RC, Watson HA, Wendland B (2003) The yeast Epsin Ent1 is recruited to membranes through multiple independent interactions. *J Biol Chem* **278:** 10737-43

Aguilar RC, Watson HA, Wendland B (2006) The yeast Epsin Ent1 is recruited to membranes through multiple independent interactions. *J Biol Chem* **278:** 10737-43

Bareford LM, Swaan PW (2007) Endocytic mechanisms for targeted drug delivery. *Adv Drug Deliv Rev* **59:** 748-758

Baudin A, Ozier-Kalogeropoulos O, Denouel A, Lacroute F, Cullin C (1993) A simple and efficient method for direct gene deletion in *Saccharomyces cerevisiae*. *Nucl Acids Res* **21:** 3329-3330

Babst M, Sato TK, Banta LM, Emr SD (1997) Endosomal transport function in yeast requires a novel AAA-type ATPase, Vps4p. *EMBO J* **16:** 1820-31

Babst M, Katzmann DJ, Estepa-Sabal EJ, Meerloo T, Emr SD (2002) Escrt-III: an endosome-associated heterooligomeric protein complex required for mvb sorting. *Dev Cell* **3:** 271-82

Bender A, Pringle JR (1991) Use of a screen for synthetic lethal and multicopy suppressee mutants to identify two new genes involved in morphogenesis in Saccharomyces cerevisiae. *Mol Cell Biol* **11:** 1295-305

Bénédetti H, Raths S, Crausaz F, Riezman H (1994) The END3 gene encodes a protein that is required for the internalization step of endocytosis and for actin cytoskeleton organization in yeast. *Mol Biol Cell* **5:** 1023-37

Benmerah A, Lamaze C, Bègue B, Schmidt SL, Dautry-Varsat A, and Cerf-Bensussan N (1998) AP-2/Eps15 interaction is required for receptor mediated endocytosis. *J Cell Biol* **140:** 1055-1062

Bonifacino JS, Rojas R (2006) Retrograde transport from endosomes to the trans-Golgi network. *Nat Rev Mol Cell Biol* **7:** 568-579

Brandt DT, Marion S, Griffiths G, Watanabe T, Kaibuchi K, Grosse R (2007) Dia1 and IQGAP1 interact in cell migration and phagocytic cup formation. *J Cell Biol* **178:** 193-200

Burri L, Lithgow T (2004). A complete set of SNAREs in yeast. *Traffic* **5:** 45-52

Carbone R, Fre S, Iannolo G, Belleudi F, Mancini P, Pelicci PG, Torrisi MR, Di Fiore PP (1997) Eps15 and Eps15R are essential components of the endocytic pathway. *Cancer Res* **57:** 5498-5504

Carroll SY, Stimpson HE, Weinberg J, Toret CP, Sun Y, Drubin DG (2012) Analysis of yeast endocytic site formation and maturation through a regulatory transition point. *Mol Biol Cell* **23:** 657-68

Chen H, Fre S, Slepnev VI, Capua MR, Takei K, Butler MH, Di Fiore PP, De Camilli P (1998) Epsin is an EH-domain-binding protein implicated in clathrin-mediated endocytosis. *Nature* **394:** 793-797

Chvatchko Y, Howald I, Riezman H (1986) Two yeast mutants defective in endocytosis are defective in pheromone response. *Cell* **46:** 355-64

Colucci-Guyon E, Niedergang F, Wallar BJ, Peng J, Alberts AS, Chavrier P. (2005) A role for mammalian diaphanous-related formins in complement receptor (CR3)-mediated phagocytosis in macrophages. *Curr Biol* **15:** 2007-12

Cong L, Ran FA, Cox D, Lin S, Barretto R, Habib N, Hsu PD, Wu X, Jiang W, Marraffini LA, Zhang F (2013) Multiplex genome engineering using CRISPR/Cas systems. *Science* **339:** 819-23

Cope MJ, Yang S, Shang C, Drubin DG (1999) Novel protein kinases Ark1p and Prk1p associate with and regulate the cortical actin cytoskeleton in budding yeast. *J Cell Biol* **144:** 1203-18

De Camilli P, Chen H, Hyman J, Panepucci E, Bateman A, Brunger AT (2002) The ENTH domain. *FEBS Lett* **513:** 11-8

Delley PA, Hall MN (1999) Cell wall stress depolarizes cell growth via hyperactivation of RHO1. *J Cell Biol* **147:** 163-74

Donnelly SF, Pocklington MJ, Pallotta D, Orr E (1993) A proline-rich protein, verprolin, involved in cytoskeletal organization and cellular growth in the yeast Saccharomyces cerevisiae. *Mol Microbiol* **10:** 585-96

Dorfman BZ (1969) The isolation of adenylosuccinate synthetase mutants in yeast by selection for constitutive behavior in pigmented strains. *Genetics* **(2):** 377-89

25

Evangelista M, Pruyne D, Amberg DC, Boone C, Bretscher A (2002) Formins direct Arp2/3-independent actin filament assembly to polarize cell growth in yeast. *Nat Cell Biol* **4:** 260-9

Farrell KB, Grossman C, Di Pietro SM (2015) New Regulators of Clathrin-Mediated Endocytosis Identified in Saccharomyces cerevisiae by Systematic Quantitative Fluorescence Microscopy. *Genetics* **201:** 1061-70

Felder S, Miller K, Moehren G, Ullrich A, Schlessinger J, Hopkins CR (1990) Kinase activity controls the sorting of the epidermal growth factor receptor within the multivesicular body. *Cell* **61:** 623-34

Ford MG, Pearse BM, Higgins MK, Vallis Y, Owen DJ, Gibson A, Hopkins CR, Evans PR, McMahon HT (2001) Simultaneous binding of PtdIns(4,5)P2 and clathrin by AP180 in the nucleation of clathrin lattices on membranes. *Science* **291:** 1051-5

Gakidis MA, Cullere X, Olson T, Wilsbacher JL, Zhang B, Moores SL, Ley K, Swat W, Mayadas T, Brugge JS (2004) Vav GEFs are required for beta2 integrin-dependent functions of neutrophils. *J Cell Biol* **166:** 273-82

Gagny B, Wiederkehr A, Dumoulin P, Winsor B, Riezman H, Haguenauer-Tsapis R (2000) A novel EH domain protein of Saccharomyces cerevisiae, Ede1p, involved in endocytosis. *J Cell Sci* **113:** 3309-19

Gerst JE, Rodgers L, Riggs M, Wigler M (1992) SNC1, a yeast homolog of the synaptic vesicle-associated membrane protein/synaptobrevin gene family: genetic interactions with the RAS and CAP genes. *Proc Natl Acad Sci* **89:** 4338-42

Ghazi-Tabatabai S, Saksena S, Short JM, Pobbati AV, Veprintsev DB, Crowther RA, Emr SD, Egelman EH, Williams RL (2008) Structure and disassembly of filaments formed by the ESCRT-III subunit Vps24. *Structure* **16:** 1345-56

Gill DJ, Teo H, Sun J, Perisic O, Veprintsev DB, Emr SD, Williams RL (2007) Structural insight into the ESCRT-I/-II link and its role in MVB trafficking. *EMBO J* **26:** 600-12

Goode BL, Eskin JA, Wendland B (2015) Actin and endocytosis in budding yeast. *Genetics* **199:** 315-58

Grant BD, Donaldson JG (2009) Pathways and mechanisms of endocytic recycling. *Nat Rev Mol Cell Biol* **10:** 597-608

Green R, Lesage G, Sdicu AM, Ménard P, Bussey H (2003) A synthetic analysis of the Saccharomyces cerevisiae stress sensor Mid2p, and identification of a Mid2p-interacting protein, Zeo1p, that modulates the PKC1-MPK1 cell integrity pathway. *Microbiology* **149:** 2487-99

Greene EA, Codomo CA, Taylor NE, Henikoff JG, Till BJ, Reynolds SH, Enns LC, Burtner C, Johnson JE, Odden AR, Comai L, Henikoff S (2003) Spectrum of chemically induced mutations from a large-scale reverse-genetic screen in Arabidopsis. *Genetics* **164:** 731-40

Gruenberg J, Maxfield FR (1995) Membrane transport in the endocytic pathway. *Curr Opin Cell Biol* **7:** 552-63

Hanson PI, Roth R, Lin Y, Heuser JE (2008) Plasma membrane deformation by circular arrays of ESCRT-III protein filaments. *J Cell Biol* **180:** 389-402

Howard JP, Hutton JL, Olson JM, Payne GS (2002) Sla1p serves as the targeting signal recognition factor for NPFX(1,2)D-mediated endocytosis. *J Cell Biol* **157:** 315-326

Huh WK, Falvo JV, Gerke LC, Carroll AS, Howson RW, Weissman JS, O'Shea EK (2003) Global analysis of protein localization in budding yeast. *Nature* **425:** 686-91

Huotari J, Heleniusa A (2011) Endosome maturation. *EMBO J* **30:** 3481-3500

Isnard AD, Thomas D, Surdin-Kerjan Y (1996) The study of methionine uptake in Saccharomyces cerevisiae reveals a new family of amino acid permeases. *J Mol Biol* **262:** 473-84

Itoh T, Koshiba S, Kigawa T, Kikuchi A, Yokoyama S, Takenawa T (2001) Role of the ENTH domain in phosphatidylinositol-4,5-bisphosphate binding and endocytosis. *Science* **291:** 1047-51

Jones EW and Fink GR (1982) Regulation of amino acid and nucleotide biosynthesis in yeast, 181-299. *In* J. N. Strathern, J. R. Broach, and E. W. Jones (ed.), The molecular biology of the yeast *Saccharomyces*: metabolism and gene expression. Cold Spring Harbor Laboratory Press, Cold Spring Harbor, N.Y.

Kaksonen M, Sun Y, Drubin DG (2003) A pathway for association of receptors, adaptors, and actin during endocytic internalization. *Cell* **115:** 475-87

Kaksonen M, Toret CP, Drubin DG (2005) A modular design for the clathrin- and actin-mediated endocytosis machinery. *Cell* **123:** 305-20

Kay BK, Yamabhai M, Wendland B, Emr SD (1999) Identification of a novel domain shared by putative components of the endocytic and cytoskeletal machinery. *Protein Sci* **8:** 435-8

Kirchhausen T, Harrison SC, Chow EP, Mattaliano RJ, Ramachandran KL, Smart J, Brosius J (1987) Clathrin heavy chain: molecular cloning and complete primary structure. *Proc Natl Acad Sci* **84:** 8805-8809

Klionsky DJ, Herman PK, Emr SD (1990) The fungal vacuole: composition, function, and biogenesis. *Microbiol Rev* **54:** 266-292

Lamaze C, Dujeancourt A, Baba T, Lo CG, Benmerah A, Dautry-Varsat A (2001) Interleukin 2 receptors and detergent-resistant membrane domains define a clathrin-independent endocytic pathway. *Mol Cell* **7:** 661-71

Lawley PD, Martin CN (1975) Molecular mechanisms in alkylation mutagenesis. Induced reversion of bacteriophage T4rII AP72 by ethyl methanesulphonate in relation to extent and mode of ethylation of purines in bacteriophage deoxyribonucleic acid. *Biochem J* **145:** 85-91

Lombardi R1, Riezman H (2001) Rvs161p and Rvs167p, the two yeast amphiphysin homologs, function together in vivo. *J Biol Chem* **276:** 6016-22

Longtine MS, McKenzie A III, Demarini DJ, Shah NG, Wach A, Brachat A, Philippsen P, Pringle JR (1998) Additional modules for versatile and economical PCR-based gene deletion and modification in Saccharomyces cerevisiae. *Yeast* **14:** 953-961

Lorenz MC, Muir RS, Lim E, McElver J, Weber SC, Heitman J (1995) Gene disruption with PCR products in *Saccharomyces cerevisiae*. *Gene* **158:** 113-117

Maldonado-Báez L, Dores MR, Perkins EM, Drivas TG, Hicke L, Wendland B (2008) Interaction between Epsin/Yap180 adaptors and the scaffolds Ede1/Pan1 is required for endocytosis. *Mol Biol Cell* **19:** 2936-48

Marcoux N, Cloutier S, Zakrzewska E, Charest PM, Bourbonnais Y, Pallotta D (2000) Suppression of the profilin-deficient phenotype by the RHO2 signaling pathway in *Saccharomyces cerevisiae*. *Genetics* **156:** 579-92

Mayers JR, Fyfe I, Schuh AL, Chapman ER, Edwardson JM, Audhya A (2011) ESCRT-0 assembles as a heterotetrameric complex on membranes and binds multiple ubiquitinylated cargoes simultaneously. *J Biol Chem* **286:** 9636-45

Mellman I, Yarden Y (2013) Endocytosis and cancer. *Cold Spring Harb Perspect Biol* **5:** a016949

McElver J, Weber S (1992) Flag^{TM} N-terminal epitope overexpression of bacterial alkaline phosphatase and Flag^{TM} C-terminal epitope tagging by PCR one-step targeted integration. *Yeast* **8:** S627

McMahon, Boucrot E (2011) Molecular mechanism and physiological functions of clathrin-mediated endocytosis. *Nat Rev Mol Cell Biol* **12:** 517-533

Mosesson Y, Mills GB, Yarden Y (2008) Derailed endocytosis: an emerging feature of cancer. *Nat Rev Cancer* **8:** 835-50

Munn AL, Stevenson BJ, Geli MI, Riezman H (1995) end5, end6, and end7: mutations that cause actin delocalization and block the internalization step of endocytosis in Saccharomyces cerevisiae. *Mol Biol Cell* **6:** 1721-42

Naqvi SN1, Zahn R, Mitchell DA, Stevenson BJ, Munn AL (1998) The WASp homologue Las17p functions with the WIP homologue End5p/verprolin and is essential for endocytosis in yeast. *Curr Biol* **8:** 959-62

Ozaki K, Tanaka K, Imamura H, Hihara T, Kameyama T, Nonaka H, Hirano H, Matsuura Y, Takai Y (1996) Rom1p and Rom2p are GDP/GTP exchange proteins (GEPs) for the Rho1p small GTP binding protein in Saccharomyces cerevisiae. *EMBO J* **15:** 2196-207

Piao HL, Machado IMP, Payne GS (2007) NPFXD-mediated endocytosis is required for polarity and function of a yeast cell wall stress sensor. *Mol Biol Cell* **18:** 57-65

Philip B, Levin DE (2001) Wsc1 and Mid2 are cell surface sensors for cell wall integrity signaling that act through Rom2, a guanine nucleotide exchange factor for Rho1. *Mol Cell Biol* **21:** 271-80

Prosser DC, Drivas TG, Maldonado-Báez L, Wendland B (2011) Existence of a novel clathrin-independent endocytic pathway in yeast that depends on Rho1 and formin. *J Cell Biology* **195:** 657-71

Prosser DC, Wendland B (2012) Conserved roles for yeast Rho1 and mammalian RhoA GTPases in clathrin-independent endocytosis. *Small GTPases* **3:** 229-35

Prosser DC, Pannunzio AE2, Brodsky JL2, Thorner J3, Wendland B4, O'Donnell AF5 (2015) α-Arrestins participate in cargo selection for both clathrin-independent and clathrin-mediated endocytosis. *J Cell Sci* **128:** 4220-34

Prosser DC, Wrasman K, Woodard TK, O'Donnell AF, Wendland B (2016) Applications of pHluorin for Quantitative, Kinetic and High-throughput Analysis of Endocytosis in Budding Yeast. *J Vis Exp* (116) doi: 10.3791/54587

Protopopov V, Govindan B, Novick P, Gerst JE (1993) Homologs of the synaptobrevin/VAMP family of synaptic vesicle proteins function on the late secretory pathway in S. cerevisiae. *Cell* **74:** 855-61

Raiborg C, Bache KG, Mehlum A, Stang E, Stenmark H (2001) Hrs recruits clathrin to early endosomes. *EMBO J* **20:** 5008-5021

Raiborg C, Bache KG, Gillooly DJ, Madshus IH, Stang E, Stenmark H (2002) Hrs sorts ubiquitinated proteins into clathrin-coated microdomains of early endosomes. *Nat Cell Biol* **4:** 394-398

Reider A, Wendland B (2011) Endocytic adaptors--social networking at the plasma membrane. *J Cell Sci* **124:** 1613-1622

Ren X, Kloer DP, Kim YC, Ghirlando R, Saidi LF, Hummer G, Hurley JH (2009) Hybrid structural model of the complete human ESCRT-0 complex. *Structure* **17:** 406-16

Robinson JS, Klionsky DJ, Banta LM, Emr SD (1998) Protein sorting in Saccharomyces cerevisiae: isolation of mutants defective in the delivery and processing of multiple vacuolar hydrolases. *Mol Cell Biol* **8:** 4936-48

Roman H (1956) Studies of gene mutation in *Saccharomyces*. *Cold Spring Harb Symp Quant Biol* **21:** 175-85

Roth TF, Porter KR (1964) Yolk protein uptake in the oocyte of the mosquito *Aedes aegypti*. L. *J Cell Biol* **20:** 313-32

Rothman JH, Howald I, Stevens TH (1989) Characterization of genes required for protein sorting and vacuolar function in the yeast Saccharomyces cerevisiae. *EMBO J* **8:** 2057-65

Sagot I, Klee SK, Pellman D (2002) Yeast formins regulate cell polarity by controlling the assembly of actin cables. *Nat Cell Biol* **4:** 42-50

Sandvig K, Torgersen ML, Raa HA, van Deurs B (2008) Clathrin-independent endocytosis: from nonexisting to an extreme degree of complexity. *Histochem Cell Biol* **129:** 267-76

Sandvig K, van Deurs B (2008) Cell biology: Viruses in camouflage. *Nature* **453:** 466-7

Schreij AM, Fon EA, McPherson PS (2016) Endocytic membrane trafficking and neurodegenerative disease. *Cell Mol Life Sci* **73:** 1529-45

Schroer TA, Fyrberg E, Cooper JA, Waterston RH, Helfman D, Pollard TD, Meyer DI (1994) Actin-related protein nomenclature and classification. *J Cell Biol* **127:** 1777-8

Schwob E, Martin RP (1992) New yeast actin-like gene required late in the cell cycle. *Nature* **355:** 179-82

Smith GP (1985) Filamentous fusion phage: novel expression vectors that display cloned antigens on the virion surface. *Science* **228:** 1315-7

Stahelin RV, Long F, Peter BJ, Murray D, De Camilli P, McMahon HT, Cho W (2003) Contrasting membrane interaction mechanisms of AP180 N-terminal homology (ANTH) and epsin N-terminal homology (ENTH) domains. *J Biol Chem* **278:** 28993-9

Tang HY, Munn A, Cai M (1997) EH domain proteins Pan1p and End3p are components of a complex that plays a dual role in organization of the cortical actin cytoskeleton and endocytosis in Saccharomyces cerevisiae. *Mol Cell Biol* **17:** 4294-304

Tang HY, Xu J, Cai M (2000) Pan1p, End3p, and S1a1p, three yeast proteins required for normal cortical actin cytoskeleton organization, associate with each other and play essential roles in cell wall morphogenesis. *Mol Cell Biol* **20:** 12-25

Teo H, Gill DJ, Sun J, Perisic O, Veprintsev DB, Vallis Y, Emr SD, Williams RL (2006) ESCRT-I core and ESCRT-II GLUE domain structures reveal role for GLUE in linking to ESCRT-I and membranes. *Cell* **125:** 99-111

Tong AH, Evangelista M, Parsons AB, Xu H, Bader GD, Pagé N, Robinson M, Raghibizadeh S, Hogue CW, Bussey H, Andrews B, Tyers M, Boone C (2001) Systematic genetic analysis with ordered arrays of yeast deletion mutants. *Science* **294:** 2364-8

Tonikian R, Zhang Y, Boone C, Sidhu SS (2007) Identifying specificity profiles for peptide recognition modules from phage-displayed peptide libraries. *Nat Protoc* **2:** 1368-1386

Ungermann C, Sato K, Wickner W (1998) Defining the functions of trans-SNARE pairs. *Nature* **396:** 543-8

Ungewickell E, Branton D (1981) Assembly units of clathrin coats. *Nature* **289:** 420-422

Wendland B, Emr SD (1998) Pan1p, yeast eps15, functions as a multivalent adaptor that coordinates protein-protein interactions essential for endocytosis. *J Cell Biol* **141:** 71-84

Wendland B, Steece KE, Emr SD (1999) Yeast epsins contain an essential N-terminal ENTH domain, bind clathrin and are required for endocytosis. *EMBO J* **18:** 4383-93

Werner E, Kheradmand F, Isberg RR, Werb Z (2001) Phagocytosis mediated by Yersinia invasin induces collagenase-1 expression in rabbit synovial fibroblasts through a proinflammatory cascade. *J Cell Sci* **114:** 3333-43

Wiederkehr A, Avaro S, Prescianotto-Baschong C, Haguenauer-Tsapis R, Riezman H (2000) The F-box protein Rcy1p is involved in endocytic membrane traffic and recycling out of an early endosome in Saccharomyces cerevisiae. *J Cell Biol* **149:** 397-410

Winzeler EA, Shoemaker DD, Astromoff A, Liang H, Anderson K, Andre B, Bangham R, Benito R, Boeke JD, Bussey H, Chu AM, Connelly C, Davis K, Dietrich F, Dow SW, El Bakkoury M, Foury F, Friend SH, Gentalen E, Giaever G, Hegemann JH,

Jones T, Laub M, Liao H, Liebundguth N, Lockhart DJ, Lucau-Danila A, Lussier M, M'Rabet N, Menard P, Mittmann M, Pai C, Rebischung C, Revuelta JL, Riles L, Roberts CJ, Ross-MacDonald P, Scherens B, Snyder M, Sookhai-Mahadeo S, Storms RK, Véronneau S, Voet M, Volckaert G, Ward TR, Wysocki R, Yen GS, Yu K, Zimmermann K, Philippsen P, Johnston M, Davis RW. (1999) Functional characterization of the S. cerevisiae genome by gene deletion and parallel analysis. *Science* **285:** 901-6

Yeo SC1, Xu L, Ren J, Boulton VJ, Wagle MD, Liu C, Ren G, Wong P, Zahn R, Sasajala P, Yang H, Piper RC, Munn AL (2003) Vps20p and Vta1p interact with Vps4p and function in multivesicular body sorting and endosomal transport in Saccharomyces cerevisiae. *J Cell Sci* **116:** 3957-70

Yu X, Cai M (2004) The yeast dynamin-related GTPase Vps1p functions in the organization of the actin cytoskeleton via interaction with Sla1p. *J Cell Sci* **117:** 3839-53

Zeng G, Cai M (1999) Regulation of the actin cytoskeleton organization in yeast by a novel serine/threonine kinase Prk1p. *J Cell Biol* **144:** 71-82

CHAPTER 2

Syp1 regulates the clathrin-mediated and clathrin-independent endocytosis of multiple

cargo proteins through a novel sorting motif

This chapter was previously published in *Molecular Biology of the Cell* (Apel, Hoban *et al*., 2017). Figures 2-1B; 2-2, B and C; 2-3, C-E; and 2-12D; as well as Table 2-1, were

contributed by coauthors. All other results in this chapter are original work.

Abstract

Internalization of proteins from the plasma membrane (PM) allows for cell-surface composition regulation, signaling network modulation, and nutrient uptake. Clathrin-mediated endocytosis (CME) is a major internalization route for PM proteins. During CME, endocytic adaptor proteins bind cargos at the cell surface and link them to the PM and clathrin coat. Muniscins are a conserved family of endocytic adaptors, including Syp1 in budding yeast and its mammalian ortholog, FCHo1. These adaptors bind cargo via a C-terminal μ-homology domain (μHD); however, few cargos exhibiting muniscin-dependent endocytosis have been identified, and the sorting sequence recognized by the μHD is unknown. To reveal Syp1 cargo-sorting motifs, we performed a phage display screen and used biochemical methods to demonstrate that the Syp1 μHD binds DxY motifs in the previously identified Syp1 cargo, Mid2, and the v-SNARE, Snc1. We also executed an unbiased visual screen, which identified the peptide transporter, Ptr2, and the ammonium permease, Mep3, as Syp1 cargos containing DxY motifs. Finally, we determined that, in addition to regulating cargo entry through CME, Syp1 can promote internalization of Ptr2 through a recently identified clathrin-independent endocytic pathway that requires the Rho1 GTPase. These findings elucidate the mechanism of Syp1 cargo recognition and its role in trafficking.

Introduction

The plasma membrane (PM) of eukaryotic cells forms an essential barrier that selectively separates the fluctuating extracellular environment from the more stable conditions maintained in the cytoplasm. It contains transmembrane proteins that allow for the establishment of vital cellular gradients, regulation of cell-surface markers, modulation of signaling networks, and uptake of vital nutrients. The PM must be continuously modified in order to precisely regulate these events and accommodate the changing needs of a cell.

Clathrin-mediated endocytosis (CME) is a key pathway for modulating the composition of the PM, and this endocytic mechanism requires the action of many cytosolic proteins to internalize a portion of the membrane by generating a clathrin-coated vesicle (CCV). CCV generation requires the ordered assembly of a large number of proteins that act in discrete steps: (1) initiation of CME, in which early-arriving proteins select the endocytic site, concentrate cargo, and facilitate clathrin coat assembly; (2) maturation of the endocytic site, during which F-actin assembly and the clathrin coat promote vesicle budding; and (3) scission, in which the bud neck constricts, and the nascent vesicle is separated from the plasma membrane (Kaksonen *et al.*, 2003; Kaksonen *et al.*, 2005).

The CME machinery is largely conserved from yeast to human, such that orthlogous proteins perform equivalent functions and are recruited in a similar order (Engqvist-Goldstein and Drubin, 2003; Taylor *et al.*, 2011; Goode *et al.*, 2015). Adaptor proteins select specific membrane-associated cargos for trafficking into the cell through

35

physical interactions and are among the first components to act in CME, subsequently recruiting later-arriving components of the endocytic machinery, including clathrin.

The muniscins are a recently identified family of endocytic adaptors that includes the budding yeast protein, Syp1, and its mammalian orthologs, FCHo1/2 and SGIP1 (Reider *et al*., 2009). The muniscins have known roles in CME and are recruited to nascent sites for this pathway (Boettner *et al*., 2009; Reider *et al*., 2009; Henne *et al*., 2010); however, whether muniscin-dependent cargo internalization occurs exclusively via CME has not been determined.

Muniscins mediate cargo selection via a C-terminal μ-homology domain (μHD), named for its structural similarity to the cargo-binding μ2 subunit of the heterotetrameric AP-2 adaptor complex (Reider *et al*., 2009). *SYP1* overexpression causes partial relocalization of Mid2 to the vacuole in a μHD-dependent manner (Reider *et al*., 2009), while the FCHo1 μHD interacts with the BMP receptor Alk8 (Umasankar *et al*., 2012). Notably, the yeast ortholog of μ2, known as Apm4, can also bind to Mid2 and affect its localization (Chapa-y-Lazo *et al*., 2014). Currently, the mechanism by which muniscins recognize their cognate cargo proteins is unclear.

Most endocytic adaptors contain one or more regions that bind short, linear peptide sequences known as cargo-sorting motifs, which are present in the cytoplasmic regions of their transmembrane cargos (Reider and Wendland, 2011). The wide variety of PM-localized cargos necessitates the use of several different sorting motifs to prevent competition for entry into the cell, as well as to allow for maximal flexibility and regulation of specific cargo internalization. Numerous sorting motifs have been identified, each of which has a distinct amino acid sequence (Traub, 2009).

AP-2 binds two different cargo sorting motifs: YxxΦ – where Φ is any amino acid with a bulky, hydrophobic side chain – through the μ2 subunit and [D/E]xxxL[L/I/M] motifs through the σ2 subunit (Boll *et al*., 1996; Doray *et al*., 2007; Kelly *et al*., 2008; Owen *et al*., 2004). Other adaptor proteins that contain variant phosphotyrosine-binding domains, such as Dab2, ARH, and Talin, bind to non-phosphorylated [F/Y]XNPXxNPx[Y/F] sorting motifs found in the tails of membrane cargos such as integrins and the LDL receptor (Keyel *et al*., 2006; Wegener *et al*., 2007). The yeast-specific adaptor protein, Sla1, interacts with NPFxD sorting motifs within its cargos, Ste2 and Wsc1, through its Sla1-homology domain 1 region (Howard *et al*., 2002; Piao *et al*., 2007). Still, other cargos lack any known sorting sequences, leading to the prediction that additional motifs have yet to be determined.

To date, the only known Syp1 cargo is the cell wall stress sensor Mid2 (Reider *et al*., 2009). The smallest fragment of Mid2 demonstrated to bind the Syp1 μHD is Mid2[251-316] (Reider *et al*., 2009; Figure 2-1A), suggesting that the sorting motif recognized by Syp1 resides in this region of the cargo. Intriguingly, Mid2 is a component of a clathrin-independent endocytosis (CIE) pathway in yeast that requires the Rho1 GTPase and its effector, the formin Bni1 (Prosser *et al*., 2011); however, a potential role for Syp1 in cargo trafficking via CIE has not yet been addressed. This is due, in part, to the fact that Mid2 localizes primarily to the PM and requires *SYP1* overexpression for observable trafficking into the cell (Reider *et al*., 2009), complicating the use of Mid2 in live-cell studies of Syp1-mediated endocytosis.

Identifying additional cargos that localize to downstream endocytic compartments would aid in examining the potential involvement of Syp1 in both endocytic pathways

under standard conditions, as well as testing the role for a potential cargo-sorting motif *in vivo*. To improve our understanding of the molecular mechanisms underlying muniscin-mediated cargo trafficking, we aimed to identify cargo-sorting motifs recognized by the Syp1 µHD. Using a phage display screen, we demonstrated that DxY is a cargo-sorting motif; moreover, visual screening revealed the peptide transporter, Ptr2, and ammonium permease, Mep3, as Syp1 cargos. Finally, we identified a role for Syp1 in clathrin-independent endocytosis of Ptr2, suggesting that Syp1 participates in multiple endocytic pathways.

Results

The Syp1 µHD binds a DxY motif within Mid2

 To reveal peptide sequences bound by the Syp1 µHD, we performed an unbiased phage display screen using a random 12-mer peptide library. The µHD was tagged with GST, expressed in bacteria, purified, and used as a target in binding selections with the phage display library. From the screen, we identified eight potential Syp1 ligand sequences and, to aid in the search for potential motifs, we compared the peptide sequences to that of Mid2$^{251-316}$, the smallest fragment of Mid2 previously shown to bind the Syp1 µHD (Figure 2-1, A and B; Reider *et al*., 2009). Two DxY sequences (Peptides 1 and 2), two YxxΦ motifs (Peptides 3 and 6), and several instances of two consecutive residues with bulky side chains, including one WY (Peptide 1) and five WW sequences (Peptides 4-8), were present in the peptides. All of these potential Syp1-interacting motifs are present in Mid2$^{251-316}$.

 Due to the abundance of consecutive, bulky side chains in our phage display results, we initially aimed to investigate the role of this candidate motif in cargo binding by Syp1. The WY motif overlaps with both a WW and a YxxΦ motif (276-WWYMLL, Figure 2-1A); therefore, we generated a mutant in which the WY residues were mutated to alanines to allow for the simultaneous disruption and investigation of all three motifs. We examined binding of the µHD to the WY>AA mutant protein using an affinity pull-down experiment. For these tests, a longer Mid2 fragment, Mid2$^{273-376}$, was used as a result of its increased amenability for use in biochemical assays. Mutation of the WY sequence (aa277-278) did not have an observable effect on binding of His$_6$-Mid2$^{273-376}$ to the Syp1 µHD; similar amounts of the WT and mutant protein were recovered in the bead

A

Mid2[251-316]: QSSRTDFIDSDGKVVTAYRANKFTKWWYMLLGKKVSDEYHSDSPLGGSASSAGGLDLDEADDVMEQ

B

Phage Display Peptides

1. DWYRDPVFDVLL
2. LWRRVVVDSYGV
3. YMWIACPDGWDC
4. WWDWAVQSETLL
5. WWVNPLGVTQDV
6. EYPWWMEQFYLE
7. WWAEAWFAWTPG
8. ISWHSDWWVELV
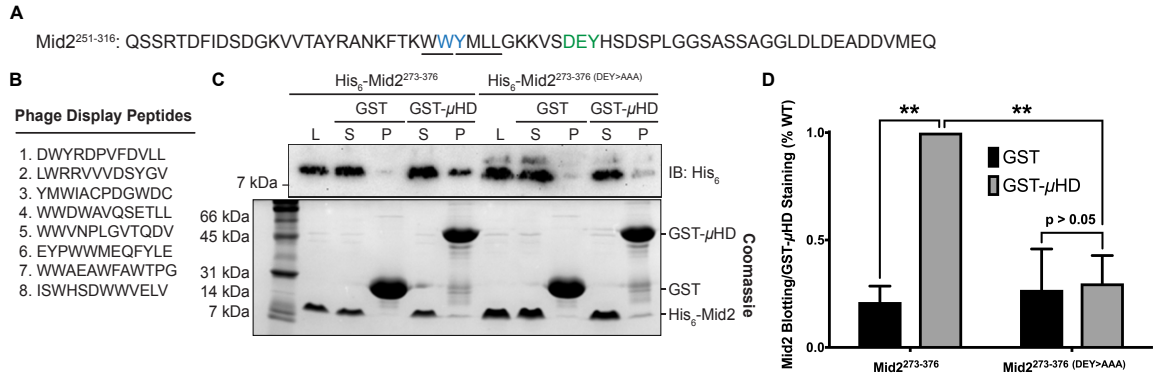
Figure 2-1. The Syp1 μHD binds a DxY motif within Mid2. (A) Amino acid sequence of Mid2[251-316]. The DxY and WY motifs are shown in green and blue, respectively, and the WW and YxxΦ motifs overlapping the WY motif are underlined. (B) Amino acid sequence of the eight 12-mer peptides identified in the Syp1 μHD phage display screen. (C) Immunoblot of recombinant binding assay in which WT and mutant His$_6$-Mid2[273-376] (DEY>AAA) fragments are tested for binding to an immobilized GST negative control or GST-Syp1 μHD; top: anti-His$_6$ immunoblot, bottom: GelCode Blue (Coomassie) protein stain. (L: loading control, S: supernatant, P: pelleted fraction). (D) Quantification of Mid2 WT and mutant fragment blotting relative to staining of GST or GST-μHD recovered from pelleted fractions (error bars indicate mean ± SD; n = 3; **, P < 0.01 compared to normalized WT).

fraction when co-precipitated with GST-µHD (Figure 2-2A). Consequently, these data indicate that WW and WY (WW/Y) motifs, along with YxxΦ motif, in the Mid2 C-terminal tail are unlikely to bind Syp1.

Based on our results indicating that these motifs are not required for Syp1 binding to Mid2, we tested the ability of the µHD to bind the DxY motif. The residues DEY (aa287-289) were mutated to alanines, and affinity pull-down experiments using His_6-$Mid2^{273-376}$ and GST-µHD revealed that, while the WT protein bound to the µHD as expected, mutation of the DxY motif significantly reduced the amount of Mid2 that co-precipitated with GST-µHD (Figure 2-1, C and D). Together, these results demonstrate that the Syp1 µHD binds the DxY motif in its known cargo protein, Mid2.

Syp1 also recognizes a DxY motif within Snc1

A previous high-throughput study demonstrated that the v-SNARE, Snc1, exhibits a decreased rate of endocytosis in mutant strains lacking some CME-associated genes, including a modest defect in *syp1Δ* cells (Burston *et al*., 2009). Although greater defects were observed in cells lacking other adaptor-encoding genes, cargo proteins are often trafficked into the cell by multiple adaptors. For example, in Burston *et al*., 2009, deletion of either *YAP1801* or *YAP1802* individually produced a mild Snc1 endocytosis defect but, when removed from the genome in combination, the inhibition of Snc1 internalization was more severe.

Of note, Snc1 also contains DxY, WY, and YxxΦ motifs in its cytoplasmic domain (Figure 2-3A). Given that Syp1 interacts directly with Mid2 to promote its internalization, we reasoned that Syp1 might similarly associate with Snc1. Thus, we
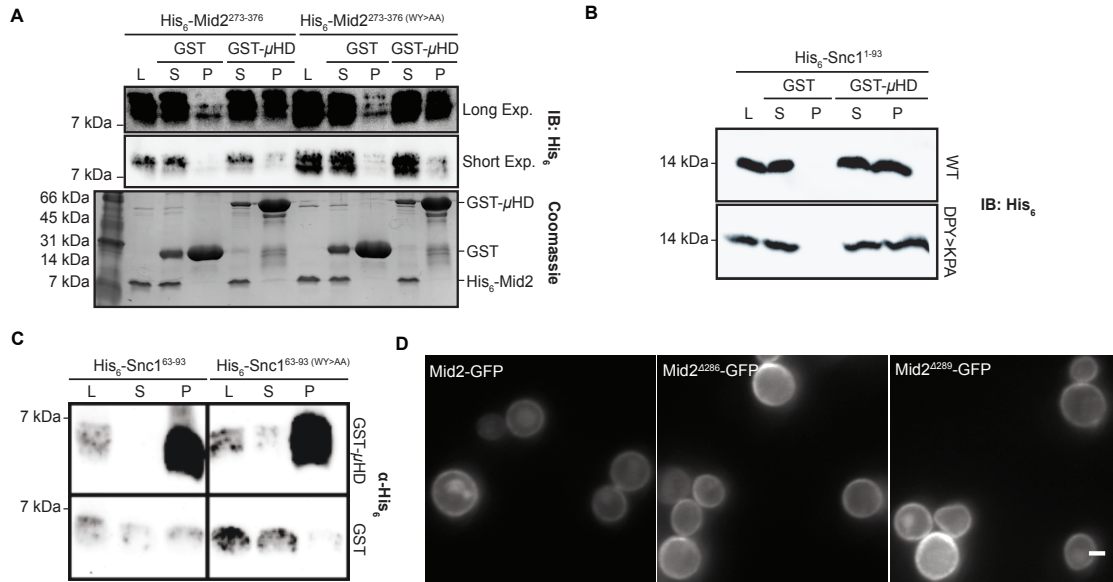
Figure 2-2. Syp1 does not recognize WY motifs. (A) Immunoblot of recombinant binding assay in which WT and mutant Mid2$^{273-376}$ (WY>AAA) fragments were tested for binding to an immobilized GST negative control or GST-Syp1 μHD; top: long exposure anti-His$_6$ immunoblot, middle: short exposure anti-His$_6$ immunoblot, bottom: GelCode Blue (Coomassie) protein stain. (L: loading control, S: supernatant, P: pelleted fraction). (B) Immunoblot of binding assay in which GST and GST-Syp1 μHD were treated with either WT His$_6$-Snc1$^{1-93}$ or a mutant in which the DPY motif was mutated to KPA (L: loading control, S: supernatant, P: pelleted fraction). (C) Immunoblot of binding assay in which GST and GST-Syp1 μHD were treated with either WT His$_6$-Snc1$^{63-93}$ or a mutant in which the WY motif was mutated to alanines (L: loading control, S: supernatant, P: pelleted fraction). (D) Cells expressing full-length Mid2-GFP, Mid2$^{\Delta286}$-GFP, or Mid2$^{\Delta289}$-GFP were grown on minimal medium and imaged via live-cell fluorescence microscopy. Scale bar, 2 μm.

A

Snc1^1-93: MSSSTPF<u>DPY</u>ALSEHDEERPQNVQSKSRTAELQAEIDDTVGIMRDNINKVAERGERLTSIEDKADNLAVSAQGFKRGANRVRKAM<u>WY</u>KDLKMK

Figure 2-3. Syp1 recognizes a DxY motif within Snc1. (A) Amino acid sequence of the cytoplasmic region of Snc1, aa1-93. Snc1$^{1-27}$ is shown in green and Snc1$^{63-93}$ in blue; the DxY and WY motifs are underlined. (B) WT cells expressing GFP-Snc1 from a low-copy plasmid were transformed with either an empty or *SYP1*-containing high-copy vector and grown on selective medium. Cells were imaged via live-cell fluorescence microscopy (arrowheads: GFP-Snc1 in medium- to large-sized buds; arrows: GFP-Snc1 in unbudded cells). Scale bar, 2 μm. (C) Immunoblot of binding assay in which GST and GST-Syp1 μHD are treated with WT His$_6$-Snc1$^{1-93}$ (L: loading control, S: supernatant, P: pelleted fraction). (D) Immunoblot of binding assay in which WT His$_6$-Snc1$^{1-27}$ and a mutant of this fragment (DPY>AAA) were tested for binding to the Syp1 μHD. (L: loading control, S: supernatant, P: pelleted fraction). (E) Immunoblot of binding assay in which Snc1$^{63-93}$ was tested for binding to GST-Syp1 μHD (L: loading control, S: supernatant, P: pelleted fraction).

investigated a potential role for Syp1 in Snc1 endocytosis. Due to the previous

observation that only a subtle reduction in Snc1 trafficking occurs in $syp1\Delta$ cells (Burston

et al., 2009), we chose to test the effect of *SYP1* overexpression on Snc1 localization.

To assess changes in Snc1 localization, we transformed WT cells expressing

GFP-Snc1 from a low-copy plasmid with either an empty high-copy vector or one

containing *SYP1* expressed from its endogenous promoter. In cells with empty vector,

GFP-Snc1 was polarized to the PM of the daughter bud in medium- to large-budded cells

(Figure 2-3B, left panel; arrowheads), as expected (Robinson *et al.*, 2006). The protein

also localized to internal punctae, likely due to constitutive endocytosis and recycling. In

contrast, the localization of GFP-Snc1 to the PM was less pronounced in buds of similar

size from cells with high-copy expression of *SYP1*. Instead, most of the protein localized

to internal compartments within buds (Figure 2-3B, right panel; arrowhead). We also

observed increased GFP-Snc1 internalization in unbudded cells, indicating that the effect

of Syp1 on Snc1 internalization is not cell cycle-dependent (Figure 2-3B, arrows).

Overall, these data demonstrate that Syp1 can contribute to Snc1 trafficking.

Due to the ability of Syp1 to promote Snc1 endocytosis *in vivo*, as well as the

presence of candidate Syp1-binding motifs in the Snc1 cytoplasmic domain, we next

tested whether recombinant Syp1 and Snc1 bind *in vitro*. The His_6-tagged, cytosolic

domain of Snc1 (aa1-93) bound to GST-μHD but not to GST alone, confirming Snc1 as a

binding partner of Syp1 (Figure 2-3C). To determine whether the DxY motif near the N-

terminus of Snc1 binds to Syp1 as did the DxY motif of Mid2, a His_6-tagged fragment of

Snc1 containing this motif, $Snc1^{1-27}$ (Figure 2-3A, green), was tested for binding to the

μHD. $Snc1^{1-27}$ bound the μHD, indicating that this region physically interacts with Syp1

(Figure 2-3D). Moreover, binding was diminished when the DxY motif in this fragment was mutated to alanines, suggesting that the DxY motif may be a common sorting sequence among Syp1 cargos.

Although the DxY motif is necessary for binding to the Syp1 µHD in the context of Snc1[1-27], results of an experiment using a longer fragment of Snc1 (aa1-93) indicated that this cargo contains more than one Syp1-binding site. Snc1[1-93] still interacted with Syp1 when the DxY motif in this fragment was mutated; even charge reversal of the aspartic acid to lysine did not abrogate the interaction (Figure 2-2B). As a result, additional fragments of the Snc1 cytoplasmic tail were constructed, and tested for binding to the Syp1 µHD. The last third of the Snc1 tail (aa63-93; Figure 2-3A, blue) also bound to the µHD (Figure 2-3E).

Snc1[63-93] does not contain a DxY motif but does have WY and YxxΦ motifs, both of which were present in the phage display peptides. Therefore, we tested the ability of Syp1 to bind these motifs in the Snc1[63-93] fragment. Mutation of the WY residues (aa86-87) to alanines, which simultaneously disrupts the WY and YxxΦ motifs, did not inhibit binding of Snc1[63-93] to the µHD (Figure 2-2C). Along with results of the Mid2 WY mutant binding experiment, this further suggests that Syp1 does not bind WY motifs in these cargos; the precise nature of association between Syp1 and Snc1[63-93] will be a subject of future study. Together, these findings indicate that Snc1 contains at least two Syp1 binding-sites, including a DxY motif, both of which are independent of the previously identified Snc1 endocytic signal V40, M43 within Snc1[28-62] (Burston *et al*., 2009; Gurunathan *et al*., 2000).

A visual screen reveals Ptr2 and Mep3 to be Syp1 cargos

Given that Syp1 and its mammalian orthologs play conserved roles as adaptor proteins, we hypothesized that Syp1 may regulate endocytosis of cargos other than Mid2 and Snc1. Since short peptide motifs, such as DxY, are likely to be found in many proteins, we attempted to identify potential Syp1-dependent cargos using an unbiased, high-throughput visual screen, as identification of further Syp1 cargos would improve our understanding of the cellular roles for this adaptor.

To establish that deletion of *SYP1* does not impair trafficking of all endocytic cargos, we first examined the localization of GFP-tagged Ste3 in WT and *syp1Δ* cells. Ste3, the yeast **a**-factor mating pheromone receptor, is constitutively endocytosed in non-mating *MATα* cells and localizes primarily to the vacuole (Davis *et al*., 1993). Ste3-GFP internalization was not disrupted in a *syp1Δ* strain, with protein localization appearing similar to WT cells (Figure 2-4A). In contrast, the absence of End3, a key endocytic protein that acts in coordination with the accessory proteins Sla1 and Pan1 (Tang *et al*., 1997; Tang *et al*., 2000), causes cargos, including Ste3, to nonspecifically accumulate at the plasma membrane (Raths *et al*., 1993).

To quantify the amount of Ste3 at the PM in each condition, we also constructed a chimera using pHluorin (Figure 2-4B), a pH-sensitive variant of GFP that allows for analysis of endocytic efficiency (Miesenbock *et al*., 1998; Prosser *et al*., 2010). Quantification of Ste3-pHluorin intensity corroborated the results obtained from Ste3-GFP imaging: the *syp1Δ* mutants did not exhibit increased Ste3-pHluorin fluorescence, unlike the significant increase observed in the *end3Δ* strain. These data suggest that loss of Syp1 does not generally interrupt endocytosis of cargo and may, instead, affect the

Figure 2-4. A visual screen reveals Ptr2 and Mep3 to be Syp1 cargos. (A) WT, *syp1Δ*, and *end3Δ* cells expressing Ste3-GFP were grown on rich medium and imaged via live-cell fluorescence microscopy. Scale bar, 2 μm. (B) Intensity of Ste3-pHluorin was quantified for each condition; intensity values were corrected for cell size and expressed in arbitrary units (a.u.) (error bars indicate mean ± SEM; ****, $P < 0.0001$ compared to WT). (C) WT and *syp1Δ* cells expressing Ptr2-GFP were grown on rich medium (YPD) and imaged via live-cell fluorescence microscopy. Scale bar, 2 μm. (D) Intensity of Ptr2-pHluorin was quantified for each condition; intensity values were corrected for cell size and expressed in arbitrary units (a.u.) (error bars indicate mean ± SEM; ****, $P < 0.0001$ compared to WT). (E) WT and *syp1Δ* cells expressing Mep3-GFP were grown on minimal, ammonium-rich medium (YNB) and imaged via live-cell fluorescence microscopy. Scale bar, 2 μm. (F) Intensity of Mep3-pHluorin was quantified for each condition; intensity values were corrected for cell size and expressed in arbitrary units (a.u.) (error bars indicate mean ± SEM; *, $P < 0.05$ compared to WT).

Figure on following page.
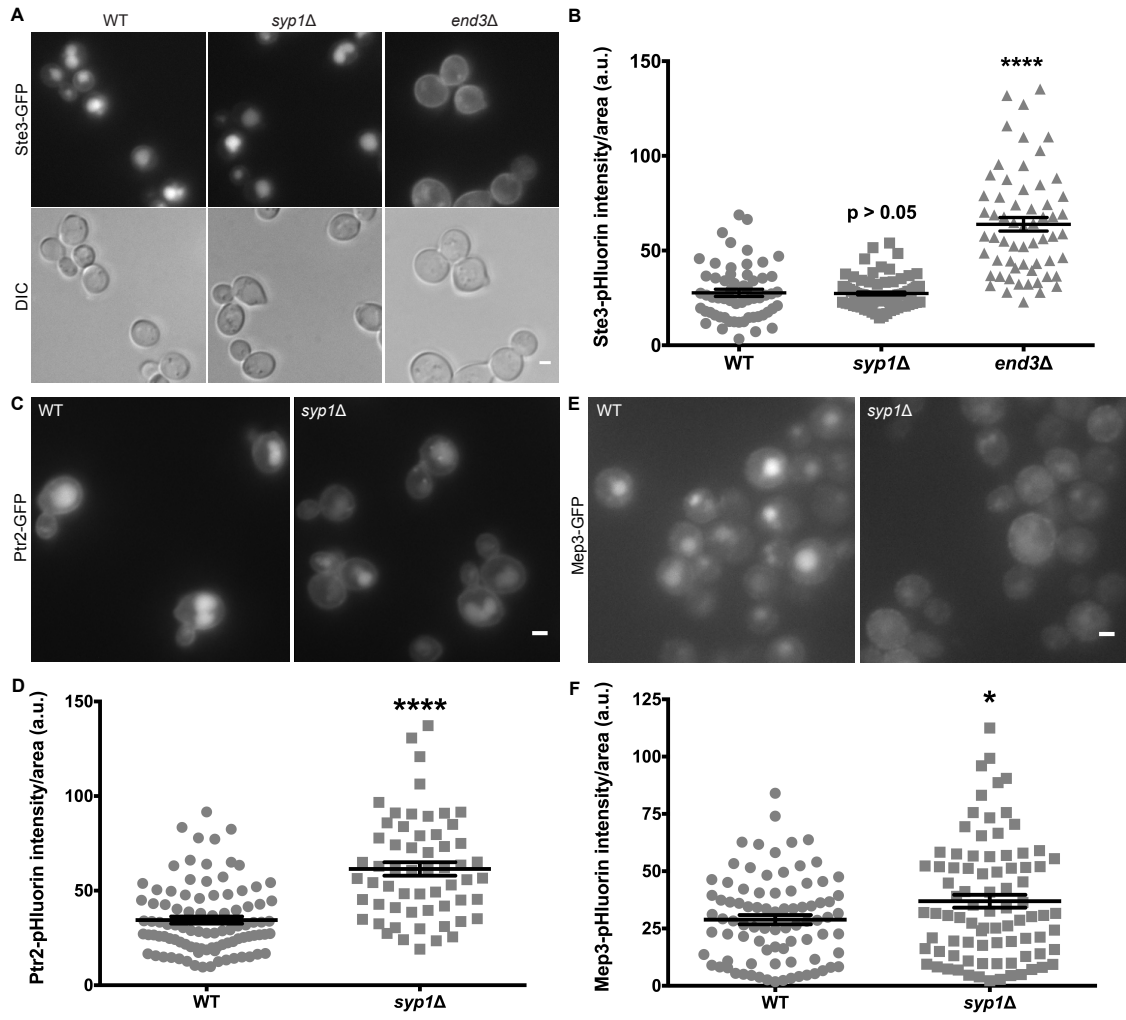
Figure 2-4. A visual screen reveals Ptr2 and Mep3 to be Syp1 cargos.

internalization of specific proteins. Therefore, a *syp1Δ* strain was used in our visual

screen to identify novel Syp1 cargos.

Using the commercially available Yeast GFP Library that expresses C-terminally

tagged genes (Huh *et al.*, 2003), we selected the complete set of 203 proteins with at least

one predicted transmembrane domain that have reported localization to one or more

regions of the cell along the endocytic route: periphery, bud neck, endosomes, and

vacuoles; these proteins represent the set of possible Syp1-dependent cargos (Table S2-

1). Strains expressing GFP-tagged proteins were mated with *syp1Δ* cells, sporulated, and

the resulting haploids selected for *syp1Δ* mutants expressing the GFP fusion (Cohen and

Schuldiner, 2011). We used live-cell fluorescence microscopy to screen for proteins with

altered localization in the *syp1Δ* strain compared to WT cells.

From the screen, ten candidate Syp1 cargos were identified. The candidates were

then reconstructed in a separate genetic background strain (W303), different from the

background of the GFP collection (BY4742), to independently verify the results of the

screen (Figure 2-5A; Figure 2-4, C-F). Two proteins, Ptr2 and Mep3, continued to exhibit

notably altered localization in the absence of Syp1 after reconstruction (Figure 2-4, C-F)

and were, consequently, chosen for further investigation.

Ptr2 is a di/tripeptide transporter that functions at the PM and is a member of a

peptide transport family of proteins conserved from archaea to humans (Steiner *et al.*,

1994; Saier, 2000). Ptr2-GFP localized mainly to the vacuole in cells grown on rich

medium, with some protein also visible at the PM (Figure 2-4C). However, trafficking of

Ptr2-GFP to the vacuole was reduced in the *syp1Δ* strain, with more protein accumulating

at the PM compared to WT cells. Though decreased, endocytosis of Ptr2 was not

Figure 2-5. Most candidate cargos possess motifs potentially recognized by Syp1. (A) Reconstructed WT and *syp1Δ* cells expressing candidate cargos tagged with GFP in strain background W303 were grown on rich medium and imaged via live-cell fluorescence microscopy. Scale bar, 2 μm. (B) Full-length candidate cargo sequences were analyzed using the SPOCTOPUS membrane protein topology prediction algorithm. DxY motifs in regions of proteins that are predicted to be cytoplasmic are indicated in black; in the absence of a DxY motif in these regions, DxΦ and ExY sequences are indicated. One DxY motif residing in a region predicted to be extracellular is indicated in red (Inside: cytoplasmic, Outside: extracellular, TM-Helix: transmembrane).

Figure on following page.
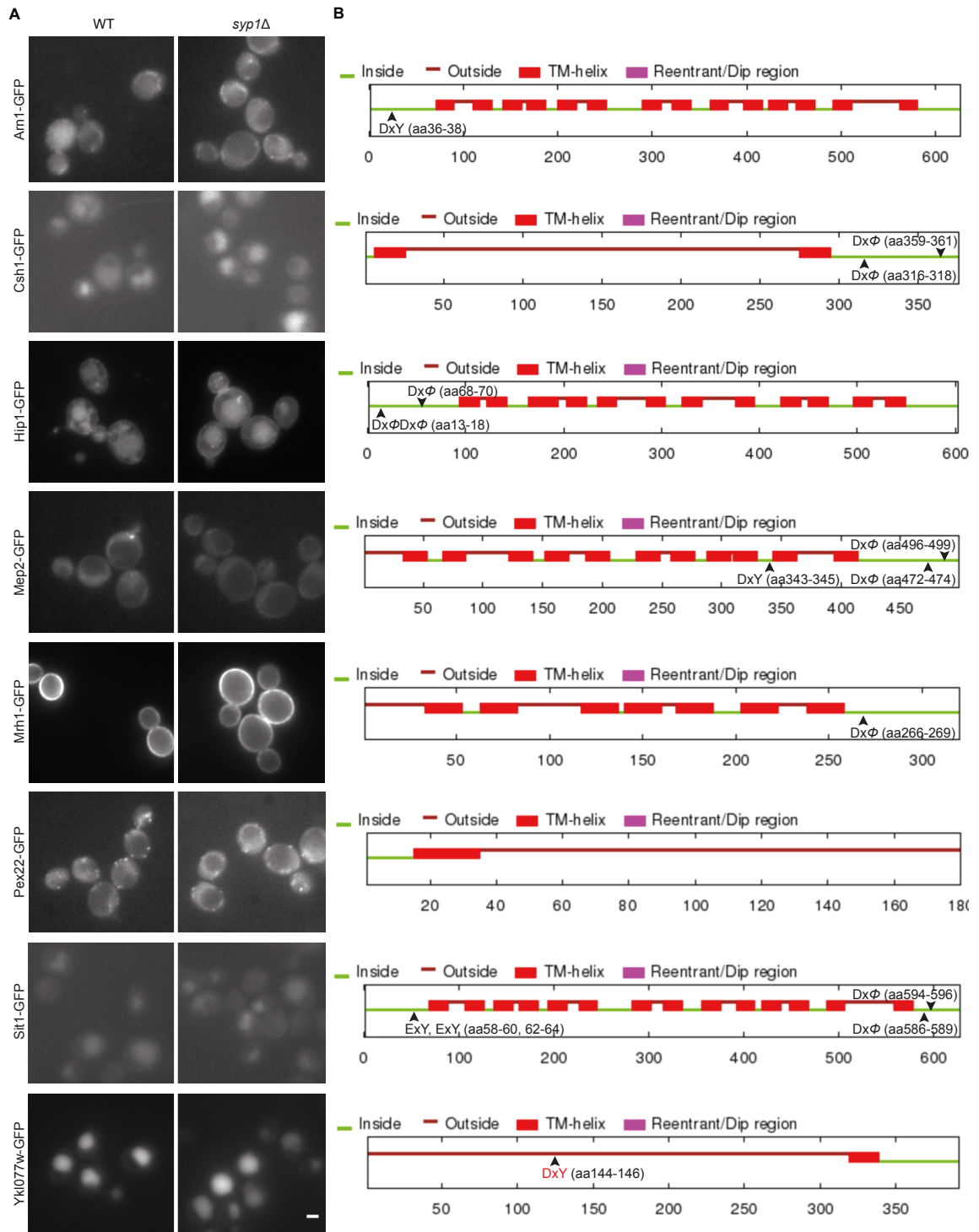
Figure 2-5. Most candidate cargos possess motifs potentially recognized by Syp1.

51

abolished in *syp1Δ* cells, indicating that there are likely additional adaptor proteins that contribute to internalization of this cargo. Quantification of Ptr2-pHluorin revealed a significant increase in Ptr2 concentration at the PM of *syp1Δ* cells compared to WT (Figure 2-4D), in agreement with findings using GFP. These results suggest that Ptr2 is a novel Syp1 cargo.

The other candidate Syp1 cargo that we chose to investigate further was the ammonium permease, Mep3 (Marini *et al.*, 1997). Ammonium-transporting Mep proteins in budding yeast share sequence homology to the Rhesus family of mammalian proteins (Heitman and Agre, 2000). Mep3-GFP localized primarily to the vacuole in a WT background when cells were grown on minimal, ammonium-rich medium; however, with the loss of Syp1, internalization of the protein was reduced, and cells exhibited diminished fluorescent signal at the vacuole (Figure 2-4E). Quantification of a Mep3-pHluorin chimera indicated that its concentration at the PM was significantly increased in a *syp1Δ* strain compared to WT cells (Figure 2-4F). This implies that Syp1 also selectively recognizes Mep3 for trafficking into the cell. Though diminished, Mep3 endocytosis continued in the absence of Syp1, suggesting that Mep3, like Ptr2, is also selected for internalization by other factors in addition to Syp1.

To rule out the possibility that differences observed in *syp1Δ* cells may not result from a loss of Syp1 function at the PM, but instead as a result of inhibiting direct Golgi-to-vacuole trafficking of cargos, we treated strains expressing fluorescently-tagged cargos with Latrunculin A (LatA). LatA inhibits the polymerization of F-actin, causing a complete block in endocytosis, but does not impair Golgi-to-vacuole transport (Ayscough *et al.*, 1997; Huang and Chang, 2011). When treated with LatA, WT cells showed a

significant increase in the amount of Ptr2 and Mep3 at the PM compared to controls

(Figure 2-6, A and B), indicating that Syp1 contributions to the localization of these

cargos is indeed due to its function at the PM.

DxY motifs mediate Syp1-dependent trafficking *in vivo*

All ten candidate Syp1 cargos possess either a DxY motif or biochemically

similar sequence, such as DxΦ or ExY. For eight of the candidates, the motifs reside in a

region of the cargo predicted to be in the cytoplasm upon analysis using the topology

prediction program, SPOCTOPUS (Viklund *et al*., 2008), specifically including several

DxY motifs (Figure 2-5B; Figure 2-7A). Notably, the two validated cargos, Mep3 and

Ptr2, contain a DxY motif, suggesting that Syp1 may promote endocytosis of an

expanded list of cargos with this sorting sequence.

The Ptr2 DxY motif (aa35-37) falls within an N-terminal region previously

predicted to reside in the cytoplasm (Hauser *et al*., 2005). The topology of Mep3,

however, is unknown. The result of the SPOCTOPUS projection for Mep3 places the

DxY sequence within a C-terminal, cytoplasmic tail (Figure 2-7A). Based on predicted

topology, DxY motifs in the cytoplasmic regions of Ptr2 and Mep3 would be accessible

for binding to the Syp1 μHD. The C-terminal DxY motif in Mep3 also permits short

truncations of the protein to test the role of the motif in Mep3 trafficking while readily

retaining the majority of the protein sequence under control of the endogenous promoter.

For this reason, we chose Mep3 over Ptr2 for further *in vivo* studies examining DxY

motifs.
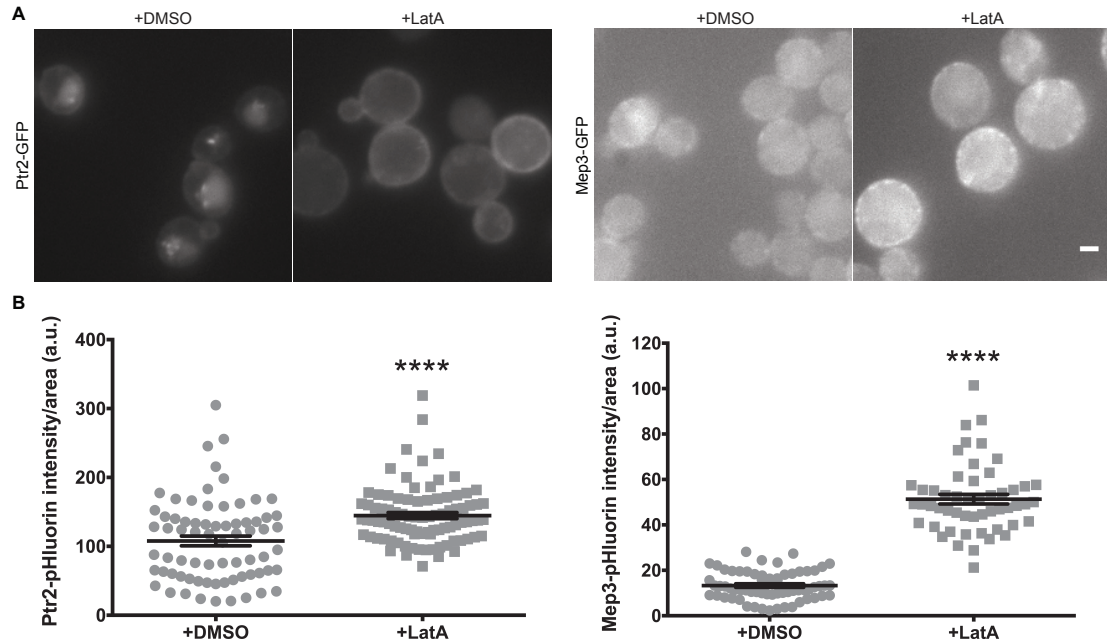
Figure 2-6. Syp1 cargos are trafficked to the PM before being delivered to vacuoles. (A) Cells expressing Ptr2-GFP or Mep3-GFP were treated with vehicle (DMSO) or Latrunculin A (LatA) prior to imaging by live-cell fluorescence microscopy. Scale bar, 2 μm. (B) Intensity of Ptr2-pHluorin or Mep3-pHluorin was quantified for each condition; intensity values were corrected for cell size and expressed in arbitrary units (a.u.) (error bars indicate mean ± SEM; ****, $P < 0.0001$ compared to WT).

Figure 2-7. A DxY motif contributes to Mep3 trafficking. (A) Full-length Mep3 sequence was analyzed using the SPOCTOPUS membrane protein topology prediction algorithm. The DxY motif (aa431-433) is indicated (Inside: cytoplasmic, Outside: extracellular, TM-Helix: transmembrane). (B) Localization of Mep3-GFP in WT or *syp1Δ* cells transformed with empty high-copy vector, high-copy *SYP1*, or high-copy *SYP1* lacking the μHD was examined by live-cell fluorescence microscopy. Scale bar, 2 µm. (C) Fluorescence intensity from cells expressing Mep3-pHluorin was quantified for each condition; intensity values were corrected for cell size and expressed in arbitrary units (a.u.; error bars indicate mean ± SEM; *, P < 0.05; ****, P < 0.0001 compared to WT). (D) Cells expressing full-length Mep3-GFP, Mep3$^{\Delta 430}$-GFP, or Mep3$^{\Delta 433}$-GFP in WT and *syp1Δ* backgrounds were grown on minimal medium and imaged via live-cell fluorescence microscopy. Scale bar, 2 µm. (E) Intensity of Mep3-pHluorin for each condition was quantified; intensity values were corrected for cell size and expressed in arbitrary units (a.u.) (error bars indicate mean ± SEM; *, P , 0.05; ****, P < 0.0001 compared to WT).

Figure on following page.
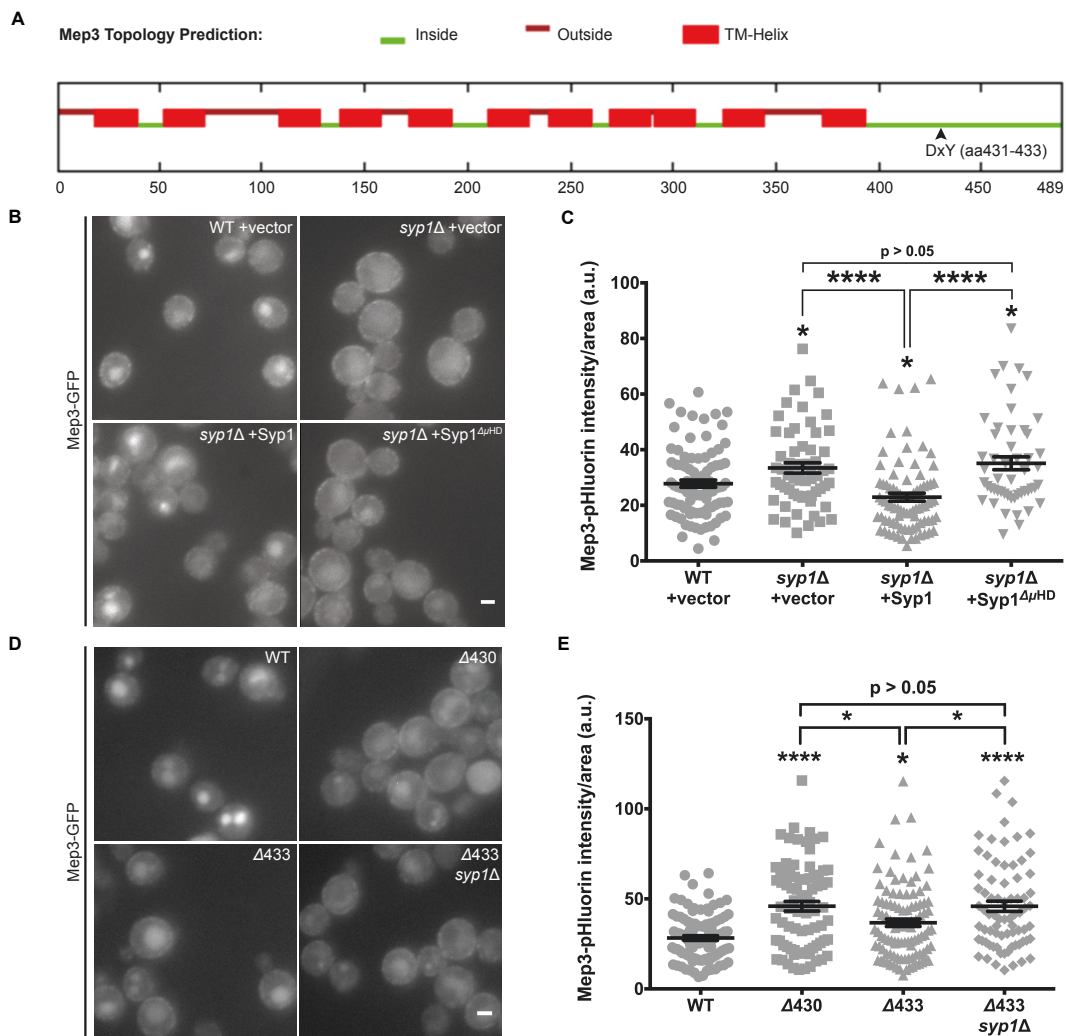
Figure 2-7. A DxY motif contributes to Mep3 trafficking.

We previously demonstrated that the Syp1 μHD is specifically responsible for

binding to and internalizing Mid2 (Reider *et al.*, 2009). In order to demonstrate that this

is true for Syp1 internalization of Mep3, we introduced full-length *SYP1* on a high-copy

plasmid, as well as a truncated form in which the μHD is absent, into *syp1Δ* cells

expressing genomically-encoded Mep3-GFP. Therefore, the plasmid-borne *SYP1* was the

sole source of Syp1 protein in this experiment. As expected, high-copy expression of full-

length *SYP1* rescued Mep3 internalization and significantly decreased the amount of

Mep3-GFP or Mep3-pHluorin at the PM below WT levels (Figure 2-7, B and C).

However, high-copy expression of truncated Syp1 lacking the μHD did not rescue the

endocytic defect. Instead, Mep3-GFP remained primarily at the PM, comparable to the

syp1Δ strain with empty vector. This result demonstrates that Mep3 behaves similarly to

the previously identified cargo, Mid2, and suggests that the Syp1 μHD is required for

internalization of both cargos.

We next utilized a truncation approach to assess the role of the DxY motif in

Mep3 trafficking. When Mep3 was truncated in an otherwise WT background by placing

a fluorescent tag just N-terminal to its DxY motif (aa431-433), thereby removing the

sorting signal and all downstream residues, the truncated Mep3$^{\Delta430}$ protein (aa1-430)

displayed significantly diminished trafficking to the vacuole and increased retention at

the PM (Figure 2-7, D and E). The localization of Mep3$^{\Delta430}$-GFP to the PM supports

results of the topological prediction that the Mep3 DxY motif resides within a

cytoplasmic region of the protein; if the DxY motif were located within an extracellular

region of Mep3, the GFP tag would translocate to the ER lumen during protein synthesis,

which presents a challenging environment for GFP folding in many contexts and can lead to aberrant retention in the ER (Jain *et al.*, 2001).

In addition, we constructed a Mep3 truncation, Mep3$^{\Delta433}$ (aa1-433), in which the DxY motif is retained, but all downstream residues are replaced with a GFP tag. Imaging and results of pHluorin quantification for this truncation demonstrated that the inclusion of these three amino acids partially, yet significantly, rescued trafficking of the Mep3$^{\Delta430}$ mutant (Figure 2-7, D and E). There are several possibilities as to why the rescue of Mep3 truncation endocytosis by reintroduction of the DxY motif was incomplete. For example, additional sorting signals regulating internalization of this cargo are present within the sequence downstream of the DxY motif; this would not be unexpected due to the existence of Syp1-independent mechanisms of Mep3 endocytosis (Figure 2-4, E and F). Deletion of *SYP1* abolished the rescue observed with reintroduction of the DxY motif, demonstrating that Syp1 is responsible for DxY-mediated rescue of Mep3 internalization in this experiment. Overall, these results indicate that a DxY motif affects Syp1 trafficking of Mep3 *in vivo*.

A similar experiment was performed for Mid2 in which truncations with (Mid2$^{\Delta289}$-GFP) and without (Mid2$^{\Delta286}$-GFP) the DxY motif were tested for internalization in cells expressing high-copy *SYP1* (Figure 2-2D). Results regarding the role of the DxY motif in Mid2 trafficking were inconclusive; many cells expressing Mid2$^{\Delta289}$-GFP, which includes the DxY motif, failed to induce trafficking of this Mid2 truncation to the vacuole. This highlights the usefulness of the alternative cargos identified in the visual screen. However, we observed that Mid2$^{\Delta286}$-GFP, which lacks the DxY motif and downstream C-terminus, but retains the Mid2 WW/Y and YxxΦ motifs,

exhibited decreased internalization even in the presence of high-copy Syp1, supporting the conclusion that these sequences do not contribute to Mid2 recognition by Syp1.

Ammonium-induced trafficking of Mep3 is interrupted in *syp1Δ* cells

In our examinations of Mep3-GFP localization, we observed that the localization of this protein is sensitive to changes in growth medium. Mep3 remained primarily at the PM during growth in nutrient-rich conditions but localized mainly to the vacuole on minimal, ammonium-rich medium. In yeast, many nutrient permeases are internalized under conditions of high extracellular ligand concentrations (Conrad *et al*., 2014); thus, we tested whether Mep3 internalization could be induced in response to ammonium. In an attempt to observe Mep3-GFP trafficking over time, cells were grown in rich conditions with a low ammonium concentration and shifted to minimal medium with high levels of ammonium.

Unlike cells grown continuously in low-ammonium (rich) conditions, those grown in high-ammonium (minimal) medium displayed trafficking of Mep3-GFP to the vacuole after four hours (Figure 2-8A). pHluorin quantification was precluded due to length of the time course being longer than a cell division cycle (Prosser *et al*., 2016), raising concern for dilution of pHluorin-tagged protein upon formation of daughter cells. However, Mep3-GFP remained almost entirely at the PM of cells grown in rich medium, in contrast to the internalization observed in response to ammonium.

To determine if trafficking of Mep3 in response to high ammonium concentration requires Syp1, we performed an experiment in which both WT and *syp1Δ* cells grown in rich conditions were treated with minimal, high-ammonium medium (Figure 2-9A). We
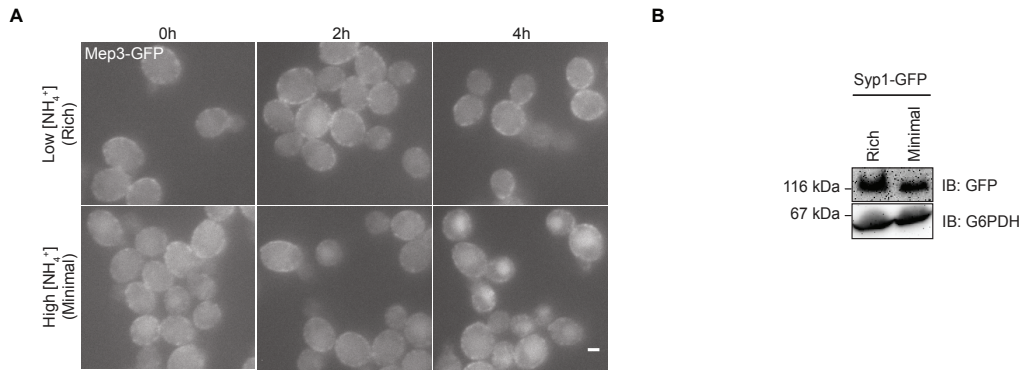
Figure 2-8. Mep3 is internalized under high ammonium conditions. (A) WT cells were grown in nutrient-rich (YPD) medium and resuspended in either fresh YPD or ammonium-rich, minimal (YNB) medium. Cells were imaged every two hours via live-cell fluorescence microscopy. Scale bar, 2 μm. (B) TCA precipitations of total protein from log phase cells expressing Syp1-GFP grown on rich or minimal medium were resolved by SDS-PAGE. Immunoblotting using anti-GFP antibody, or anti-glucose-6-phosphate dehydrogenase (G6PDH) antibody as a loading control, was then performed.

Figure 2-9. Ammonium-induced trafficking of Mep3 is interrupted in *syp1Δ* cells. (A) WT and *syp1Δ* cells were grown to mid-logarithmic phase in rich medium (YPD), and were then resuspended in minimal medium (YNB). Cells were imaged every two hours via live-cell fluorescence microscopy. Scale bar, 2 μm. (B) WT and *syp1Δ* cells at 0- and 4-hour time points post-shift to high ammonium medium were categorized as having strong, moderate, or weak/absent localization of Mep3-GFP to the vacuole (black, gray, and white bars, respectively; ***, $P < 0.001$; each mutant phenotypic class per time point was compared to its respective WT class of the same time point). (C) Cells expressing Syp1-GFP and Ede1-GFP were grown on either rich medium or high ammonium-containing minimal medium and imaged via live-cell fluorescence microscopy. Scale bar, 2 μm. (D) Intensity of Syp1- or Ede1-GFP fluorescence per cell was quantified for each condition; intensity values were corrected for cell size and expressed in arbitrary units (a.u.) (error bars indicate mean ± SEM; ***, $P < 0.001$; ****, $P < 0.0001$ compared to WT).

Figure on following page.
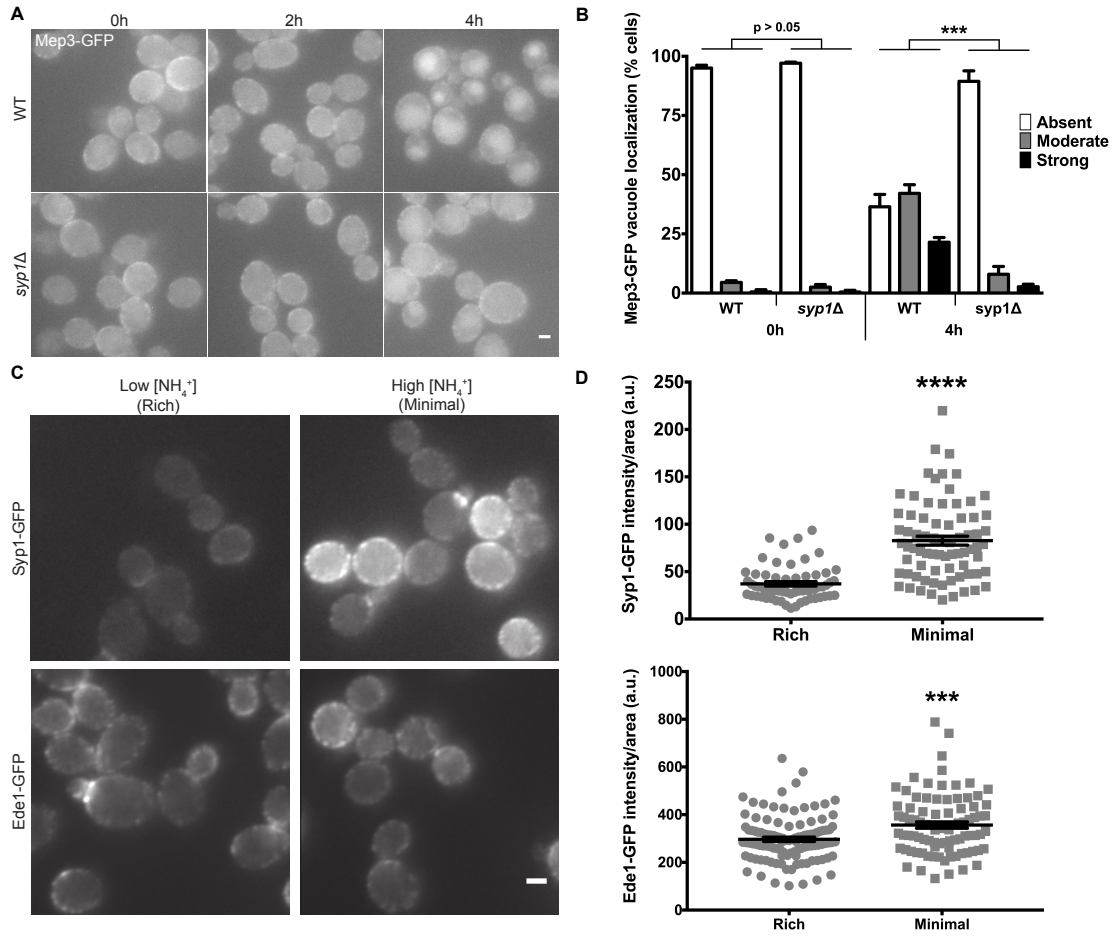
Figure 2-9. Ammonium-induced trafficking of Mep3 is interrupted in *syp1Δ* cells.

quantified trafficking by categorizing cells as having either strong, moderate, or weak/absent localization of Mep3-GFP to the vacuole (Figure 2-9B). Both strains displayed a similar predominance of Mep3-GFP at the PM at the start of the time course (0 h), with no obvious differences between WT and $syp1\Delta$ cells. Conversely, at four hours post-shift to ammonium-rich medium, the WT strain exhibited greater trafficking of Mep3-GFP into the cell than the $syp1\Delta$ strain for all three localization classes. These results indicate that the ammonium-induced internalization of Mep3-GFP is Syp1-dependent.

We hypothesized that altered Mep3 trafficking under different growth conditions might result from changes in the expression of Syp1 or amount of Syp1 at sites of CME. To examine this possibility, we grew cells expressing Syp1-GFP in either rich or minimal, high-ammonium medium. The intensity of Syp1-GFP punctae at the PM appeared brighter in cells grown on minimal medium compared to rich (Figure 2-9C). This condition-dependent change in fluorescence was greater for Syp1-GFP than Ede1-GFP, which, along with Syp1, is the earliest-arriving protein to nascent CME events in yeast.

Quantification of cells expressing each chimeric protein demonstrated that the fluorescence intensity of Syp1- and Ede1-GFP increased on minimal medium; however, the enhancement was greater for Syp1 compared to Ede1 (Figure 2-9D). These data indicate that, although the earliest-arriving CME factors appear to exhibit generally increased levels at endocytic sites in cells grown with minimal media, the intensity of Syp1 fluorescence is elevated to a greater extent under these conditions.

To determine if the increased Syp1-GFP intensity during growth on minimal medium is due to an altered level of Syp1 expression, as opposed to changes in recruitment to endocytic sites, we examined the total amount of Syp1-GFP in cells grown in rich and minimal medium. Immunoblotting against Syp1-GFP with anti-GFP antibodies, demonstrated that the growth on rich media did not decrease cellular levels of Syp1 (Figure 2-8B). Together, these data suggest that enhanced Syp1-mediated trafficking of Mep3 in cells exposed to high levels of ammonium is due to increased concentration of Syp1 at sites of CME.

Ptr2 can be trafficked via Rho1-mediated clathrin-independent endocytosis

Previous studies established that Syp1 and its homologue, FCHo1, are involved in the initiation and regulation of CME, and that Syp1 acts as an adaptor to internalize cargo (Boettner *et al.*, 2009; Stimpson *et al.*, 2009; Reider *et al.*, 2009; Henne *et al.*, 2010). However, an exclusive role for Syp1 in clathrin-mediated cargo internalization has not been demonstrated. Notably, the Syp1 cargo, Mid2, plays a role in activation of Rho1-mediated CIE (Prosser *et al.*, 2011), suggesting that Syp1 may have additional functions in cargo trafficking via CIE.

To evaluate the role of CME in Syp1-mediated internalization, we tagged cargos in *end3Δ* strains in which CME is disrupted. We first tested the ability of high-copy Syp1 to promote internalization of Mid2 from PM to vacuole in *end3Δ* cells. As expected, high-copy expression of *SYP1* in WT cells increased trafficking of Mid2 to the vacuole (Reider *et al.*, 2009; Figure 2-10A), whereas Syp1-dependent internalization was blocked in *end3Δ* cells, suggesting that Mid2 is a CME-specific cargo despite its role in activating

64

Figure 2-10. Syp1 traffics cargo via CME and Rho1-dependent CIE. (A) WT and *end3Δ* cells expressing Mid2-GFP were transformed with either an empty or *SYP1*-containing high-copy vector and imaged via live-cell fluorescence microscopy. Scale bar, 2 μm. (B) WT and *end3Δ* cells expressing GFP-Snc1 were transformed with either an empty or *SYP1*-containing high-copy vector and imaged via live-cell fluorescence microscopy. Scale bar, 2 μm. (C) Cells expressing Ptr2-pHluorin were grown on rich medium (YPD) with or without 1M sorbitol. Scale bar, 2 μm. (D) WT and *end3Δ* cells expressing Ptr2-GFP were transformed with either an empty or *ROM1*-containing high-copy vector and imaged via live-cell fluorescence microscopy. Scale bar, 2 μm. (E) Intensity of Ptr2-pHluorin was quantified for each condition; intensity values were corrected for cell size and expressed in arbitrary units (a.u.) (error bars indicate mean ± SEM; ****, P < 0.0001 compared to WT). (F) WT and *end3Δ* cells expressing Ptr2-GFP were transformed with either an empty, *ROM1*-, or *SYP1*-containing high-copy vector, grown in selective media containing protease inhibitors, and imaged via live-cell fluorescence microscopy. Scale bar, 2 μm.

Figure on following page.
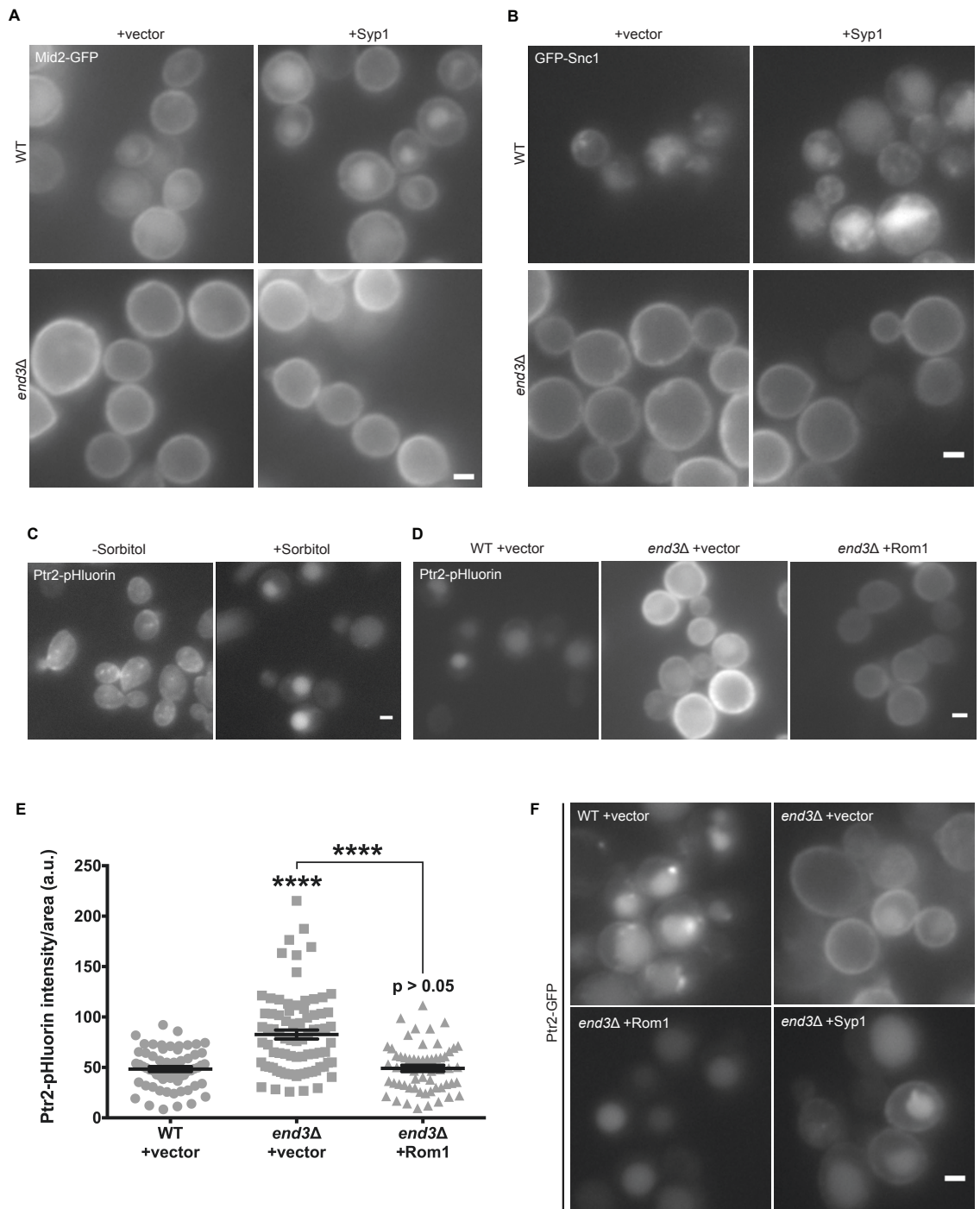
Figure 2-10. Syp1 traffics cargo via CME and Rho1-dependent CIE.

Rho1-dependent CIE. Similarly, the results of an experiment with Snc1, in which the internalization of GFP-Snc1 in cells with high-copy *SYP1* was disrupted by the loss of End3, lead to the conclusion that this cargo is also trafficked predominantly via CME (Figure 2-10B).

We utilized the same strategy for determining the role of CME in the internalization of our newly identified Syp1 cargos, Mep3 and Ptr2. In *end3Δ* cells, both Mep3 and Ptr2 trafficking was largely blocked, compared to WT, leading to their accumulation at the PM (Figure 2-11, A-C). These results indicate that CME contributes predominantly to the internalization of Syp1 cargos identified by the visual screen as well. However, Ptr2 displayed continued trafficking into cells despite the CME deficiency (Figure 2-11A, arrows), a phenotype that was not observed for other cargos in an *end3Δ* mutant.

To determine if Rho1-dependent CIE may be responsible for continued Ptr2 trafficking in CME mutants, we grew cells expressing Ptr2-GFP in the presence of 1 M sorbitol, which has been shown to upregulate CIE in yeast (Prosser et al, 2011). Trafficking of Ptr2-GFP into *end3Δ* cells was improved by the addition of sorbitol to the medium (Figure 2-11A). In contrast, Mep3 showed only subtle improvement in endocytosis with osmotic support. This result suggests that the rescue of internalization by osmotic support is more specific to Ptr2. Unfortunately, the addition of sorbitol to the growth medium inhibits pHluorin quenching within vacuoles, barring the use of pHluorin chimeras for quantification of endocytosis (Figure 2-10C; D. Prosser, unpublished results). Thus, we utilized the same approach of counting the proportion of cells with strong, moderate, or weak/absent vacuole fluorescence as in previous experiments. We

Figure 2-11. Ptr2 can be trafficked via clathrin-independent endocytosis. (A) Cells expressing Mep3-GFP or Ptr2-GFP and lacking End3 were grown on rich medium alongside WT strains in the absence or presence of osmotic support (1M sorbitol) and imaged by fluorescence microscopy. Arrows indicate cells with internalized Ptr2-GFP. Scale bar, 2 μm. (B) Intensity of Mep3-pHluorin was quantified; intensity values were corrected for cell size and expressed in arbitrary units (a.u.) (error bars indicate mean ± SEM; **, P < 0.01 compared to WT). (C) Intensity of Ptr2-pHluorin was quantified; intensity values were corrected for cell size and expressed in arbitrary units (a.u.) (error bars indicate mean ± SEM; ****, P < 0.0001 compared to WT). (D) For each condition, Ptr2-GFP expressing cells were quantified as having a strong, moderate, or weak/absent vacuolar signal, and the percentage in each category was plotted (error bars indicate mean ± SD; n = 2; *, P < 0.05; **, P < 0.01; ***, P < 0.001 compared to WT). (E) WT, *bni1Δ*, and *bnr1Δ* cells expressing Ptr2-GFP were grown on rich medium and imaged by fluorescence microscopy. Scale bar, 2 μm. (F) Intensity of Ptr2-pHluorin was quantified for each condition; intensity values were corrected for cell size and expressed in arbitrary units (a.u.) (error bars indicate mean ± SEM; *, P < 0.05 compared to WT).

Figure on following page.
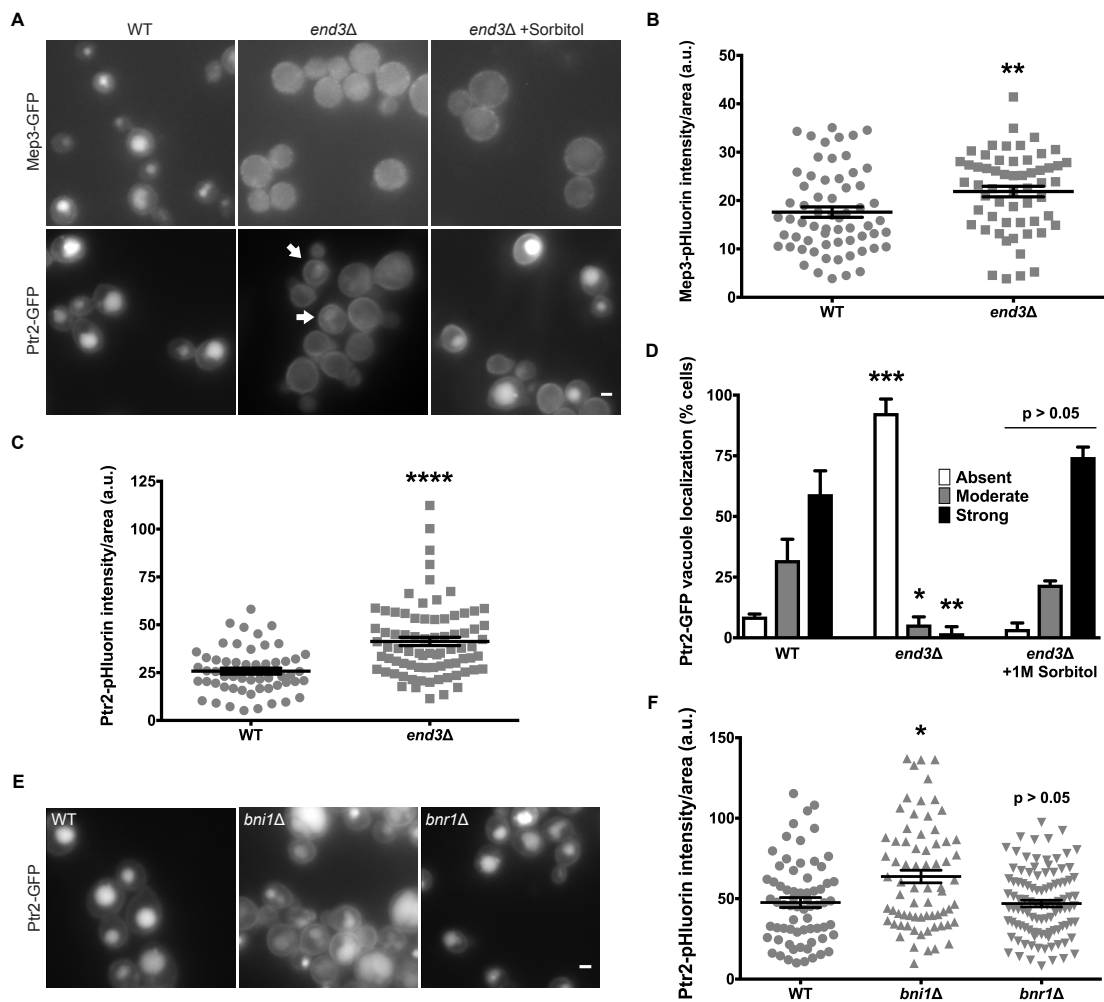
Figure 2-11. Ptr2 can be trafficked via clathrin-independent endocytosis.

observed that endocytosis of Ptr2-GFP in *end3Δ* cells was rescued to near WT levels by addition of sorbitol to the media (Figure 2-11D).

This result was encouraging, but the role of End3 in Rho1-dependent CIE has not yet been assessed. To address this, we expressed high-copy *ROM1*, a guanine nucleotide exchange factor for Rho1 that was shown to activate this CIE pathway in CME-deficient cells (Prosser *et al.*, 2011). High-copy *ROM1* decreased the concentration of Ptr2 at the PM in *end3Δ* cells (Figure 2-10, D and E), indicating that End3 is not involved in Rho1-dependent CIE.

Despite the rescue of Ptr2 trafficking from the PM with Rom1 overexpression, vacuoles were not visible in many of the cells. We postulated that this might be due to the outpacing of GFP degradation within the vacuole by the trafficking of Ptr2 to this compartment. To test this, we repeated the experiment with the addition of protease inhibitors to the growth medium. In the presence of protease inhibitors, the vacuoles of *end3Δ* cells expressing high-copy *ROM1* became visible (Figure 2-10F). However, many of the CME mutants possessing the empty vector exhibited no vacuolar fluorescence, similar to untreated cells (Figure 2-11A; lower, middle panel), indicating that treatment with protease inhibitors does not induce vacuolar autofluorescence. This result supports the conclusion that decreased levels of Ptr2 at the PM in CME mutant cells are due to enhanced Rho1-dependent CIE.

To further investigate a role for CIE in Ptr2 trafficking, we constructed *bni1Δ* strains expressing either GFP- or pHluorin-tagged Ptr2. Bni1 is a yeast formin that promotes elongation of linear actin filaments and is required for this CIE pathway (Pruyne *et al.*, 2002; Prosser *et al.*, 2011). In the absence of Bni1, fluorescently tagged

Ptr2 accumulated at the PM to a greater extent than in WT cells (Figure 2-11, E and F). In contrast, cells lacking Bnr1, the second yeast formin that is not involved in CIE (Prosser *et al.*, 2011), showed localization of Ptr2 chimeras that was indistinguishable from WT cells. Therefore, the accumulation of Ptr2 at the PM in a *bni1Δ* strain is not a result of altered actin regulation, but is instead due to the loss of Rho1-dependent CIE. These data suggest this CIE pathway contributes observably to Ptr2 internalization in WT cells under standard conditions.

Syp1 contributes to internalization of Ptr2 via Rho1-dependent CIE in addition to CME

Based on our observation that Ptr2 can internalize via Rho1-dependent CIE, we aimed to determine if Syp1 mediates trafficking of Ptr2 via this pathway by functioning in the Rho1-dependent CIE pathway. We introduced a high-copy plasmid containing *SYP1* into *end3Δ* cells expressing fluorescently tagged Ptr2 to test if Syp1 overexpression can rescue Ptr2 endocytosis in this CME-deficient strain. Cells lacking End3 and possessing an empty vector exhibited high levels of Ptr2 at the plasma membrane, as expected. However, in the *end3Δ* strain transformed with high-copy *SYP1*, a significant decrease in the amount of Ptr2 at the PM was observed (Figure 2-12, A and B). Ptr2 concentration within buds appeared diminished compared to mother cells, and we also noted that the buds often appeared elongated with Syp1 overexpression.

Vacuoles were not visible in many *end3Δ* cells with high-copy *SYP1*, as was observed in similar experiments with Rom1 overexpression (Figure 2-10D). However, addition of protease inhibitors to the growth medium allowed the vacuoles of cells with high-copy *SYP1* to be observed (Figure 2-10F). The results of this experiment support the

Figure 2-12. Syp1-mediated internalization of Ptr2 occurs via CIE in addition to CME. (A) WT and *end3Δ* cells expressing Ptr2-GFP were transformed with either an empty or *SYP1*-containing high-copy vector and imaged via live-cell fluorescence microscopy. Scale bar, 2 μm. (B) Intensity of Ptr2-pHluorin was quantified for each condition; intensity values were corrected for cell size and expressed in arbitrary units (a.u.) (error bars indicate mean ± SEM; ****, $P < 0.0001$ compared to WT). (C) WT and *end3Δ* cells expressing Sla2-GFP and Abp1-mCherry were transformed with either an empty or *SYP1*-containing high-copy vector and imaged via live-cell fluorescence microscopy. Maximum intensity projection images generated from Z stacks are shown. Scale bar, 2 μm. (D) Cells expressing Ptr2-GFP in WT, *end3Δ*, *end3Δ syp1Δ*, or *end3Δ bni1Δ* strains were grown on rich medium in the presence or absence of 1M sorbitol and imaged by fluorescence microscopy. Scale bar, 2 μm.
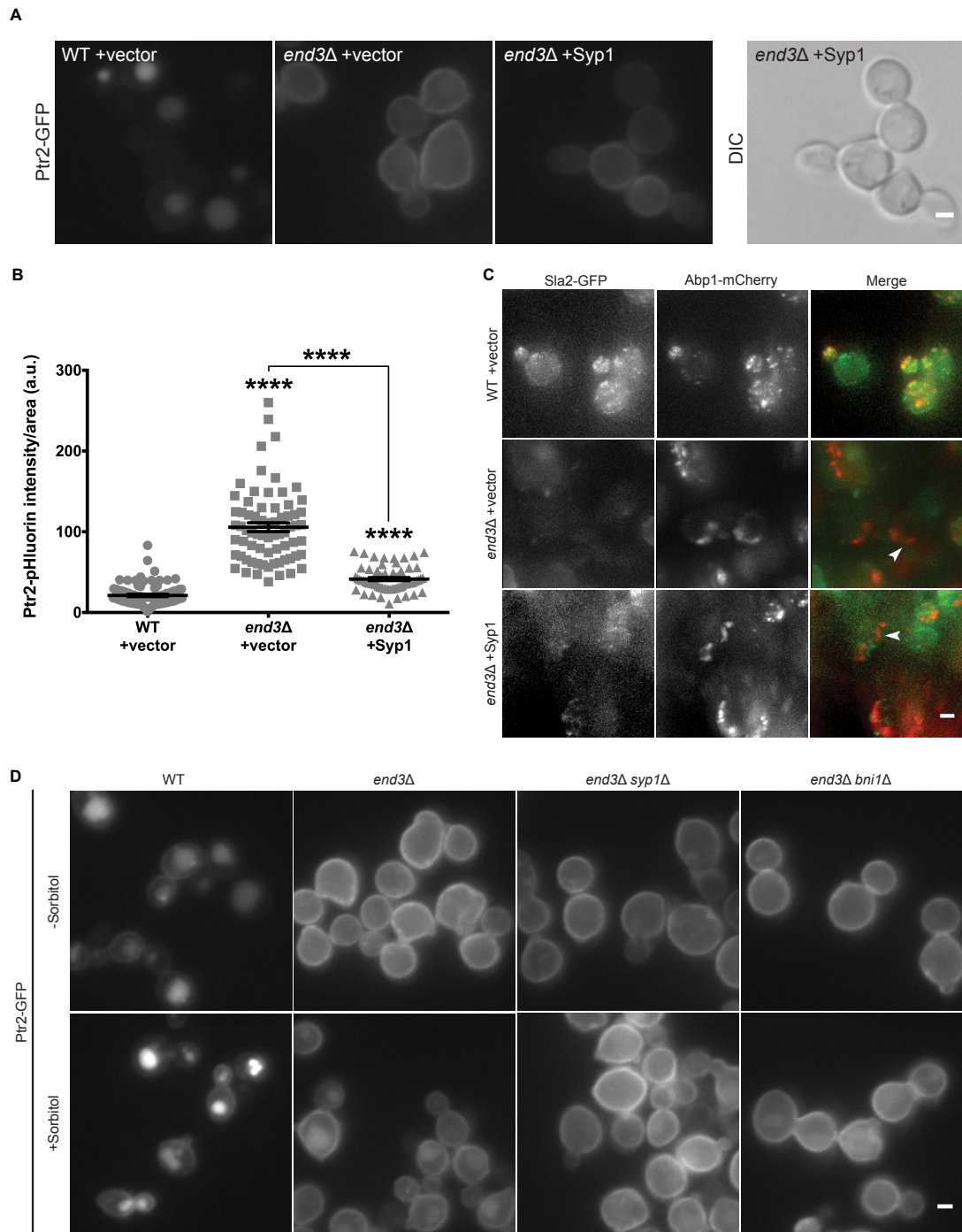
Figure 2-12. Syp1-mediated internalization of Ptr2 occurs via CIE in addition to CME.

conclusion that decreases in Ptr2 levels at the PM in these studies are indeed the result of upregulated cargo trafficking into the cell.

To confirm that high-copy *SYP1* restores Ptr2 endocytosis in *end3Δ* cells via CIE, and not by upregulating CME, we investigated the effect of high-copy *SYP1* on actin patches associated with CME; previous experiments showed that cortical actin patches are larger and fewer in *end3Δ* cells (Bénédetti *et al*., 1994). We examined *end3Δ* cells expressing a GFP-tagged CME protein, Sla2, as well as Abp1-mCherry, an F-actin binding protein that marks actin patches, in the presence and absence of high-copy *SYP1*. As previously reported, actin patches in *end3Δ* cells with empty vector appeared to be larger and fewer in number compared to those in a WT strain (Figure 2-12C), as well as less dynamic (Videos 1-3). Structures similar to actin comet tails, which are observed in many endocytic mutants (Kaksonen *et al*., 2005; Newpher and Lemmon, 2006; Prosser *et al*., 2011; Bradford *et al*., 2015), were also seen in the absence of End3, and these mutant phenotypes were not rescued by high-copy *SYP1* (Figure 2-12C, arrowheads; Videos 2 and 3).

We also tested the ability of osmotic support to rescue Ptr2 endocytosis in an *end3Δ* strain lacking functional Rho1-dependent CIE. Ptr2 internalization in an *end3Δ* strain was improved by the addition of sorbitol to the growth medium (Figure 2-12D), as shown above (Figure 2-11A). However, this enhanced trafficking was largely abolished in an *end3Δ bni1Δ* double mutant that is deficient in both CME and CIE. Additionally, we observed that high osmolarity was unable to improve Ptr2 internalization in an *end3Δ syp1Δ* strain, further suggesting that Ptr2 trafficking via both pathways is Syp1-

Video S1. WT cells expressing Sla2-GFP and Abp1-mCherry were transformed with an empty, high-copy vector. Equatorial images were taken every two seconds for two minutes; time lapse frame rate, 10 fps. Scale bar, 10 μm.

Video S2. Mutant *end3Δ* cells expressing Sla2-GFP and Abp1-mCherry were transformed with an empty, high-copy vector. Equatorial images were taken every two seconds for two minutes; time lapse frame rate, 10 fps. Scale bar, 10 μm.

Video S3. Mutant *end3Δ* cells expressing Sla2-GFP and Abp1-mCherry were transformed with a *SYP1*-containing, high-copy vector. Equatorial images were taken every two seconds for two minutes; time lapse frame rate, 10 fps. Scale bar, 10 μm.

See supplement for videos.

dependent. Together, these results indicate that Syp1 functions in Rho1-dependent CIE

and can direct Ptr2 internalization via this pathway.

Discussion

A role for cargo-sorting DxY motifs in endocytosis

DxY motifs appear to be a common feature of Syp1 cargos, important for recognition and trafficking into the cell; however, DxY was not the most abundant motif present in the phage display peptides. We anticipated the presence of clues regarding the mechanism of physical interaction between Syp1 and its higher-affinity binding partners such as Ede1, which also binds to the region of Syp1 used in the phage display screen (Reider *et al*., 2009). The large number of WW sequences may be one such indicator, pointing to a separate mechanism dependent on a hydrophobic interaction.

Syp1 may also recognize similar sequences, such as ExY or DxΦ, although we have not yet tested roles for these variants. All of the candidate cargos that do not possess a DxY motif have a biochemically similar sequence, most of which reside within a predicted cytoplasmic region of the protein. The Snc1$^{63-93}$ fragment, which binds Syp1 but does not include a DxY motif, contains a DxΦ sequence, DxL (aa 65-67; Figure 2-3A). This offers a potential recognition site for Syp1. This Snc1 fragment also contains a YxxΦ motif. However, it is unlikely that this motif mediates the interaction between the μHD and this portion of Snc1, since a mutation that disrupted the Snc1 YxxΦ motif still bound efficiently to the Syp1 μHD (Fig S1C).

Mep3 exhibited condition-dependent endocytic trafficking, and the mechanisms underlying precise regulation of cargo internalization in changing growth conditions will continue to be an important area of future research. PhosphoGRID data indicates that the DxY motif in Ptr2, DSY (aa35-37), can be phosphorylated on both S and Y residues, presenting the possibility that phosphoregulation mediates uptake of this cargo (Stark *et*

al., 2010); controlled trafficking of protein cargos by the μ subunit of AP-2 has been observed in mammalian cells (Rapetti-Mauss *et al*., 2013).

The ability of mammalian Syp1 orthologs to recognize DxY motifs has not yet been tested. The Mep3 and Ptr2 orthologs, RhAG and PepT1, respectively, do not contain DxY motifs but do have DxΦ motifs; it will be interesting to see if similar interactions between these transporters and FCHo1/2 or SGIP1 occur in mammalian cells. DxΦ sequences are also present in the Ptr2-related protein, PepT2, which possesses a DxY motif as well (aa217-219), and in the FCHo1 cargo, Alk8.

Although this study focused on the role of DxY motifs in cargo sorting, biochemically similar sequences also appear to be important for interactions between components of the endocytic machinery. In addition to the role in cargo sorting, DPF motifs are also present in many endocytic proteins such as Eps15, auxilin, amphiphysin, AP180/PICALM, synaptojanin, and HIP1 (Owen *et al*., 1999). Recent investigations have demonstrated that the μHD of FCHo1 binds consecutive DPF motifs in Eps15, the homologous domain of FCHo2 interacts with DPF motifs in Dab2, and the μHD of SGIP1 binds successive DPF motifs as well (Ma *et al*., 2016; Mulkearns and Cooper, 2012; Shimada *et al*., 2016). Together, this suggests that DxY and/or DxΦ motifs may play a ubiquitous role in muniscin-cargo interactions.

Future studies will aim to identify further cargo-sorting motifs recognized by muniscins and pinpoint their potentially separate cargo-binding sites, as well as reveal additional cargos of these adaptors.

Trafficking of Snc1 and its mammalian ortholog, VAMP2 (synaptobrevin)

The large number of adaptor proteins that are known to participate in SNARE endocytosis highlights the importance of SNARE regulation in maintaining cellular physiology (Maritzen *et al*., 2012). Syp1 is the first adaptor protein observed to bind Snc1 at two sites (Figure 2-3, D and E), one within and one outside of the SNARE motif, leading to the prediction that Syp1 plays a unique role in Snc1 internalization. Snc1[1-27] is predicted to be unstructured (Strop *et al*., 2008).

Binding of adaptor proteins to the SNARE motif of SNAREs, which is primarily reserved for association with the other SNARE complex members (e.g. syntaxin/SNAP-25 in mammals), was once thought to be uncommon (Sutton *et al*., 1998). Two recent reports reveal that this is not as unusual as originally thought. Both CALM and AP180 were shown to traffic and interact with several VAMP family proteins through direct interaction of the AP180/CALM ANTH domain with the N-terminal half of the SNARE motif (Koo *et al*., 2011; Miller *et al*., 2011). Together with our data, these results suggest a novel mechanism of SNARE motif-dependent endocytic sorting.

Since Syp1 and the other SNARE motif-binding adaptors associate with v-SNAREs at the sites of SNARE-SNARE interaction, it is likely that NSF-mediated disassembly of cis-SNARE complexes will be a prerequisite for Syp1 and AP180/CALM-mediated endocytic recycling of Snc1 and the VAMPs, and that the SNARE motif binding site only becomes accessible to Syp1 after NSF-mediated dissociation. However, Syp1 also binds to a region outside of the SNARE motif, making the range of Syp1-Snc1 interactions an interesting subject of future research.

Identifying additional cargos of Syp1

Approximately five percent of the complete set of potential cargo proteins tested in the visual screen were identified as candidate Syp1 cargos, and only one percent were successfully confirmed as *bona fide* cargos of this adaptor after testing the Syp1-dependence of candidates in multiple genetic backgrounds. It is likely that additional Syp1 cargos exist that were not detected using this approach, potentially including those candidates that did not appear to be true cargo proteins upon validation of results from the visual screen.

There are many possibilities as to why only a fraction of the tested proteins appeared to exhibit Syp1-dependent localization. One such reason is redundancy in cargo protein recognition by other endocytic adaptors, which might become increasingly common when the preferred adaptor is absent and cargo concentration at the PM begins to rise. Moreover, ubiquitination is a major signal for cargo internalization in yeast, and binding of Epsin/AP180 proteins, which are the primary endocytic adaptors in yeast, occurs largely via recognition of ubiquitinated cargo (Polo *et al*., 2002; Shih *et al*., 2002). The absence of Syp1 in combination with other adaptors may reveal additional cargos.

Alternatively, the findings in one recent study allows for the possibility of sequential binding by FCHo1/2 and other adaptors to explain the lack of complete penetrance of *syp1* mutant cargo trafficking phenotypes (Ma *et al*., 2016). Additionally, a C-terminally tagged protein library was used in this screen; therefore, it is possible that some Syp1 cargos are unable to support modifications at their C-terminus. Use of newly available N-terminal libraries may reveal further cargo proteins in cases where a C-terminal GFP tag impedes internalization (Yofe *et al*., 2016).

Finally, subtle differences in cargo trafficking between WT and *syp1Δ* strains may not be visible using GFP and, instead, would only become apparent upon pHluorin quantification or overexpression of Syp1, as seen for Mid2 and Snc1 (Reider *et al.*, 2009; Figure 2-3B). Growth under altered conditions may also affect cellular requirements for the function and localization of a particular cargo, during which Syp1-dependent regulation may become more observable. This was true for Mep3, which exhibited a more pronounced Syp1-dependent internalization on medium containing high levels of ammonium (Figure 2-9, A and B). Testing a wider range of growth conditions might also reveal roles for Syp1 in endocytosis of other proteins. Similar visual screens for changes in cargo localization might provide analogous information for other adaptors as well.

Role of multiple endocytic pathways in Syp1-mediated cargo internalization

Budding yeast possess a Rho1-dependent CIE pathway (Prosser *et al.*, 2011); however, few cargos that can be trafficked via this pathway have been identified. Additionally, experiments revealing components of the Rho1-dependent CIE machinery have largely relied on overexpression of CIE factors to demonstrate the endocytosis of cargo. This is consistent with these cargos being preferentially internalized via CME, while also possessing the capacity for uptake via CIE.

We observed partial defects in endocytosis of Ptr2 by simply inactivating CIE (Figure 2-11, E and F), suggesting that Ptr2 is the first known dual cargo, exhibiting a contribution from CIE for its internalization under standard conditions. Thus, Ptr2 may become a powerful tool for future analysis of CIE mechanisms. Although CIE does not appear to contribute to Mep3 endocytosis, it is possible that other Syp1 cargos behave

similarly to Ptr2 and are trafficked via CIE as well. The discovery of additional Syp1 cargos may not only shed light on the function of Syp1, but also on roles for CIE.

Evidence that Ptr2 is partially internalized via CIE, and that high-copy expression of *SYP1* can induce trafficking via this pathway, indicates that Syp1 is among the first adaptors linked to both CME and CIE mechanisms. It is possible that Syp1 localizes to two distinct sets of endocytic sites, helping to establish those corresponding to nascent CME and CIE events. Syp1 may be recruited to sites of CIE via physical interaction with Mid2 when cargos are signaled for internalization via this pathway. Our results suggesting a role in both pathways make Syp1 an important regulator of yeast endocytosis.

Materials and Methods

Strains and plasmids

A complete list of strains and plasmids used in this study can be found in Table 2-1 and Table 2-2, respectively. Strains were constructed using PCR-based genomic integration as described previously (Longtine *et al.*, 1998; Goldstein and McCusker, 1999; Nishimura *et al.*, 2009). For genomic integration of GFP or pHluorin, we designed primers using the F2 and R1 plasmid-specific sequences (Longtine *et al.*, 1998). Transformations were performed according to standard procedures using the lithium acetate method, and integrations were confirmed by colony PCR and/or Western immunoblotting (data not shown).

Phage display screen

Phage display 12-mer peptide libraries (of random sequence) fused to the N-terminus of pVIII of M13 filamentous phage were used to select peptide ligands for GST-Syp1 μHD. Phage display selection was carried out as described previously (Tonikian *et al.*, 2007).

Protein purification

Proteins were purified as described previously (Reider *et al.*, 2009). In brief, His$_6$- and GST-tagged proteins were purified from Rosetta cells (Novagen) transformed with plasmids derived from pET28a or pGEX-KG-KAN. 0.3 mM IPTG was used to induce protein expression in these cells, which were then harvested, frozen to -80°C, and resuspended in buffer containing protease inhibitor cocktail (Roche). His$_6$-tagged protein

Table 2-1. Strains used in this chapter.

Strain	Genotype	Source
W303	*MATα ura3-1 ade2-1 his3-11 leu2,3112 trp1-1 can1-100 ade2::ADE2*	Laboratory strain
BWY3597	*MATα ura3-1 ade2-1 his3-11 leu2,3112 trp1-1 can1-100 ade2::ADE2 Ste3-GFP::KAN*	This study
BWY6376	*MATα ura3-1 ade2-1 his3-11 leu2,3112 trp1-1 can1-100 ade2::ADE2 Ste3-GFP::KAN syp1::HIS3*	This study
BWY6361	*MATα ura3-1 ade2-1 his3-11 leu2,3112 trp1-1 can1-100 ade2::ADE2 Ste3-GFP::KAN end3::NAT*	This study
BWY6002	*MATα ura3-1 ade2-1 his3-11 leu2,3112 trp1-1 can1-100 ade2::ADE2 Ste3-pHluorin::KAN*	This study
BWY6483	*MATα ura3-1 ade2-1 his3-11 leu2,3112 trp1-1 can1-100 ade2::ADE2 Ste3-pHluorin::KAN syp1::HIS3*	This study
BWY6480	*MATα ura3-1 ade2-1 his3-11 leu2,3112 trp1-1 can1-100 ade2::ADE2 Ste3-pHluorin::KAN end3::NAT*	This study
BWY5735	*MATa ura3-1 ade2-1 his3-11 leu2,3112 trp1-1 can1-100 ade2::ADE2 Ptr2-GFP::KAN*	This study
BWY6015	*MATα ura3-1 ade2-1 his3-11 leu2,3112 trp1-1 can1-100 ade2::ADE2 Ptr2-GFP::KAN syp1::HIS3*	This study
BWY6228	*MATα ura3-1 ade2-1 his3-11 leu2,3112 trp1-1 can1-100 ade2::ADE2 Ptr2-pHluorin::KAN*	This study
BWY6229	*MATa ura3-1 ade2-1 his3-11 leu2,3112 trp1-1 can1-100 ade2::ADE2 Ptr2-pHluorin::KAN syp1::HIS3*	This study
BWY6329	*MATα ura3-1 ade2-1 his3-11 leu2,3112 trp1-1 can1-100 ade2::ADE2 Mep3-GFP::KAN*	This study
BWY5744	*MATa ura3-1 ade2-1 his3-11 leu2,3112 trp1-1 can1-100 ade2::ADE2 Mep3-GFP::KAN syp1::HIS3*	This study
BWY6371	*MATa ura3-1 ade2-1 his3-11 leu2,3112 trp1-1 can1-100 ade2::ADE2 Mep3-pHluorin::KAN*	This study
BWY6375	*MATα ura3-1 ade2-1 his3-11 leu2,3112 trp1-1 can1-100 ade2::ADE2 Mep3-pHluorin::KAN syp1::HIS3*	This study
BWY5739	*MATa ura3-1 ade2-1 his3-11 leu2,3112 trp1-1 can1-100 ade2::ADE2 Arn1-GFP::KAN*	This study
BWY5740	*MATa ura3-1 ade2-1 his3-11 leu2,3112 trp1-1 can1-100 ade2::ADE2 Arn1-GFP::KAN syp1::HIS3*	This study
BWY5733	*MATa ura3-1 ade2-1 his3-11 leu2,3112 trp1-1 can1-100 ade2::ADE2 Csh1-GFP::KAN*	This study
BWY5734	*MATα ura3-1 ade2-1 his3-11 leu2,3112 trp1-1 can1-100 ade2::ADE2 Csh1-GFP::KAN syp1::HIS3*	This study
BWY5729	*MATa ura3-1 ade2-1 his3-11 leu2,3112 trp1-1 can1-100 ade2::ADE2 Hip1-GFP::KAN*	This study
BWY5730	*MATa ura3-1 ade2-1 his3-11 leu2,3112 trp1-1 can1-100 ade2::ADE2 Hip1-GFP::KAN syp1::HIS3*	This study

BWY6380	*MATα ura3-1 ade2-1 his3-11 leu2,3112 trp1-1 can1-100 ade2::ADE2 Mep2-GFP::KAN*	This study
BWY6370	*MATα ura3-1 ade2-1 his3-11 leu2,3112 trp1-1 can1-100 ade2::ADE2 Mep2-GFP::KAN syp1::HIS3*	This study
BWY5737	*MATa ura3-1 ade2-1 his3-11 leu2,3112 trp1-1 can1-100 ade2::ADE2 Mrh1-GFP::KAN*	This study
BWY5738	*MATa ura3-1 ade2-1 his3-11 leu2,3112 trp1-1 can1-100 ade2::ADE2 Mrh1-GFP::KAN syp1::HIS3*	This study
BWY5745	*MATa ura3-1 ade2-1 his3-11 leu2,3112 trp1-1 can1-100 ade2::ADE2 Pex22-GFP::KAN*	This study
BWY5746	*MATa ura3-1 ade2-1 his3-11 leu2,3112 trp1-1 can1-100 ade2::ADE2 Pex22-GFP::KAN syp1::HIS3*	This study
BWY5741	*MATa ura3-1 ade2-1 his3-11 leu2,3112 trp1-1 can1-100 ade2::ADE2 Sit1-GFP::KAN*	This study
BWY5742	*MATα ura3-1 ade2-1 his3-11 leu2,3112 trp1-1 can1-100 ade2::ADE2 Sit1-GFP::KAN syp1::HIS3*	This study
BWY6434	*MATa ura3-1 ade2-1 his3-11 leu2,3112 trp1-1 can1-100 ade2::ADE2 Ykl077w-GFP::KAN*	This study
BWY6435	*MATα ura3-1 ade2-1 his3-11 leu2,3112 trp1-1 can1-100 ade2::ADE2 Ykl077w-GFP::KAN syp1::HIS3*	This study
BWY6227	*MATα ura3-1 ade2-1 his3-11 leu2,3112 trp1-1 can1-100 ade2::ADE2 mep3(aa1-430)-GFP::KAN*	This study
BWY6757	*MATa ura3-1 ade2-1 his3-11 leu2,3112 trp1-1 can1-100 ade2::ADE2 mep3(aa1-433)-GFP::KAN*	This study
BWY6908	*MATα ura3-1 ade2-1 his3-11 leu2,3112 trp1-1 can1-100 ade2::ADE2 mep3(aa1-433)-GFP::KAN syp1::HIS3*	This study
BWY6226	*MATα ura3-1 ade2-1 his3-11 leu2,3112 trp1-1 can1-100 ade2::ADE2 mep3(aa1-430)-pHluorin::KAN*	This study
BWY6758	*MATa ura3-1 ade2-1 his3-11 leu2,3112 trp1-1 can1-100 ade2::ADE2 mep3(aa1-433)-pHluorin::KAN*	This study
BWY6910	*MATa ura3-1 ade2-1 his3-11 leu2,3112 trp1-1 can1-100 ade2::ADE2 mep3(aa1-433)-pHluorin::KAN syp1::HIS3*	This study
BWY2919	*MATa ura3-1 ade2-1 his3-11 leu2,3112 trp1-1 can1-100 ade2::ADE2 Mid2-GFP::KAN*	Reider *et al*., 2009
BWY6755	*MATa ura3-1 ade2-1 his3-11 leu2,3112 trp1-1 can1-100 ade2::ADE2 mid2(aa1-286)-GFP::KAN*	This study
BWY6756	*MATa ura3-1 ade2-1 his3-11 leu2,3112 trp1-1 can1-100 ade2::ADE2 mid2(aa1-289)-GFP::KAN*	This study
BWY3893	*MATα ura3-1 ade2-1 his3-11 leu2,3112 trp1-1 can1-100 ade2::ADE2 Syp1-GFP::KAN*	Reider *et al*., 2009
BWY3210	*MATα ura3-1 ade2-1 his3-11 leu2,3112 trp1-1 can1-100 ade2::ADE2 Ede1-GFP::KAN*	Reider et al., 2009
BWY6368	*MATα ura3-1 ade2-1 his3-11 leu2,3112 trp1-1 can1-100 ade2::ADE2 Mep3-GFP::KAN end3::NAT*	This study
BWY6396	*MATa ura3-1 ade2-1 his3-11 leu2,3112 trp1-1 can1-100 ade2::ADE2 Mep3-pHluorin::KAN end3::NAT*	This study

BWY6363	*MATa ura3-1 ade2-1 his3-11 leu2,3112 trp1-1 can1-100 ade2::ADE2 Ptr2-GFP::KAN end3::NAT*	This study
BWY6366	*MATα ura3-1 ade2-1 his3-11 leu2,3112 trp1-1 can1-100 ade2::ADE2 Ptr2-pHluorin::KAN end3::NAT*	This study
BWY6254	*MATa ura3-1 ade2-1 his3-11 leu2,3112 trp1-1 can1-100 ade2::ADE2 Ptr2-GFP::KAN bni1::NAT*	This study
BWY6387	*MATa ura3-1 ade2-1 his3-11 leu2,3112 trp1-1 can1-100 ade2::ADE2 Ptr2-GFP::KAN bnr1::NAT*	This study
BWY6388	*MATα ura3-1 ade2-1 his3-11 leu2,3112 trp1-1 can1-100 ade2::ADE2 Ptr2-pHluorin::KAN bni1::NAT*	This study
BWY6391	*MATa ura3-1 ade2-1 his3-11 leu2,3112 trp1-1 can1-100 ade2::ADE2 Ptr2-pHluorin::KAN bnr1::NAT*	This study
BWY6378	*MATa ura3-1 ade2-1 his3-11 leu2,3112 trp1-1 can1-100 ade2::ADE2 Mid2-GFP::KAN end3::NAT*	This study
BWY6781	*MATα ura3-1 ade2-1 his3-11 leu2,3112 trp1-1 can1-100 ade2::ADE2 Sla2-GFP::KAN Abp1-mCherry::HPH*	This study
BWY6782	*MATα ura3-1 ade2-1 his3-11 leu2,3112 trp1-1 can1-100 ade2::ADE2 Sla2-GFP::KAN Abp1-mCherry::HPH end3::NAT*	This Study
BWY6386	*MATα ura3-1 ade2-1 his3-11 leu2,3112 trp1-1 can1-100 ade2::ADE2 Ptr2-GFP::KAN end3::NAT syp1::HIS3*	This study
BWY6426	*MATα ura3-1 ade2-1 his3-11 leu2,3112 trp1-1 can1-100 ade2::ADE2 Ptr2-GFP::KAN end3::NAT bni1::NAT*	This Study

Table 2-2. Plasmids used in this chapter.

Plasmid	Details	Source
pBW1546	pGEX-KG-KAN	Reider *et al.*, 2009
pBW1503	pGEX-KG-KAN::*Syp1*(aa602-870)	Reider *et al.*, 2009
pBW2250	pET28aC/U::*Mid2*(aa273-376)	This study
pBW2505	pET28aC/U::*mid2*(aa273-376; W277A, Y278A)	This study
pBW2515	pET28aC/U::*mid2*(aa273-376; D14A, E15A, Y16A)	This study
pBW2019	pRS316::*GFP-Snc1*	Quenneville *et al.*, 2006
pRS425	2*μ*, *LEU2*	Laboratory Plasmid
pBW1034	pRS425::*SYP1* (2*μ*, *LEU2*)	This study
pBW1916	pET28aC/U::*Snc1*(aa1-93)	This study
pBW2326	pET28aC/U::*Snc1*(aa1-27)	This study
pBW2336	pET28aC/U::*snc1*(aa1-27; D8A, P9A, Y10A)	This study
pBW1973	pET28aC/U::*snc1*(aa1-93; D8K, Y10A)	This study
pBW2330	pET28aC/U::*Snc1*(aa63-93)	This study
pBW2439	pET28aC/U::*snc1*(aa63-93; W86A, Y87A)	This study
pRS426	2*μ*, *URA3*	Laboratory Plasmid
pBW1446	pRS426::*Syp1* (2*μ*, *URA3*)	Reider *et al.*, 2009
pBW1562	pRS426::S*yp1* (aa1-601) (2*μ*, *URA3*)	Reider *et al.*, 2009
pBW1622	pYEP352::*Rom1* (2*μ*, URA3)	Ozaki *et al.*, 1996

lysates were immobilized on Talon metal affinity resin (Clontech) and GST-tagged

proteins were isolated with glutathione-agarose (Thermo Fisher).

Binding assays

GST-tagged protein lysates were incubated with glutathione-agarose beads

(Sigma) for 2 h at 4°C, washed twice with wash buffer [20 mM HEPES-NaOH, 30 mM

NaCl, pH 7.6], and mixed with His_6-tagged protein lysates for 2 h at 4°C. After

incubation, the immobilized proteins were washed three times with cold wash buffer

before adding SDS-PAGE sample buffer. Supernatant and pellet fractions were resolved

by SDS-PAGE, transferred to nitrocellulose, and immunoblotted with mouse anti-His_6

antibody (1:5,000; Clontech). Blots were then treated with horseradish peroxidase (HRP)-

conjugated goat anti-mouse secondary antibodies (1:10,000) prior to exposure.

Protein binding quantification

AlphaView SA software was used to quantify the results of binding assays. The

intensity of bands visualized by immunoblotting was quantified and the background-

corrected (BC) averages were compared to that of appropriate GST or GST-μHD protein

detected by GelCode Blue staining. Unpaired t-tests were used to determine statistical

significance.

Media and growth conditions

Standard yeast extract/peptone medium with 2% dextrose (YPD) was used for

growth of yeast under rich conditions. For ammonium-rich conditions or plasmid

maintenance, standard yeast nitrogen base (YNB) medium; containing 38mM ammonium sulfate, 2% dextrose, and appropriate amino acids and nutrients; was used. All yeast were grown at 30°C.

Bacteria were grown in LB supplemented with 50 μg/ml carbenicillin, 30 μg/ml kanamycin, and/or 34 μg/ml chloramphenicol, as appropriate. Materials were from Fisher Scientific Co. or Sigma Chemical Co, unless otherwise stated.

SGA

All genetic manipulations for the high-throughput visual screen were performed using Synthetic Genetic Array (SGA) techniques as previously described (Cohen and Schuldiner, 2011; Tong and Boone, 2006) to allow efficient introduction of various mutant backgrounds (*syp1Δ* and *end3Δ*) into a collection of secretory pathway-localized proteins harboring a transmembrane domain and tagged with GFP at the C-terminus (Huh *et al.*, 2003).

Briefly, using a RoToR colony arrayer (Singer Instruments, UK) to manipulate libraries in 384-colony high-density formats, haploid strains from opposing mating types, each harboring a different genomic alteration, were mated on YPD plates. Diploid cells were selected on plates containing all selection markers found on both parent haploid strains. Sporulation was then induced by transferring cells to nitrogen-starvation plates for 5 days. Haploid cells containing all desired mutations were selected for by transferring cells to plates containing all selection markers alongside the toxic amino acid derivatives Canavanine and Thialysine (S-AEC) to select against remaining diploids.

High-throughput fluorescence microscopy

Microscopic screening was performed using an automated microscopy setup as described previously (Breker *et al*., 2013). Cells were moved from agar plates into liquid 384-well polystyrene growth plates using the RoToR arrayer. Liquid cultures were grown overnight in SD -His medium in a shaking incubator (LiCONiC Instruments) at 30°C. A JANUS liquid handler (PerkinElmer), which is connected to the incubator, was used to back-dilute the strains into plates containing the same medium. Plates were then transferred back to the incubator and were allowed to grow for 4 h at 30°C to reach logarithmic growth phase.

The liquid handler was then used to transfer strains into glass-bottom 384-well microscope plates (Matrical Bioscience) coated with Concanavalin A (Sigma-Aldrich) to allow cell adhesion. Wells were washed four times in an imaging medium without fluorescence (SD -His -Riboflavin -folic acid) to remove floating cells and reach cell monolayer. Plates were then transferred into an automated inverted fluorescent microscopic ScanR system (Olympus) using a swap robotic arm (Hamilton). Imaging of plates was performed in 384-well format using a 60× air lens (NA 0.9) in SD -His -Riboflavin -folic acid medium. Images were acquired using the GFP (excitation at 490/20 nm, emission at 535/50 nm) channel.

For cases in which protein topology is currently undetermined, motifs within Syp1 cargos were assessed for residence in cytoplasmic regions of the protein using membrane topology prediction software, SPOCTOPUS (Viklund *et al*., 2008; http://octopus.cbr.su.se/).

<u>Live-cell fluorescence microscopy and quantification of fluorescence intensity</u>

Images were acquired and quantified as described previously (Prosser *et al.*, 2010). In brief, images were obtained at 30°C using an inverted microscope (Axiovert 200; Carl Zeiss) equipped with a Sensicam (Cooke), an X-Cite 120 PC fluorescence illumination system, and a 100×, 1.4 NA Plan-Apochromat objective lens. Within an experiment, images were acquired using identical exposure conditions; subsequently, brightness and contrast adjustments were applied equally to all images.

For quantification of fluorescence intensity, background subtraction was performed using ImageJ, and integrated density was measured for a minimum of 50 cells per condition. All integrated density values were then corrected for cell size. Fluorescence intensity measurements were performed for all cells in a minimum of two separate fields per experimental group. Statistical analysis was performed using Prism (GraphPad); either Welch's unequal variances *t*-test or one-way ANOVA with Tukey's correction was used.

When use of pHluorin was precluded, trafficking of GFP-tagged protein into cells was assessed via blind quantification of the percentage of cells in each experimental group with one of three vacuolar fluorescence phenotypes; at least 50 cells per condition, per replicate, were categorized as having either a weak/absent, moderate, or strong fluorescent signal at the vacuole. Unpaired *t*-tests of all replicates were then performed, comparing each experimental phenotypic class to its respective WT class at the same time point.

Z stacks were acquired for maximum intensity projections using 0.25 μm-step intervals. Projections were generated using ImageJ.

LatA treatment

Cells were grown to logarithmic phase and resuspended in synthetic medium containing 200 μM LatA (Invitrogen) or an equivalent volume of DMSO. Cells were incubated for 2 h at 30°C prior to imaging to allow for protein accumulation at the plasma membrane.

Urea extraction and tricholoracetic acid (TCA) precipitation

For urea extraction of membrane proteins, 5 ODs of mid-log phase cells expressing Ptr2-GFP or Mep3-GFP were grown in rich or ammonium-rich medium, respectively, collected, and washed with 1 ml of phosphate-buffered saline. Cells were then vortexed for 90 seconds with 100 μl of acid-washed glass 0.5 mm beads and 100 μl of 1x Laemmli urea sample buff (LUSB) and incubated at room temperature for 5 min prior to analysis.

For TCA precipitation of soluble proteins, 5 ODs of mid-log phase cells expressing Syp1-GFP were grown in rich and ammonium-rich media, collected, and resuspended in 1 ml of 10% TCA. Cells were incubated on ice for 20 min and were then pelleted at 14,000 rpm for 10 min at 4°C. The pellets were washed twice with cold acetone, dried, and resuspended in SDS sample buffer. Samples were then heated to 65°C for 5 min prior to analysis.

Samples were resolved by SDS-PAGE, transferred to nitrocellulose, and immunoblotted with mouse anti-GFP antibody (1:2,000; Santa Cruz Biotechnology) and HRP-conjugated goat anti-mouse secondary antibodies (1:5,000) prior to exposure.

<u>Growth assays</u>

Growth curves were generated using a Tecan Infinite M200 plate reader. WT or *syp1Δ* cultures were grown in YNB medium with or without methylammonium in 24-well, flat bottom tissue culture plates (Corning). Cultures were adjusted to equivalent starting density and volume, and were then grown at 30°C with shaking, with the OD_{600} for each condition measured every 30 min for 16 h.

References

Ayscough KR, Stryker J, Pokala N, Sanders M, Crews P, Drubin DG (1997) High rates of actin filament turnover in budding yeast and roles for actin in establishment and maintenance of cell polarity revealed using the actin inhibitor latrunculin-A. *J Cell Biol* **137:** 399-416

Bénédetti H, Raths S, Crausaz F, Riezman H (1994) The END3 gene encodes a protein that is required for the internalization step of endocytosis and for actin cytoskeleton organization in yeast. *Mol Biol Cell* **5:** 1023-37

Boettner DR, D'Agostino JL, Torres OT, Daugherty-Clarke K, Uygur A, Reider A, Wendland B, Lemmon SK, Goode BL (2009) The F-BAR protein Syp1 negatively regulates WASp-Arp2/3 complex activity during endocytic patch formation. *Curr Biol* **19:** 1979-1987

Boll W, Ohno H, Songyang Z, Rapoport I, Cantley LC, Bonifacino JS, Kirchhausen T (1996) Sequence requirements for the recognition of tyrosine-based endocytic signals by clathrin AP-2 complexes. *EMBO J* **15:** 5789-95

Bradford MK, Whitworth K, Wendland B (2015) Pan1 regulates transitions between stages of clathrin-mediated endocytosis. *Mol Biol Cell* **26:** 1371-85

Breker M, Gymrek M, Schuldiner M (2013) A novel single-cell screening platform reveals proteome plasticity during yeast stress responses. *J Cell Biol* **200:** 839-50

Burston HE, Maldonado-Báez L, Davey M, Montpetit B, Schluter C, Wendland B, Conibear E (2009) Regulators of yeast endocytosis identified by systematic quantitative analysis. *J Cell Biol* **185:** 1097-1110

Chapa-y-Lazo B, Allwood EG, Smaczynska-de Rooij II, Snape ML, Ayscough KR (2014) Yeast endocytic adaptor AP-2 binds the stress sensor Mid2 and functions in polarized cell responses. *Traffic* **15:** 546-57

Cohen Y, Schuldiner M (2011) Advanced methods for high-throughput microscopy screening of genetically modified yeast libraries. *Methods Mol Biol* **781:** 127-159

Conrad M, Schothorst J, Kankipati HN, Van Zeebroeck G, Rubio-Texeira M, Thevelein JM (2014) Nutrient sensing and signaling in the yeast Saccharomyces cerevisiae. *FEMS Microbiol Rev* **38:** 254-99

Davis NG, Horecka JL, Sprague GF Jr (1993) Cis- and trans-acting functions required for endocytosis of the yeast pheromone receptors. *J Cell Biol* **122:** 53-65

Doray B, Lee I, Knisely J, Bu GJ, Kornfeld S (2007) The gamma/sigma 1 and alpha/sigma 2 hemicomplexes of clathrin adaptors AP-1 and AP-2 harbor the dileucine recognition site. *Mol Biol Cell* **18:** 1887-1896

Engqvist-Goldstein AEY, Drubin DG (2003) Actin assembly and endocytosis: From yeast to mammals. *Annual Review of Cell and Developmental Biology* **19:** 287-332

Goldstein AL, McCusker JH (1999) Three new dominant drug resistance cassettes for gene disruption in Saccharomyces cerevisiae. *Yeast* **15:** 1541-53

Goode BL, Eskin JA, Wendland B (2015) Actin and endocytosis in budding yeast. *Genetics* **199:** 315-58

Gurunathan S, Chapman-Shimshoni D, Trajkovic S, Gerst JE (2000) Yeast exocytic v-SNAREs confer endocytosis. *Mol Biol Cell* **11:** 3629-3643

Hauser M, Kauffman S, Naider F, Becker JM (2005) Substrate preference is altered by mutations in the fifth transmembrane domain of Ptr2p, the di/tri-peptide transporter of Saccharomyces cerevisiae. *Mol Mem Biol* **22:** 215-227

Heitman J and Agre P (2000) A new face of the Rhesus antigen. *Nature Genetics* **26:** 258-259

Henne WM, Boucrot E, Meinecke M, Evergren E, Vallis Y, Mittal R, McMahon HT (2010) FCHo proteins are nucleators of clathrin-mediated endocytosis. *Science* **328:** 1281-1284.

Howard JP, Hutton JL, Olson JM, Payne GS (2002) Sla1p serves as the targeting signal recognition factor for NPFX(1,2)D-mediated endocytosis. *Journal of Cell Biology* **157:** 315-326

Huang C, Chang A (2011) pH-dependent cargo sorting from the Golgi. *J Biol Chem* **286:** 10058-10065

Huh WK, Falvo JV, Gerke LC, Carroll AS, Howson RW, Weissman JS, O'Shea EK (2003) Global analysis of protein localization in budding yeast. *Nature* **425:** 686-691

Jain RK, Joyce PB, Molinete M, Halban PA, Gorr SU (2001) Oligomerization of green fluorescent protein in the secretory pathway of endocrine cells. *Biochem J* **360:** 645-649

Kaksonen M, Sun Y, Drubin DG (2003) A pathway for association of receptors, adaptors, and actin during endocytic internalization. *Cell* **115:** 475-87

Kaksonen M, Toret CP, Drubin DG (2005) A modular design for the clathrin- and actin-mediated endocytosis machinery. *Cell* **123:** 305-20

Kelly BT, McCoy AJ, Spate K, Miller SE, Evans PR, Honing S, Owen DJ (2008) A structural explanation for the binding of endocytic dileucine motifs by the AP2 complex. *Nature* **456:** 976-U981

Keyel PA, Mishra SK, Roth R, Heuser JE, Watkins SC, Traub LM (2006) A single common portal for clathrin-mediated endocytosis of distinct cargo governed by cargo-selective adaptors. *Mol Biol Cell* **17:** 4300-4317

Koo SJ, Markovic S, Puchkov D, Mahrenholz CC, Beceren-Braun F, Maritzen T, Dernedde J, Volkmer R, Oschkinat H, Haucke V (2011) SNARE motif-mediated sorting of synaptobrevin by the endocytic adaptors clathrin assembly lymphoid myeloid leukemia (CALM) and AP180 at synapses. *Proc Natl Acad Sci U S A* **108:** 13540-13545

Longtine MS, McKenzie A III, Demarini DJ, Shah NG, Wach A, Brachat A, Philippsen P, Pringle JR (1998) Additional modules for versatile and economical PCR-based gene deletion and modification in Saccharomyces cerevisiae. *Yeast* **14:** 953-961

Ma L, Umasankar PK, Wrobel AG, Lymar A, McCoy AJ, Holkar SS, Jha A, Pradhan-Sundd T, Watkins SC, Owen DJ, Traub LM (2016) Transient Fcho1/2 . Eps15/R . AP-2 Nanoclusters Prime the AP-2 Clathrin Adaptor for Cargo Binding. *Dev Cell* **37:** 428-43

Marini AM, Soussi-Boudekou S, Vissers S, Andre B (1997) A family of ammonium transporters in Saccharomyces cerevisiae *Mol Cell Biol* **17:** 4282-93

Maritzen T, Koo SJ, Haucke V (2012) Turning CALM into excitement: AP180 and CALM in endocytosis and disease. *Biol Cell* Miller SE, Sahlender DA, Graham SC, Honing S, Robinson MS, Peden AA, Owen DJ (2011) The molecular basis for the endocytosis of small R-SNAREs by the clathrin adaptor CALM. *Cell* **147:** 1118-1131

Miesenbock G, De Angelis DA, Rothman JE (1998). Visualizing secretion and synaptic transmission with pH-sensitive green fluorescent proteins. *Nature* **394**:192-195

Miller SE, Sahlender DA, Graham SC, Höning S, Robinson MS, Peden AA, Owen DJ (2011) The molecular basis for the endocytosis of small R-SNAREs by the clathrin adaptor CALM. *Cell* **147:** 1118-1131

Mulkearns EE, Cooper JA (2012) FCH domain only-2 organizes clathrin-coated structures and interacts with Disabled-2 for low-density lipoprotein receptor endocytosis. *Mol Biol Cell* **23:** 1330-1342

Newpher TM, Lemmon SK (2006) Clathrin is important for normal actin dynamics and progression of Sla2p-containing patches during endocytosis in yeast. *Traffic* **7:** 574-588

Nishimura K, Fukagawa T, Takisawa H, Kakimoto T, Kanemaki M (2009) An auxin-based degron system for the rapid depletion of proteins in nonplant cells. *Nat Methods* **6:** 917-922

Owen DJ, Collins BM, Evans PR (2004) Adaptors for clathrin coats: Structure and function. *Annual Review of Cell and Developmental Biology* **20:** 153-191

Owen DJ, Vallis Y, Noble MEM, Hunter JB, Dafforn TR, Evans PR, McMahon HT (1999) A structural explanation for the binding of multiple ligands by the alphaadaptin appendage domain. *Cell* **97:** 805-815

Ozaki K, Tanaka K, Imamura H, Hihara T, Kameyama T, Nonaka H, Hirano H, Matsuura Y, Takai Y (1996) Rom1p and Rom2p are GDP/GTP exchange proteins (GEPs) for the Rho1p small GTP binding protein in Saccharomyces cerevisiae. *EMBO J* **15:** 2196-207

Piao HL, Machado IM, Payne GS (2007) NPFXD-mediated endocytosis is required for polarity and function of a yeast cell wall stress sensor. *Mol Biol Cell* **18:** 57-65

Polo S, Sigismund S, Faretta M, Guidi M, Capua MR, Bossi G, Chen H, De Camilli P, Di Fiore PP (2002) A single motif responsible for ubiquitin recognition and monoubiquitination in endocytic proteins. *Nature* **416:** 451-5

Prosser DC, Drivas TG, Maldonado-Báez L, Wendland B (2011) Existence of a novel clathrin-independent endocytic pathway in yeast that depends on Rho1 and formin. *J Cell Biology* **195:** 657-71

Prosser DC, Whitworth K, Wendland B (2010) Quantitative analysis of endocytosis with cytoplasmic pHluorin chimeras. *Traffic* **11:** 1141-50

Prosser DC, Wrasman K, Woodard TK, O'Donnell AF, Wendland B (2016) Applications of pHluorin for Quantitative, Kinetic and High-throughput Analysis of Endocytosis in Budding Yeast. *J Vis Exp* (116)

Pruyne D, Evangelista M, Yang C, Bi E, Zigmond S, Bretscher A, Boone C (2002) Role of formins in actin assembly: nucleation and barbed-end association. *Science* **297:** 612-615

Quenneville NR, Chao TY, McCaffery JM, Conibear E (2006) Domains within the GARP subunit Vps54 confer separate functions in complex assembly and early endosome recognition. *Mol Biol Cell* **17:** 1859-70

Rapetti-Mauss R, O'Mahony F, Sepulveda FV, Urbach V, Harvey BJ (2013) Oestrogen promotes KCNQ1 potassium channel endocytosis and postendocytic trafficking in colonic epithelium. *J Physiol* **591:** 2813-31

Raths S, Rohrer J, Crausaz F, Riezman H (1993) end3 and end4: two mutants defective in receptor-mediated and fluid-phase endocytosis in Saccharomyces cerevisiae. *J Cell Biology* **120:** 55-65

Reider A, Barker SL, Mishra SK, Im YJ, Maldonado-Báez L, Hurley JH, Traub LM, Wendland B (2009) Syp1 is a conserved endocytic adaptor that contains domains involved in cargo selection and membrane tubulation. *Embo J* **28:** 3103-3116

Reider A, Wendland B (2011) Endocytic adaptors--social networking at the plasma membrane. *J Cell Sci* **124:** 1613-1622

Robinson M, Poon PP, Schindler C, Murray LE, Kama R, Gabriely G, Singer RA, Spang A, Johnston GC, Gerst JE (2006) The Gcs1 Arf-GAP mediates Snc1,2 v-SNARE retrieval to the Golgi in yeast. *Mol Biol Cell* **17:** 1845-58

Saier MH Jr (2000) A functional-phylogenetic classification system for transmembrane solute transporters. *Microbiol Mol Biol Rev* **64:** 354-411

Shih SC, Katzmann DJ, Schnell JD, Sutanto M, Emr SD, Hicke L (2002) Epsins and Vps27p/Hrs contain ubiquitin-binding domains that function in receptor endocytosis. *Nat Cell Biol* **4:** 389-93

Shimada A, Yamaguchi A, Kohda D (2016) Structural basis for the recognition of two consecutive mutually interacting DPF motifs by the SGIP1 μ homology domain. *Sci Rep* **6:** 19565

Stark C, Su TC, Breitkreutz A, Lourenco P, Dahabieh M, Breitkreutz BJ, Tyers M, Sadowski I (2010) PhosphoGRID: a database of experimentally verified in vivo protein phosphorylation sites from the budding yeast Saccharomyces cerevisiae. Database (Oxford)

Steiner HY, Song W, Zhang L, Naider F, Becker JM, Stacey G (1994) An Arabidopsis peptide transporter is a member of a new class of membrane transport proteins *Plant Cell* **6:** 1289-99

Stimpson HE, Toret CP, Cheng AT, Pauly BS, Drubin DG (2009) Early-arriving Syp1p and Ede1p function in endocytic site placement and formation in budding yeast. *Mol Biol Cell* **20:** 4640-51

Strop P, Kaiser SE, Vrljic M, Brunger AT (2008) The structure of the yeast plasma membrane SNARE complex reveals destabilizing water-filled cavities. *J Biol Chem* **283:**1113-1119

Sutton RB, Fasshauer D, Jahn R, Brunger AT (1998) Crystal structure of a SNARE complex involved in synaptic exocytosis at 2.4 A resolution. *Nature* **395:** 347-353

Tang HY, Munn A, Cai M (1997) EH domain proteins Pan1p and End3p are components of a complex that plays a dual role in organization of the cortical actin cytoskeleton and endocytosis in Saccharomyces cerevisiae. *Mol Cell Biol* **17:** 4294-304

Tang HY, Xu J, Cai M (2000) Pan1p, End3p, and S1a1p, three yeast proteins required for normal cortical actin cytoskeleton organization, associate with each other and play essential roles in cell wall morphogenesis. *Mol Cell Biol* **20:** 12-25

Taylor MJ, Perrais D, Merrifield CJ (2011) A high precision survey of the molecular dynamics of mammalian clathrin-mediated endocytosis. *PLoS Biol* **9:** e1000604

Tong AH, Boone C (2006) Synthetic genetic array analysis in *Saccharomyces cerevisiae*. *Methods Mol Biol* **313:** 171-92

Tonikian R, Zhang Y, Boone C, Sidhu SS (2007) Identifying specificity profiles for peptide recognition modules from phage-displayed peptide libraries. *Nat Protoc* **2:** 1368-1386

Traub LM (2009) Tickets to ride: selecting cargo for clathrin-regulated internalization. *Nat Rev Mol Cell Biol* **10:** 583-596

Umasankar PK, Sanker S, Thieman JR, Chakraborty S, Wendland B, Tsang M, Traub LM (2012) Distinct and separable activities of the endocytic clathrin-coat components Fcho1/2 and AP-2 in developmental patterning. *Nat Cell Biol* **14:** 488-501

Viklund H, Bernsel A, Skwark M, Elofsson A (2008) SPOCTOPUS: a combined predictor of signal peptides and membrane protein topology. *Bioinformatics* **24:** 2928-2929

Wegener KL, Partridge AW, Han J, Pickford AR, Liddington RC, Ginsberg MH, Campbell ID (2007) Structural basis of integrin activation by talin. *Cell* **128:** 171-182

Yofe I *et al*. (2016) One library to make them all: streamlining the creation of yeast libraries via a SWAp-Tag strategy. *Nat Methods* **13:** 371-8

CHAPTER 3

Vps4 is required for clathrin-mediated endocytosis mutant viability and cargo trafficking

from the plasma membrane

Abstract

Endocytic trafficking from the plasma membrane (PM) regulates many processes, including lipid and protein turnover, signaling, and nutrient uptake. During clathrin-mediated endocytosis (CME), the predominant internalization pathway for most known cargos in budding yeast, endocytic adaptors bind cytosolic regions of transmembrane cargo proteins. Many of these adaptors are directly involved in the recruitment of clathrin. The clathrin-associated sorting protein family of adaptors includes the yeast epsins, Ent1/2, and the AP180/PICALM homologues, Yap1801/2. Previous work has shown that cells lacking these four adaptor-encoding genes are inviable; however, in a quadruple adaptor deletion background, the presence of a single ENTH domain from one of the epsins produces viable cells with severe endocytic defects such as cargo accumulation at the PM. This CME-deficient, quadruple adaptor mutant strain provides a sensitized background ideal for revealing cellular components that provide supporting or redundant roles to clathrin adaptors. A mutagenic screen was performed to identify alleles that are lethal when combined with the quadruple adaptor mutant using a colony-sectoring reporter assay. Upon sequencing of plasmids from a genomic library that complemented the synthetic lethal mutations, members of one complementation group possessed mutations in *VPS4*. Moreover, deletion of *VPS4* in the original adaptor mutant background replicated the synthetic lethality phenotype from the reporter assay. Interestingly, loss of Vps4 in an otherwise WT background resulted in aberrant accumulation of the cargo Ste3 at the PM, which appears to result from the upregulation of endocytic recycling. Other negative interactions were identified, such as adaptor mutants that lack Vps24, as well as the synthetic lethality of Vps4 deletion in an *end3Δ*

strain that is also CME-deficient. These findings reveal a previously unappreciated

genetic interaction between Vps4, as well as other MVB-associated factors, and CME

adaptors.

Introduction

In addition to providing a barrier that isolates the cytosol from the variable conditions in the extracellular environment, the PM contains proteins with a variety of functions, including ion channels, transporters, enzymes, and receptors. In response to fluctuating conditions in the extracellular space, the contents of the PM must be continuously adjusted for optimal cell physiology. In one method by which the cell accomplishes this, a portion of the lipid bilayer and its contents are moved into the cell by producing an intracellular vesicle in a process called endocytosis. Endocytosis allows the cell to take up nutrients from the environment, up- or down-regulate signaling pathways, and tune the protein composition of the PM. The main mechanism acting at the PM to move cargos into the cell is clathrin-mediated endocytosis (CME), a process in which dozens of proteins work together to form a clathrin-coated vesicle (CCV).

In the first phase of CME, components of the early coat localize to nascent sites of endocytosis. Subsequently, middle and then late coat proteins bind to the early coat, and the late coat recruits actin remodelers that generate force toward the cell interior, leading to invagination of the endocytic site and formation of a pit in the PM. Once a clathrin-coated pit is formed, scission factors cleave the pit from the rest of the outer cell membrane, releasing a CCV into the cytoplasm (Kaksonen *et al.*, 2003, 2005). CME is present in budding yeast and mammalian cells, and the process is highly conserved, with most components of mammalian CME sharing homology with at least one yeast endocytosis protein (Engqvist-Goldstein and Drubin, 2003; Taylor *et al.*, 2011; Goode *et al.*, 2015). Proteins that are internalized from the cell surface and concentrated into endocytic vesicles are referred to as cargos. After leaving the PM, endocytosed material

is then delivered along a series of compartments within the cytoplasm that make up the endocytic pathway.

The first compartment to which an endocytic vesicle is trafficked is the early endosome (Allen *et al.*, 1992). After fusion of the vesicle with the early endosome, multiple processes manage the fate of cargo proteins. Some cargos are returned to the PM in a process known as recycling (Dunn *et al.*, 1989; Stoorvogel *et al.*, 1991; van der Sluijs *et al.*, 1992; Mayor *et al.*, 1993), while others are delivered to further endocytic organelles. Compartments downstream of the early endosome along the endocytic route are known as late endosomes. Late endosomes contain intralumenal vesicles generated via invagination and scission of the membrane, thereby forming multivesicular bodies (MVBs) (Felder *et al.*, 1990; Gruenberg and Maxfield, 1995). The formation of intralumenal vesicles is mediated by complexes of proteins called endosomal sorting complexes required for transport (ESCRTs) in a process that can be described as similar to endocytosis, yet in reverse (Babst, 2011); whereas endocytosis generates vesicles that bud into the cytoplasm, ESCRTs act to produce vesicles that bud away from the cytoplasm. Cargos then move to the late endosome and, ultimately, to vacuoles, the yeast equivalent of the lysosome in mammalian cells (Futter *et al.*, 1996).

Adaptor proteins are among the first proteins to arrive at sites of endocytosis, where they bind to cargo, lipids in the PM, and other CME components, including clathrin itself (Reider and Wendland, 2011). Adaptors target specific proteins for endocytosis, which are referred to as cargo. One example of a cargo protein in the budding yeast, *Saccharomyces cerevisiae*, is Ste3, which is the receptor for mating pheromones released by *MAT***a** cells. In the absence of the **a**-factor pheromone, a

fluorescent Ste3-GFP chimera expressed in a wild-type strain (WT) will be delivered to the PM and constitutively internalized (Shaw *et al*., 2003). Among the CME adaptors are four similar proteins: the yeast epsins, Ent1 and Ent2; additionally, the AP180/PiCALM homologues, Yap1801 and Yap1802 (Aguilar *et al*., 2006; Maldonado-Báez *et al*., 2008). All of these adaptors possess C-terminal clathrin-binding motifs, as well as multiple NPF motifs, and Yap1801 and Yap1802 each contain an AP180 N-terminal homology (ANTH) domain while the epsins possess an epsin N-terminal homology (ENTH) domain, along with ubiquitin-interacting motifs (Aguilar *et al*., 2003). Unlike the non-essential Yap180s, the loss of both Ent1 and Ent2 from the cell is lethal; however, retention of a single copy of the ENTH domain-expressing region of either gene is sufficient for viability (2Δ+ENTH; Wendland *et al*., 1999; Aguilar *et al*., 2006). In cells lacking both Ent1 and Ent2, aside from a single ENTH domain for viability, endocytosis phenotypes remain largely compared to WT, whereas deletion of *YAP1801* and *YAP1802* in conjunction with the epsin mutant background leads to defects in endocytic protein dynamics and nonspecific cargo accumulation at the PM (4Δ+ENTH; Maldonado-Báez *et al*., 2008); for example, Ste3-GFP localizes almost exclusively to the vacuole in WT cells, but accrues at the PM in these adaptor mutants.

The adaptor mutant strain provides a unique opportunity to identify factors that cooperate or function in parallel with endocytic adaptor proteins. Using a colony-sectoring assay similar to one reported by Bender and Pringle (1991), we aimed to identify genes that become essential in the adaptor mutant context. Here, we investigate a lethal interaction between our adaptor mutant strain and the loss of *VPS4* from the genome. Our findings indicate that Vps4 is necessary for efficient trafficking of cargo

from the PM, and that this may be due to upregulated endocytic recycling in a *vps4Δ* strain; Vps4 is an ATPase best known for its role in ESCRT-III complex disassembly at endosomes that allows for MVB formation (Robinson *et al*., 1988; Rothman *et al*., 1989; Babst *et al*., 1997). In addition, Vps4-mediated ESCRT-III disassembly is shown to be the necessary function required for the viability of adaptor mutants and normal cargo trafficking. Finally, Vps4 also becomes essential in other CME mutants, and the absence of another ESCRT component yields a similarly negative genetic interaction, suggesting that synthetic lethality is a common feature when CME deficiencies and ESCRT mutants are combined.

Results

<u>Isolating and identifying lethal alleles in the adaptor mutant background</u>

To isolate mutations that are lethal with the 4Δ+ENTH1 background, we

generated a cover plasmid that contains the full-length *ENT1* gene, since reintroduction

of just Ent1 is able to rescue known phenotypes associated with this "adaptor mutant"

strain (Maldonado-Báez *et al*., 2008). In an effort to simplify the task of distinguishing

synthetic lethal mutants from those that remain viable without the Ent1 plasmid, we

utilized a peculiarity of an adenine synthesis pathway mutant in a colony-sectoring assay,

much like the one presented in Bender and Pringle (1991). Ade2 is an aminoamidozole

ribonucleotide (AIR)-carboxylase, and the AIR substrate molecules are red in color;

without the Ade2 enzyme, AIR accumulates within yeast, pigmenting the cells red along

with colonies formed by them (Roman, 1956; Dorfman, 1969; Jones and Fink, 1982). We

deleted both *ADE2* and *ADE8*, an additional enzyme in this pathway that acts upstream of

AIR formation (Jones and Fink, 1982), from adaptor mutants. In the absence of both of

proteins, the strain produces cells and colonies that are white in appearance, like WT

cells; however, the Ent1 cover plasmid also contains the gene encoding Ade8, coloring

any cells that possess it red (Figure 3-1). Therefore, yeast that do not require full-length

Ent1 for viability after mutagenesis will be able to lose the plasmid during division,

becoming white and producing sectored colonies that are both red and white. Cells with

lethal mutations, however, would be inviable without the Ent1-Ade8 plasmid, producing

completely red, non-sectoring colonies that are easily distinguished from those that are

sectored.

We treated adaptor mutant parent strains containing the Ent1 cover plasmid with

107
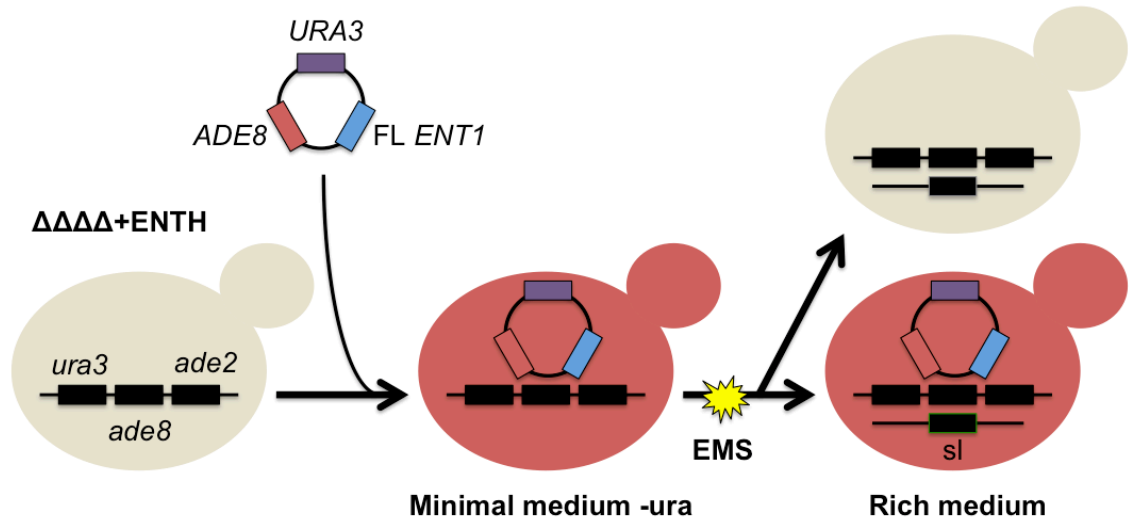
Figure 3-1. Diagram of colony-sectoring assay.

ethyl methanesulfonate (EMS), a mutagen that introduces point mutations into the genome. After mutagenesis, colonies were allowed to form on rich medium and non-sectoring, red colonies were then confirmed to be dependent on the Ent1 plasmid for viability. Next, we performed multiple rounds of backcrossing, mating each mutant to the untreated parent strain of appropriate mating type and selecting non-sectoring spores after tetrad dissection; this was done with the goal of removing mutations introduced during EMS-treatment that do not cause inviability. Backcrossing also allowed for identification of mutations as either dominant or recessive. Dominant alleles conveyed the non-sectoring phenotype to diploid cells produced by mating to a parent strain, whereas recessive alleles produced diploids with the ability to form sectored colonies. We next mated every recessive strain to each recessive mutant of the opposite mating type to identify complementation groups, comprised of strains that are likely to have mutant alleles of the same gene. Strains that produced non-sectoring diploids were categorized as being in the same complementation group, and those for which diploid colonies regained the ability to sector were assigned to different groups. From this analysis, we were able to identify eight complementation groups with multiple members.

Having generated and grouped mutants by the ability to complement the non-sectoring phenotype, we next aimed to pinpoint loci affected during EMS mutagenesis. To that end, we transformed representative mutants from each complementation group with a low-copy genomic library (Figure 3-2A, left panel). Our aim was to isolate cells that acquired a plasmid possessing a WT copy of the causative mutant gene that are then able to survive without the full-length Ent1 plasmid and form sectoring colonies. However, this represents the ideal outcome, and other scenarios could allow plasmids to
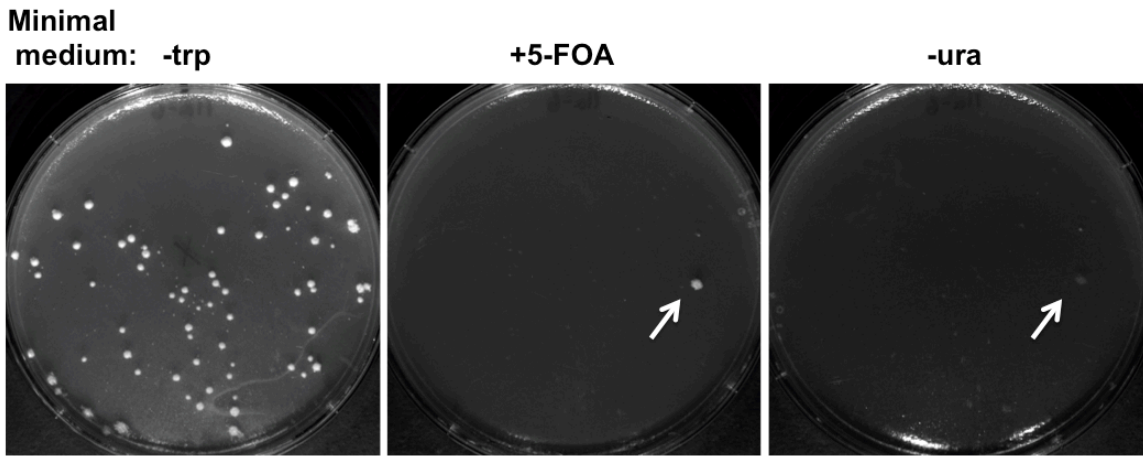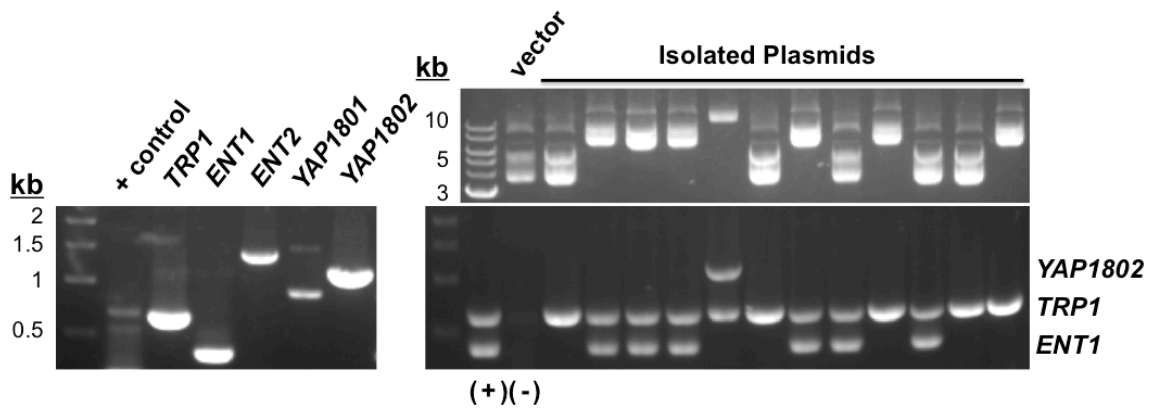
Figure 3-2. Rescuing plasmids isolated through counter-selection and tested for adaptors. (A) Example synthetic lethal mutant strain that was transformed with genomic library. Transformants were selected on YNB -tryptophan (-trp) and the original Ent1 plasmid selected against on YNB +5-FOA. After counter-selection, cells from rescued colonies are no longer viable in media lacking uracil (-ura). (B) Example of rescuing plasmids from one group, which were tested by PCR for any of the four genes deleted in adaptor mutants. Size of PCR product for each adaptor, along with a *TRP1* control, are shown in left gel. A positive Ent1 control is also indicated by (+) and negative control by (-).

confer the ability to grow without Ent as well. Due to the added presence of the *URA3* gene on the cover plasmid, we were able to simplify the identification of rescued cells by replica plating transformants onto medium containing 5-fluoroorotic acid (5-FOA), since the presence of 5-FOA is toxic to cells possessing a functional copy of *URA3* (Boeke *et al*., 1987). After replica plating, plasmids were rescued from any cells confirmed to be positive for growth on 5-FOA that, therefore, had gained the ability to grow without the original Ent1 plasmid (Figure 3-2A). The plasmids were then tested for the presence of either Ent1, Ent2, Yap1801, or Yap1802 (Figure 3-2B), and those lacking any of the four adaptors were sequenced to identify the novel, rescuing gene.

Mutation of Vps4 is lethal in combination with the adaptor mutant background

From rescued colonies of one complementation group, we isolated two distinct library plasmids that contained an overlapping genomic interval with three full-length genes present on both. These genes encode two proteins with unconfirmed functions, Ypr172w and Ypr174c, as well as Vps4, an ATPase associated with diverse cellular activities (AAA) that allows for ESCRT-III complex disassembly and release of cargo-containing vesicles into the lumen of MVBs (Robinson *et al*., 1988; Rothman *et al*., 1989; Babst *et al*., 1997) (Figure 3-3A). Of these genes, *VPS4* appeared to be the most likely candidate for synthetic lethality with adaptor mutants due to its functioning along the endocytic route, even if its functioning is generally known to occur at intracellular locations and not at the PM.

VPS4 mutants aberrantly secrete hydrolytic enzymes, which normally localize to the vacuole, into extracellular space (Babst *et al*., 1997). To test for this phenotype, we

111

Figure 3-3. Strains in one complementation group possess mutations in Vps4. (A) Diagram depicting genomic intervals present in plasmids that rescued mutants from one complementation group. (B) CPY assay in which a parent (ΔΔΔΔ+ENTH), *vps4Δ*, and synthetic lethal mutant strains were grown against nitrocellulose and probed with anti-CPY antibodies. Negative control: (-), positive control (+). (C) Live-cell fluorescence microscopy of WT, parent, and synthetic lethal mutant strains transformed with low-copy GFP-CPS and grown on minimal medium. Scale bar, 2μ. (D) Protein sequence of mutant Vps4 compared to WT.

Figure on following page.

A

B

IB: CPY

ΔΔΔΔ+ENTH (-)

lethal mutant

*vps4*Δ (+)

C

WT   ΔΔΔΔ+ENTH   lethal mutant

+GFP-CPS

D
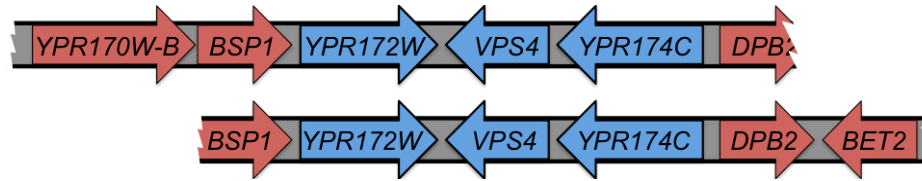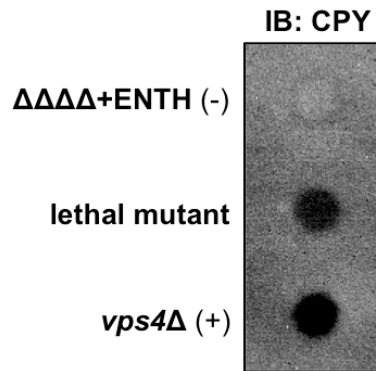
WT: MSTGDFLTKGIELVQKAI…EGN437*

mut: MSTGDFL**LRE***
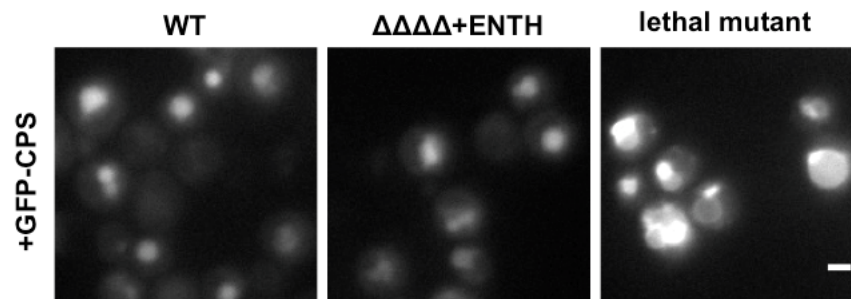
WT: …274GATNIPWQL**D**SAIRRRF290…

mut: …274GATNIPWQL**V**SAIRRRF290…

Figure 3-3. Strains in one complementation group possess mutations in Vps4.

utilized an assay in which cells are grown in direct contact with nitrocellulose; after overnight growth, the nitrocellulose is then probed for the presence of a vacuolar enzyme, carboxypeptidase Y (CPY). While the parent strain exhibited no CPY staining, a synthetic lethal mutant from this complementation group was CPY-positive, much like the positive control, a *vps4Δ* strain (Figure 3-3B). After obtaining this result, we transformed the mutant with a plasmid expressing a distinct vacuolar protein, carboxypeptidase S (CPS), that is fused with green fluorescent protein (GFP) at the N-terminus. In WT cells, GFP-CPS is trafficked to the lumen of vacuoles via the MVB pathway. However, in the absence of Vps4, the enzyme remains at the vacuole membrane and accumulates in E-Class compartments adjacent to the vacuole (Stuchell-Brereton *et al.*, 2007); these cargo-dense Class E compartments are named for the class of vacuolar protein sorting mutants in which they were first observed (Raymond *et al.*, 1992). Upon imaging, GFP-CPS localized to the interior of vacuoles in WT and adaptor mutant cells, as expected (Figure 3-3C). In the synthetic lethal mutant, the fluorescent protein instead appeared at vacuole surfaces and also revealed bright, E-Class compartments. Together, these defects indicative of vacuolar protein sorting misregulation suggested that *VPS4* is altered in the members of this complementation group and is likely the synthetic lethal mutation.

Having gained confidence from these data that *VPS4* was altered, we sequenced the gene in two representative strains of the complementation group, and analysis of the results confirmed the presence of mutations in the Vps4 coding sequence. One *VPS4* mutation results in a frame-shift mutation at the eighth amino acid of Vps4, introducing a stop codon at residue 11. In the other, a missense mutation incorporates a valine at

position 283, where aspartic acid is located in the WT protein (Figure 3-3D). Though we have not been able to confirm that Vps4^{D283V} is expressed and properly folded within the cell, this aspartic acid residue is adjacent to a phosphate-sensing asparagine at residue 277 within the active site of the ATPase (Figure 3-4A); it would be interesting if this mutation interferes with the enzymatic activity of Vps4. Nonetheless, the strains in this complementation group possess Vps4 mutations, further supporting the idea that the loss of *VPS4* activity is lethal without the Yap180s or full-length epsins.

To verify the requirement for Vps4 in cells lacking adaptor proteins, we attempted to reproduce the non-sectoring, synthetic lethal phenotype by deleting *VPS4* in the adaptor mutant parent strain. The loss of *VPS4* made cells dependent on the full-length Ent1- and Ade8-expressing plasmid, producing colonies that were completely red and non-sectored, unlike the original parent (Figure 3-5A). The additional *vps4Δ* mutation also inhibited the ability of adaptor mutant cells to grow on medium containing 5-FOA, further demonstrating an acquired dependence on the Ent1-Ura3 plasmid. We also tested deletion of multiple other genes from this background to determine if lethality is specific to Vps4. The genes investigated were those for Vps5, a Class B vacuolar protein sorting mutant (Raymond *et al*., 1992); Yta6, an AAA enzyme unrelated to endosomal traffic (Schnall *et al*., 1994); and Vta1, a binding partner of Vps4 that enhances its oligomerization (Yeo et al., 2003; Azmi *et al*., 2006). Despite a shared function in vacuole protein sorting, identity as a fellow AAA, or physical interaction with Vps4, respectively, cells lacking endocytic adaptors tolerated these deletions and continued to grow well on 5-FOA-containing medium (Figure 3-4B). Additionally, diploid cells formed by mating the *vps4Δ* synthetic lethal mutant to one of the *vps4* allele strains

115

A
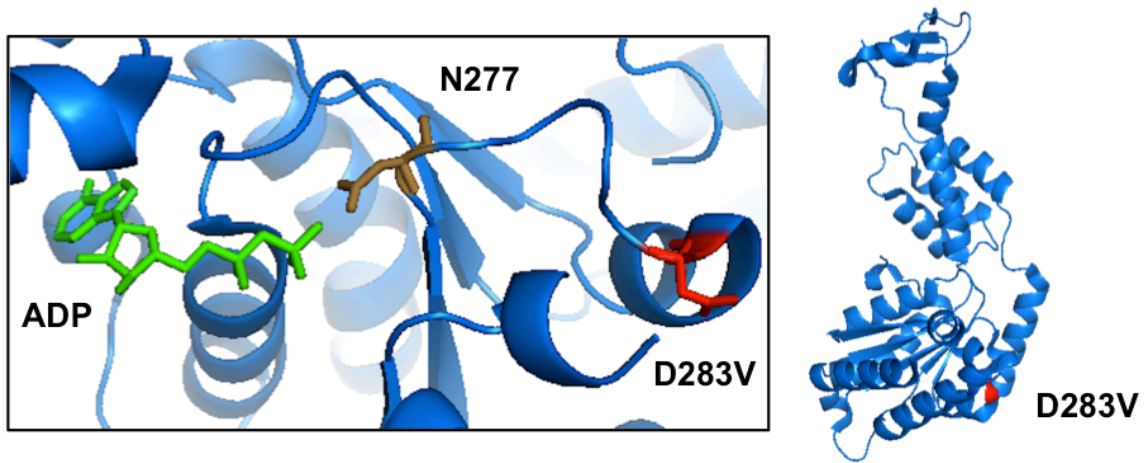
B
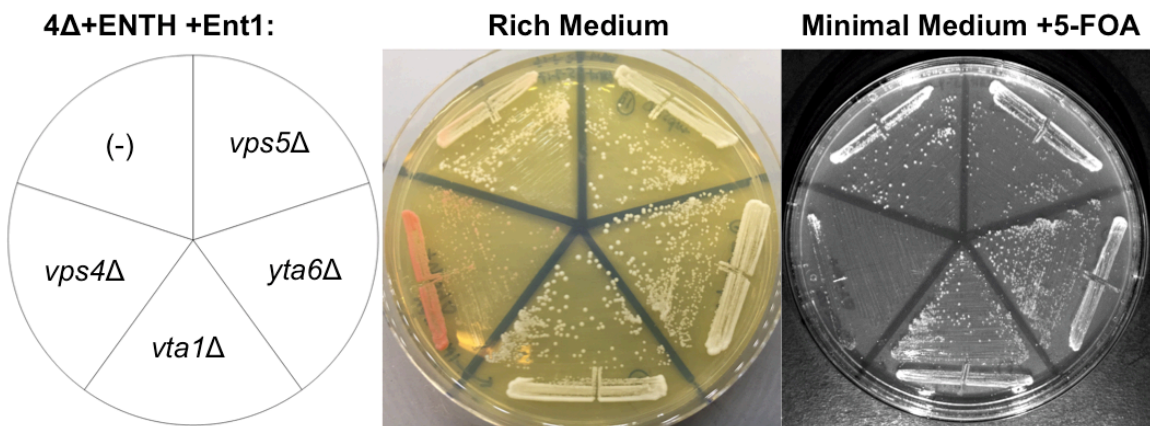
Figure 3-4. Location of a Vps4 mutation and test for interactions with adaptor mutants. (A) PyMOL-generated depiction of D283V mutation in Vps4 protein (right; D283V, red). Vps4 active site with ADP molecule (left; ADP, green). Phosphate-sensing N277 residue also highlighted (brown) (The PyMOL Molecular Graphics System, Version 1.8 Schrödinger, LLC). (B) Sectoring and growth assays, middle and right panels, respectively, of either a parent strain containing the original Ent1 plasmid (4Δ+ENTH +Ent1) alone (-), a positive control for sectoring and growth on medium with 5-FOA, or with additional mutations of *VPS4* (negative control), *VTA1*, *YTA6*, or *VPS5*.

Figure 3-5. Loss of Vps4 is lethal in the adaptor mutant background. (A) Sectoring and growth assays, shown in upper and lower panels, respectively, for a parent strain [ΔΔΔΔ(ENTH1)], synthetic lethal mutant isolated from the screen, and parent strain in which *VPS4* was deleted. Cells were tested for sectoring on rich medium and growth on medium containing 5-FOA. (B) Sectoring and growth assays, shown in upper and lower panels, respectively, for a parent strain [ΔΔΔΔ(ENTH1)] and diploid strain generated from the mating of the parent strain with an additional *vps4Δ* and a synthetic lethal mutant isolated from the screen. Cells were tested for sectoring on rich medium and growth on medium containing 5-FOA. (C) Assay in which the parent strain lacking Vps4 was transformed with either an empty *URA3* vector or one expressing high-copy Rom1 and tested for growth on minimal medium containing 5-FAA.

Figure on following page.

A

ΔΔΔΔ(ENTH1) + :   -   **lethal mutant**   ***vps4Δ***

-Ent1: White
+Ent1: Red

Rich
medium

Minimal
medium
+5-FOA

B

ΔΔΔΔ(ENTH1)   ΔΔΔΔ(ENTH1) *vps4Δ*
x
lethal mutant

Rich
media

Minimal
media
+5-FOA

C

Minimal medium -uracil   **Minimal medium +5-FAA**

+vector   +Rom1   +vector   +Rom1

4Δ(ENTH) *vps4Δ*
+Ent1 *TRP1*
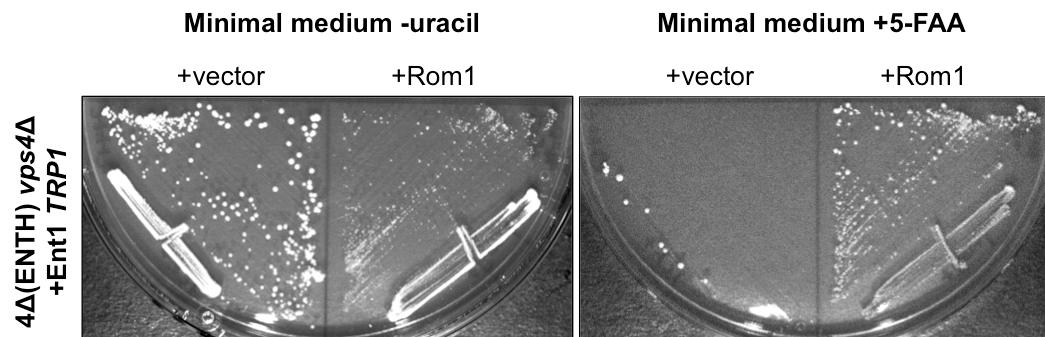
Figure 3-5. Loss of Vps4 is lethal in the adaptor mutant background.

118
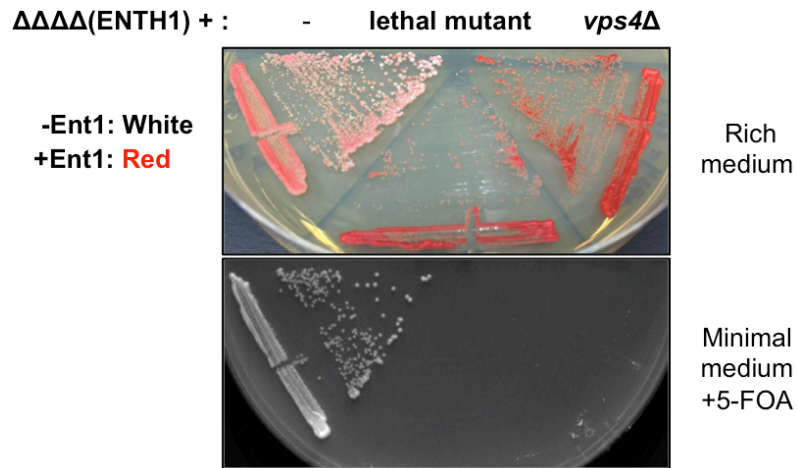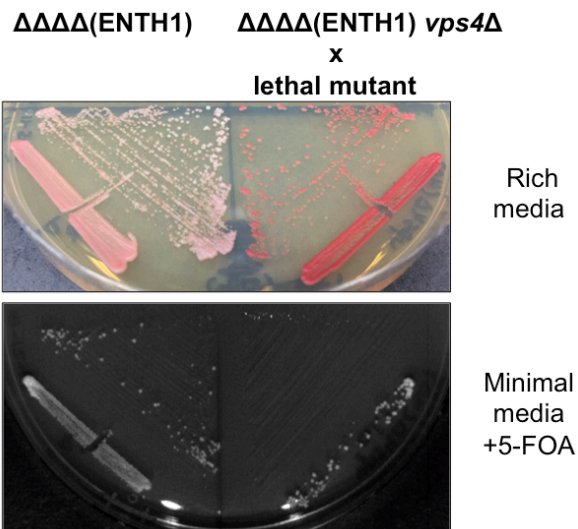
identified in the screen, shown to encode a truncated Vps4 protein, were also unable to sector or grow in the presence of 5-FOA (Figure 3-5B). Together, these findings confirm that Vps4 is essential for the viability of 4Δ+ENTH1 cells.

Interestingly, we also found that upregulation of another endocytic mechanism, one that is not mediated by clathrin, was able to restore the viability of adaptor mutants lacking Vps4. In addition to CME, a Rho1-mediated clathrin-independent endocytic pathway (CIE) pathway also exists in budding yeast. We transformed synthetic lethal cells containing a full-length copy of *ENT1*, in this case on a Trp1-expressing plasmid, with either an empty high-copy vector or one including the *ROM1* gene. Rom1 is a guanine nucleotide exchange factor (GEF) for Rho1 that enhances functioning of Rho1-dependent CIE when overexpressed (Prosser *et al.*, 2011). Only cells transformed with the *ROM1*-containing plasmid were able to lose the Trp1 cover plasmid and grow in the presence of 5-fluoroanthranilic acid (5-FAA), which is toxic to cells with functional Trp1 enzyme (Toyn *et al.*, 2000) (Figure 3-5C). The fact that the increased activity of another endocytic pathway can rescue the synthetic lethality of *VPS4* deletion from adaptor mutants suggests that the cause of inviability might not be specific to CME, but instead results from decreased endocytic efficiency in general.

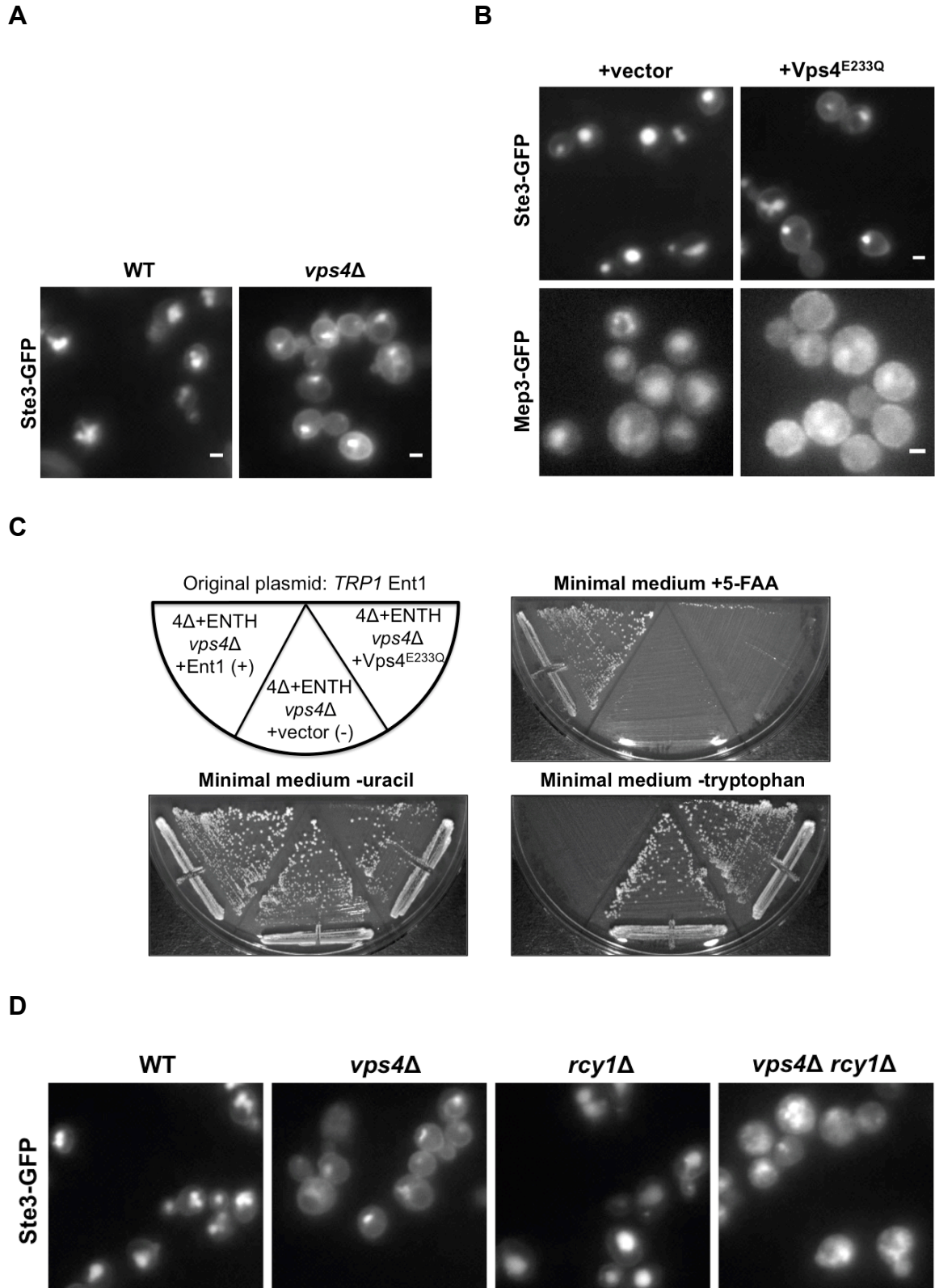Vps4 ESCRT-disassembly activity is required for efficient cargo trafficking from the PM

Having determined that Vps4 becomes essential in adaptor mutant cells, we aimed to understand the mechanism of this negative genetic interaction, particularly because Vps4 is thought to act at the surface of MVBs, whereas the endocytic adaptors Ent1, Ent2, Yap1801, and Yap1802 function at the cell cortex. One phenotype associated with

119

4Δ+ENTH1 cells is the nonspecific accumulation of cargo proteins at the PM due to deficient CME functioning. We hypothesized that cargo trafficking from the PM might be disrupted by the loss of Vps4 as well. To investigate this, we observed the localization of Ste3 in live cells. As described in previous reports (Maldonado-Báez *et al*., 2008; Prosser *et al*., 2010), Ste3-GFP localized primarily to the vacuoles of WT, haploid yeast cells (Figure 3-6A); however, in an otherwise WT strain, the deletion of *VPS4* caused Ste3 to remain at the vacuolar membrane and mark the neighboring Class-E compartments that are typical in the absence of Vps4 protein. Surprisingly, we also noticed a pool of Ste3-GFP accumulating at the PM of *vps4Δ* cells, suggesting that mutation of Vps4 hinders the ability of the cell to efficiently traffic Ste3 away from the PM.

We wondered whether the ESCRT-disassembly activity of Vps4 is necessary for normal trafficking of Ste3, and also whether this is a general phenotype of cargo trafficking in *vps4* mutants that is not specific to Ste3. Thus, we utilized a dominant negative allele of Vps4 that contains a missense mutation making the protein nonfunctional, Vps4^{E233Q} (Babst *et al*., 1997). We transformed a plasmid carrying Vps4^{E233Q} into cells expressing either fluorescent Ste3 or Mep3, a high-capacity ammonium permease, which is an additional endocytic cargo (Marini *et al*., 1997; Apel, Hoban *et al*., 2017). As in the *vps4Δ* cells, Ste3-GFP accumulated at the PM to a greater extent in the Vps4^{E233Q}-transformed strain as compared to those with vector alone (Figure 3-6B); yet, the phenotype was not as pronounced as with the deletion of *VPS4*. One potential explanation for this is that the missense allele does not completely block activity of the WT Vps4 that remains present within these cells. Though results with Ste3 were

Figure 3-6. Vps4 ESCRT disassembly is necessary for cargo trafficking from the PM.

(A) Live-cell fluorescence microscopy of WT and *vps4Δ* strains expressing Ste3-GFP.

Scale bar, 2μ. (B) Strains expressing Ste3-GFP or Mep3-GFP were transformed with

either an empty low-copy vector or one containing mutant Vps4^{E233Q} and imaged via live-

cell fluorescence microscopy. Scale bar, 2μ. (C) Assay in which a parent strain lacking

Vps4 was transformed with either an empty vector as a negative control (-) or one

expressing Vps4^{E233Q} and tested for growth on 5-FAA. Cells were also transformed with

an Ent1 plasmid containing a different marker as a positive control for growth (+). (D)

Live-cell fluorescence microscopy of Ste3-GFP localization in WT, *vps4Δ*, *rcy1Δ*, and

vps4Δ rcy1Δ strains grown on rich media. Scale bar, 2μ.

Figure on following page.

A

WT   *vps4*Δ

Ste3-GFP

B

+vector   +Vps4^{E233Q}

Ste3-GFP

Mep3-GFP

C

Original plasmid: *TRP1* Ent1

4Δ+ENTH *vps4*Δ +Ent1 (+)

4Δ+ENTH *vps4*Δ +Vps4^{E233Q}

4Δ+ENTH *vps4*Δ +vector (-)

Minimal medium +5-FAA

Minimal medium -uracil

Minimal medium -tryptophan

D

WT   *vps4*Δ   *rcy1*Δ   *vps4*Δ *rcy1*Δ

Ste3-GFP

Figure 3-6. Vps4 ESCRT disassembly is necessary for cargo trafficking from the PM.

122

subtle, Mep3 exhibited a more pronounced phenotype. Whereas Mep3-GFP localized predominantly to the vacuole in WT conditions, this cargo accumulated at the PM after introduction of the Vps4^{E233Q} plasmid, and few distinct vacuoles were visible (Figure 3-6B). This suggests that the ESCRT disassembly function of Vps4 is indeed necessary for efficient cargo trafficking from the PM, and that this is a general cargo-trafficking phenotype not specific to Ste3.

We next examined if the inability to disassemble ESCRT complexes is the reason that Vps4 becomes necessary for the viability of adaptor mutants. We used the same Vps4^{E233Q} allele in a plasmid-shuffling assay to investigate this. Adaptor mutants carrying a plasmid with *ENT1* and *TRP1* were transformed with the Vps4^{E233Q}-expressing plasmid and tested for the capacity to grow in the absence of full-length Ent1; this experiment was performed in a *vps4Δ* strain to address the possibility that Vps4^{E233Q} does not completely inhibit activity of the WT ATPase. In the presence of growth medium containing 5-FAA, cells with Vps4^{E233Q} were inviable without Ent1, as was true for a negative control strain in which the only ENTH domain source was a Trp1 plasmid (Figure 3-6C; right and middle sectors, respectively). In contrast, adaptor mutants receiving an empty vector as opposed to the nonfunctional *vps4* allele remained viable without Ent1, growing on medium with 5-FAA, as expected. In a similar experiment, we were able to verify the prediction that Vps4^{E233Q} is not fully dominant negative; an adaptor mutant strain expressing Vps4^{E233Q} that retained a WT copy of *VPS4* was able to survive without full-length Ent1 (Figure 3-7; YNB +5-FAA, right sector). Nevertheless, this result supports the conclusion that Vps4-mediated disassembly of ESCRTs is necessary not only for normal cargo trafficking from the PM, but also for viability of the adaptor mutant strain.
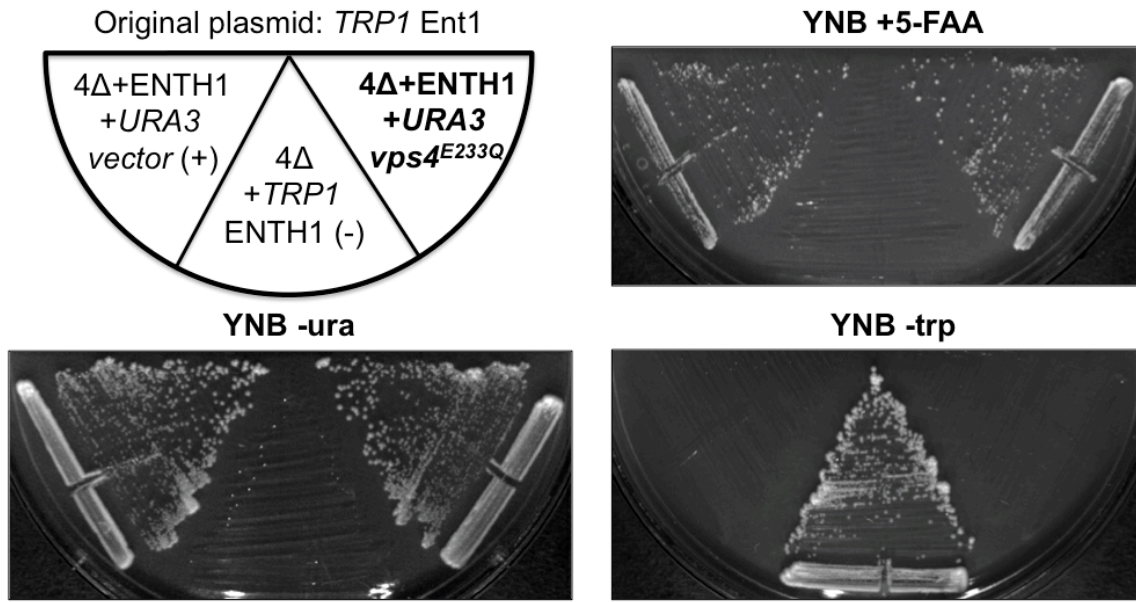
Figure 3-7. Dominant negative phenotype of Vps4^{E233Q} is not fully penetrant. Assay in which a parent strain was transformed with either an empty vector as a positive control (+) or one expressing Vps4^{E233Q} and tested for growth on 5-FAA. Untransformed cells possessing a single copy of an ENTH domain gene on a Trp1 plasmid were included as a negative control for growth on 5-FAA (-).

To determine if the increased cargo concentration seen at the PM in *vps4* mutants is a result of increased endocytic recycling, as opposed to a potentially direct role for Vps4 at the PM of budding yeast, we generated a *vps4Δ rcy1Δ* double mutant expressing Ste3-GFP. Rcy1 is involved in the recycling of endocytosed proteins, returning them to the PM from endosomes (Wiederkehr *et al.*, 2000). As shown above, a pool of Ste3-GFP localized to the PM at higher levels in the absence of Vps4 than in WT cells, in addition to lining vacuoles and revealing E-Class compartments. Ste3-GFP trafficking in an *rcy1Δ* strain alone, however, appeared similar to WT (Figure 3-6D). The double mutant, in contrast, exhibited a distinct cargo trafficking phenotype. In the *vps4Δ rcy1Δ* cells, Ste3-GFP did not accumulate at the PM; instead, the cargo localized mainly to compartments within the cell, which often appeared diffuse (Figure 3-6D; right panel). Though the precise organellar location of Ste3 in the double mutant remains unclear, the fact that this cargo requires Rcy1 to concentrate at the PM indicates that increased endocytic recycling in response to the nonfunctioning of Vps4 contributes to the inefficient trafficking of Ste3 away from the PM.

Interaction between ESCRT and endocytosis mutants appears to be a general phenotype

With the knowledge that adaptor mutants require Vps4 for viability, we assessed several other genes associated with vacuolar protein sorting for synthetic lethality in the 4Δ+ENTH1 background. Unlike genes in the previously presented assay (Figure 3-4B), *VPS24*, which encodes a subunit of the ESCRT-III complex (Babst *et al.*, 1998), does interact genetically with the adaptor mutant. When *VPS24* was deleted from the genome of a parent adaptor mutant strain that possesses the Ent1-Ade8 plasmid, the resulting

Figure 3-8. Interactions exist between other ESCRTs and endocytosis mutants as well.

(A) Sectoring and growth assays, shown in upper and lower panels, respectively, for a parent strain [ΔΔΔΔ(ENTH1)], along with strains that additionally lack either Vps4, as a negative control, or Vps24. Cells were tested for sectoring on rich medium and growth on medium containing 5-FOA. (B) Assay in which a WT, *end3Δ*, *vps4Δ*, and *end3Δ vps4Δ* strain were transformed with an Ura3-End3 plasmid and tested for growth on 5-FOA. Untransformed WT cells were also included to act as a as a negative and positive control for growth on medium lacking uracil and with 5-FOA, respectively. Lower left: WT and *end3Δ* cells expressing Ste3-GFP were grown on rich medium and imaged via live-cell fluorescence microscopy.

Figure on following page.

A

ΔΔΔΔ(ENTH1) + :   -   *vps4Δ*   *vps24Δ*

-Ent1: White
+Ent1: Red

Rich media

Minimal media +5-FOA

B

Minimal medium -uracil

Minimal medium +5-FOA

Ste3-GFP   WT   *end3Δ*
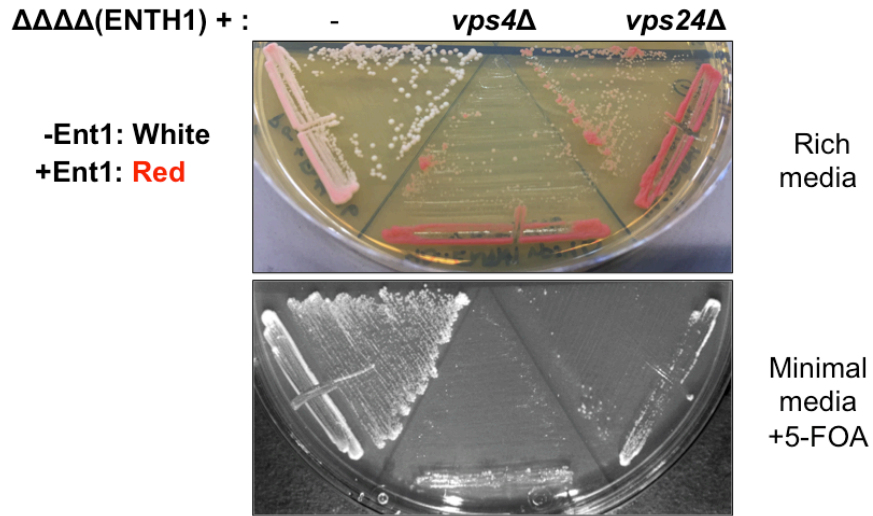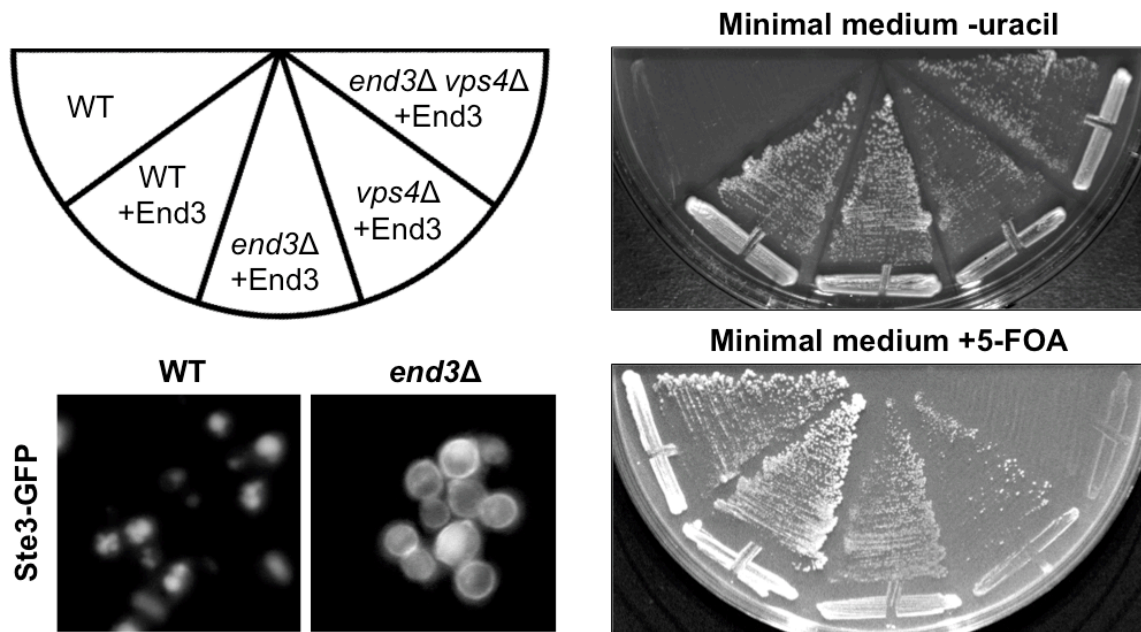
Figure 3-8. Interactions exist between other ESCRTs and endocytosis mutants as well.

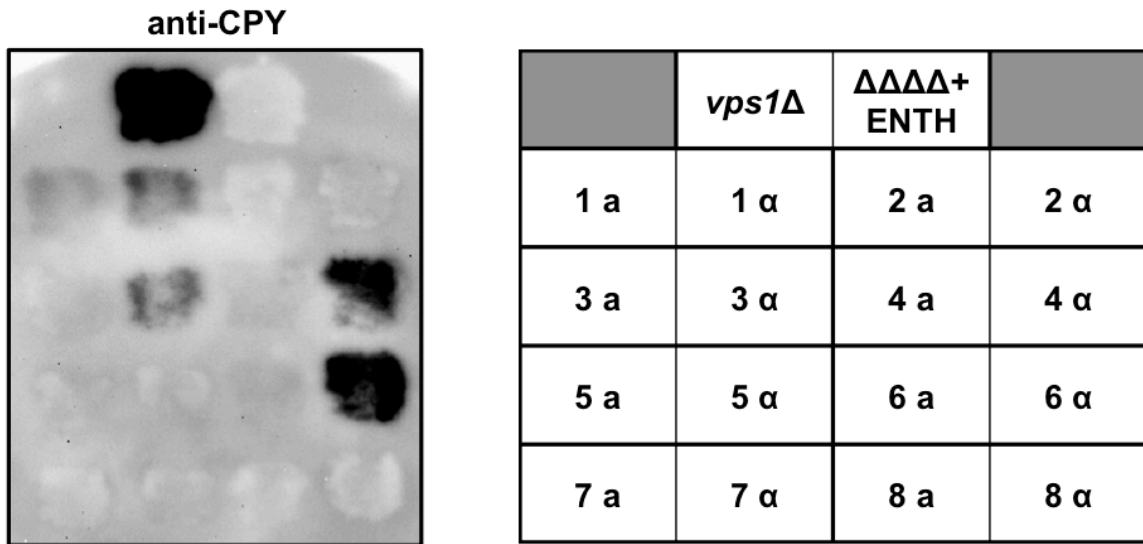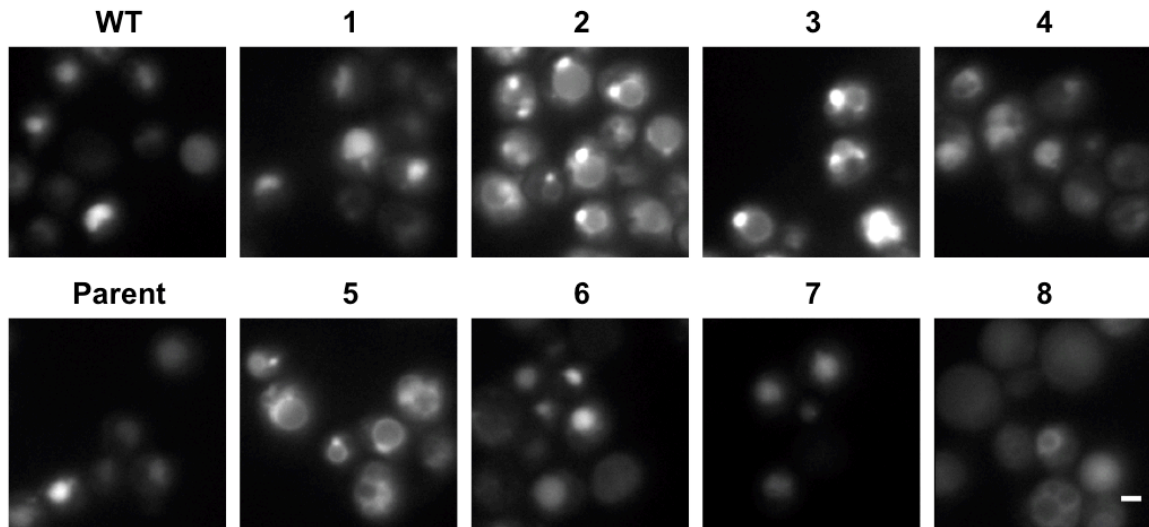mutant formed non-sectoring colonies (Figure 3-8A). Though the colonies formed by these cells appeared non-sectored on rich medium, this strain with an additional *vps24* mutation did generate several slow-forming colonies on medium with 5-FOA. From these results, we conclude that while the loss of Vps24 activity is not completely lethal to adaptor mutant cells, it does produce a strongly negative genetic interaction.

We also deleted *VPS4* in combination with a gene that is vital to the functioning of CME to determine if interaction with this AAA is specific to the adaptor mutant background. End3 is an endocytic protein that acts in conjunction with Pan1 and Sla1 (Tang *et al*., 1997; Tang *et al*., 2000). Without functional End3, cells exhibit endocytosis defects that are similar to adaptor mutants, including the nonspecific concentration of protein cargos at the PM (Raths *et al*., 1993) (Figure 3-8B; lower left). We transformed *end3Δ* cells with a *URA3* cover plasmid that expresses End3, subsequently deleting *VPS4* from the genome and testing the resulting double mutants ability to lose the End3 plasmid. Similar to a WT strain, the individual *end3Δ* and *vps4Δ* strains were able to grow on medium with 5-FOA; in contrast, the double mutant did not form colonies (Figure 3-8B). This finding indicates that cells lacking both End3 and Vps4 are inviable and reveals the existence of negative genetic interactions between multiple different mutations that interrupt CME functioning and the deletion of *VPS4*.

Additional CPY assays, in which representative mutants from the other seven complementation groups were tested, also indicated that proper vacuolar protein sorting becomes essential in endocytosis mutants. Data from this experiment demonstrated that many of these mutants also display abnormal vacuolar protein sorting, secreting CPY into the surrounding environment (Figure 3-9A). Though almost all of the tested strains

A

anti-CPY

	vps1Δ	ΔΔΔΔ+ ENTH	
1 a	1 α	2 a	2 α
3 a	3 α	4 a	4 α
5 a	5 α	6 a	6 α
7 a	7 α	8 a	8 α

B

WT   1   2   3   4

Parent   5   6   7   8

Figure 3-9. Other complementation group members exhibit vacuolar protein sorting defects. (A) CPY assay in which synthetic lethal mutant strains were grown against nitrocellulose and probed with anti-CPY antibodies. Positive control: *vps4Δ*; negative control: parent (ΔΔΔΔ+ENTH). (B) Synthetic lethal mutants were transformed with a plasmid expressing GFP-CPS and imaged via live-cell fluorescence microscopy. Scale bar, 2μ.

exhibited greater CPY secretion than the negative control parent strain, members of Groups 1, 3, 4, and 6 also exhibited pronounced staining. Localization of GFP-CPS was also examined. The fluorescently-tagged protein was found in Class-E mutant compartments and not trafficked to the lumen of vacuoles in mutants from Groups 2 and 5, in addition to the Vps4-associated Group 3 (Figure 3-9B). The localization of GFP-CPS also appeared abnormal in many Group 4 cells, and a Group 8 strain exhibited a range of phenotypes, with some cells containing vacuoles ringed with fluorescent protein while others showed no distinct vacuoles. These images further indicate that vacuolar protein sorting defects are common in the synthetic lethal mutants isolated in the colony-sectoring screen. Together, these findings support the hypothesis that proper vacuole protein sorting becomes essential in endocytosis mutants that do not efficiently internalize cargo from the PM.

Discussion

The findings presented here reveal a genetic interaction between Vps4 and the adaptor mutant background. Budding yeast that lack endocytic adaptors and, therefore, exhibit multiple phenotypes associated with the dysfunction of CME, are inviable when Vps4 is also absent from the cell. This interaction was unanticipated, since CME adaptors act at the cytoplasmic surface of the PM while Vps4 is known to act at the surface of MVBs to complete ESCRT-mediated cargo sorting. Cargos nonspecifically concentrate at the PM of adaptor mutant cells, a phenomenon we also observed in *vps4Δ* cells. Whereas cargo accumulation results from interrupted CME in adaptor mutants, it appears that the increased return of proteins to the PM via endocytic recycling is responsible for the buildup that occurs without Vps4. Unlike in cells lacking the *VPS4* gene alone, Ste3 did not appear to localize strongly to the PM in *vps4Δ rcy1Δ* double mutants, which are deficient in endocytic recycling. This suggests that the loss of Vps4 does not directly hinder endocytosis but, instead, directs cargo to return to the cell surface. This redirection is might be related to the inability of *vps4* mutants to move protein into the lumen of endocytic compartments; the cell may utilize the PM as a type of sink for cargo that cannot be processed as quickly by the compromised degradation system.

Determining the reason for the existence of the negative genetic interaction that occurs with the loss of the Vps4 ATPase in endocytic adaptor mutant cells will be an exciting direction for further inquiry. Vps4 has been shown to function in several cellular processes and at many locations within the cell (Christ *et al.*, 2017). For instance, Vps4 has been shown to regulate sterol synthesis (Wang *et al.*, 2005); perhaps this activity is necessary for the viability of adaptor mutant cells. A currently favored hypothesis to

explain this synthetic lethality is that the PM becomes overloaded when these mutations are combined. Though the cell can tolerate the buildup of cargo, or certain cargos, at the PM that occurs with either individual mutant, it is possible that an additive effect makes inefficiency of trafficking from the cell surface intolerable for budding yeast. The discovery of a genetic interaction between a *vps4Δ* strain and the loss of another protein important to CME, End3, supports this idea, since synthetic lethality with non-functional Vps4 does not appear specific to a particular endocytosis mutant. The ability of upregulated Rho1-dependent CIE to rescue the lethality of Vps4 loss from adaptor mutants also suggests that the source of the negative interaction is a reduced rate of endocytosis in general. Together, these findings indicate that a relationship with Vps4 is not specific to the adaptor mutant background but is likely a general phenotype of yeast CME mutants.

Similarly, experiments with another ESCRT, Vps24, demonstrated that it interacts negatively with the adaptor mutant cells as well; although, mutation of this gene is not completely lethal under these conditions. Perhaps many ESCRT proteins will demonstrate a similar relationship. The fact that adaptor mutants remain viable with deletion of *VPS24*, while the absence of Vps4 is synthetic lethal, implies that some ESCRT-related mutations in cells without fully functional CME are more severe than others. This finding also supports the idea that genetic interactions may be common between adaptor mutants other genes encoding ESCRT proteins. In the future, it will be interesting to determine the importance of additional ESCRTs and vacuolar protein sorting-associated genes in the adaptor mutant.

Finally, is there a maximum concentration of cargo, or particular cargos, at the PM that a cell can tolerate? Methionine becomes toxic to the cell at high concentrations, which is the reason that its transporter, Mup1, is rapidly downregulated after a shift from low to high methionine conditions via removal from the PM (Isnard *et al*., 1996; Farrell *et al*., 2015; Prosser *et al*., 2016). Though cargo overloading at the PM leading to inviability of cells under standard growth conditions has not been previously reported, we may have identified a genetic scenario in which this occurs. Perhaps the combined loss of endocytic adaptors and Vps4 function leaves the cell unable to sufficiently remove certain transporters or other proteins from the PM. Alternative hypotheses to explain the synthetic lethality of nonfunctional Vps4 in the adaptor mutant strain include the idea that ubiquitin, a modifier important for cargo trafficking at the PM as well as MVBs (Cenciarelli *et al*., 1992; Katzmann *et al*., 2001), becomes depleted within the cytoplasm. With ubiquitinated cargos largely trapped at the PM and in ESCRT complexes that fail to disassemble, the cytoplasmic pool of this important protein may decrease below a threshold concentration required for cell viability under these conditions. Another possibility is that loss of this ATPase causes aberrant recycling of damaged proteins. In a WT strain, the cell may accommodate the recycling of these damaged cargos; however, without CME, cargo internalization is already generally inhibited. A CME deficiency may cause the damaged molecules to accumulate to concentrations above a range of the cell can tolerate.

Another question arising from data obtained in the screen is why Vps4 was identified, specifically, as opposed to other ESCRT-related factors. Vps4 might be the only such endosomal protein whose presence is absolutely essential in the adaptor

mutant, with all other ESCRT complex-associated mutants eventually sectoring during our confirmation tests and unselected for further research. This may have occurred for *vps24* mutants, for example. It is also possible that mutations of additional ESCRT proteins are represented in other complementation groups for which the causative gene has yet to be identified. The eventual discovery of other ESCRT mutations in these additional groups appears highly probable, as many of the synthetic lethal complementation groups possess mutants exhibiting vacuolar protein sorting defects. This work describes an important relationship between endocytosis and ESCRT complexes, and results of the colony-sectoring screen that identified this interaction may continue to yield important clues for understanding interactions between endocytic mechanisms and vacuole protein sorting in general.

Materials and Methods

Strains and plasmids

A complete list of strains and plasmids used in this study can be found in Table 3-1 and Table 3-2, respectively. Strains were constructed using PCR-based genomic integration as described previously (Longtine *et al*., 1998; Goldstein and McCusker, 1999; Nishimura *et al*., 2009). For genomic integration of GFP or pHluorin, we designed primers using the F2 and R1 plasmid-specific sequences (Longtine *et al*., 1998). Transformations were performed according to standard procedures using the lithium acetate method, and integrations were confirmed by colony PCR and/or Western immunoblotting (data not shown).

Genomic library

The genomic library utilized in this study was generated by cloning of 8-10 kb fragments of genomic DNA from *Saccharomyces cerevisiae* into BamHI/Bgl II digested pRS200 vector (Connelly and Hieter, unpublished).

CPY assay

Cells were struck on agar plates and a nitrocellulose membrane placed directly onto the agar, covering all areas of the plate with cells. Cells were then allowed to grow overnight. The membrane was then lifted from the agar and the cells washed away from the membrane with TBST buffer. The nitrocellulose was then immunoblotted with mouse anti-CPY antibodies (1:1,000; Molecular Probes) and HRP-conjugated goat anti-mouse secondary antibodies (1:5,000) prior to exposure.

Table 3-1. Strains used in this chapter.

Strain	Genotype	Source
BWY5678	*MATa leu2-3,112 ura3-52 his3-Δ200 trp1-Δ901 suc2-Δ9 lys2-801; GAL ent1::ENTH1::KAN ent2::HIS3 yap1801::HIS3 yap1802::LEU2 ade2::NAT ade8::NAT +pBW2141*	This study
BWY5679	*MATα leu2-3,112 ura3-52 his3-Δ200 trp1-Δ901 suc2-Δ9 lys2-801; GAL ent1::ENTH1::KAN ent2::HIS3 yap1801::HIS3 yap1802::LEU2 ade2::HPH ade8::HPH +pBW2141*	This study
BWY6968	*MATa his3Δ1 leu2Δ0 met15Δ0 ura3Δ0 vps4::KAN*	Winzeler *et al.*, 1999
SEY6210	*MATa leu2-3,112 ura3-52 his3-Δ200 trp1-Δ901 suc2-Δ9 lys2-801; GAL*	Laboratory strain
BWY6684	*MATα leu2-3,112 ura3-52 his3-Δ200 trp1-Δ901 suc2-Δ9 lys2-801; GAL ent1::ENTH1::KAN ent2::HIS3 yap1801::HIS3 yap1802::LEU2 ade2::HPH ade8::HPH vps4::NAT +pBW2141*	This study
BWY6950	*MATα leu2-3,112 ura3-52 his3-Δ200 trp1-Δ901 suc2-Δ9 lys2-801; GAL ent1::ENTH1::KAN ent2::HIS3 yap1801::HIS3 yap1802::LEU2 ade2::HPH ade8::HPH vta1::NAT +pBW2141*	This study
BWY6951	*MATα leu2-3,112 ura3-52 his3-Δ200 trp1-Δ901 suc2-Δ9 lys2-801; GAL ent1::ENTH1::KAN ent2::HIS3 yap1801::HIS3 yap1802::LEU2 ade2::HPH ade8::HPH yta6::NAT +pBW2141*	This study
BWY6952	*MATα leu2-3,112 ura3-52 his3-Δ200 trp1-Δ901 suc2-Δ9 lys2-801; GAL ent1::ENTH1::KAN ent2::HIS3 yap1801::HIS3 yap1802::LEU2 ade2::HPH ade8::HPH vps5::NAT +pBW2141*	This study
BWY6685	*MATa leu2-3,112 ura3-52 his3-Δ200 trp1-Δ901 suc2-Δ9 lys2-801; GAL ent1::ENTH1::KAN ent2::HIS3 yap1801::HIS3 yap1802::LEU2 ade2::NAT ade8::NAT vps4 +pBW2141/ MATα leu2-3,112 ura3-52 his3-Δ200 trp1-Δ901 suc2-Δ9 lys2-801; GAL ent1::ENTH1::KAN ent2::HIS3 yap1801::HIS3 yap1802::LEU2 ade2::HPH ade8::HPH vps4::NAT +pBW2141*	This study
BWY5752	*MATα his3Δ1 leu2Δ0 met15Δ0 ura3Δ0 Ste3-GFP::KAN*	Prosser *et al.*, 2015
BWY6724	*MATα his3Δ1 leu2Δ0 met15Δ0 ura3Δ0 Ste3-GFP::KAN vps4::KAN*	This study
BWY6329	*MATα ura3-1 ade2-1 his3-11 leu2,3112 trp1-1 can1-100 ade2::ADE2 Mep3-GFP::KAN*	Apel, Hoban *et al.*, 2017

BWY6744	*MATα his3Δ1 leu2Δ0 met15Δ0 ura3Δ0 Ste3-GFP::KAN rcy1::KAN*	This study
BWY6743	*MATα his3Δ1 leu2Δ0 met15Δ0 ura3Δ0 Ste3-GFP::KAN vps4::KAN rcy1::KAN*	This study
BWY3037	*MATα leu2-3,112 ura3-52 his3-Δ200 trp1-Δ901 suc2-Δ9 lys2-801; GAL ent1::LEU2 ent2::HIS3 yap1801::HIS3 yap1802::LEU2 Ste3-pHluorin::KAN +pBW778*	Prosser *et al.*, 2011
BWY6949	*MATα leu2-3,112 ura3-52 his3-Δ200 trp1-Δ901 suc2-Δ9 lys2-801; GAL ent1::ENTH1::KAN ent2::HIS3 yap1801::HIS3 yap1802::LEU2 ade2::HPH ade8::HPH vps24::NAT +pBW2141*	This study
BWY3597	*MATα ura3-1 ade2-1 his3-11 leu2,3112 trp1-1 can1-100 ade2::ADE2 Ste3-GFP::KAN*	Prosser, unpublished
BWY6361	*MATα ura3-1 ade2-1 his3-11 leu2,3112 trp1-1 can1-100 ade2::ADE2 Ste3-GFP::KAN end3::NAT*	This study
BWY3012	*MATa his3Δ1 leu2Δ0 met15Δ0 ura3Δ0*	Reider *et al.*, 2009
BWY4991	*MATa his3Δ1 leu2Δ0 met15Δ0 ura3Δ0 end3::KAN*	This study
BWY5730	*MATa his3Δ1 leu2Δ0 met15Δ0 ura3Δ0 end3::KAN vps4::KAN*	This study

Table 3-2. Plasmids used in this chapter.

Plasmid	Details	Source
pBW2141	pRS416::*Ent1, pMET-CEN+Ade8*	This study
pBW1063	pRS416::*GFP-CPS*	Cowles *et al.*, 1997
pRS426	2μ, *URA3*	Laboratory plasmid
pBW1622	pYEP352::*Rom1* (2μ, *URA3*)	Ozaki *et al.*, 1996
pRS416	CEN, *URA3*	Laboratory plasmid
pBW1641	pRS416::*vps4*^{E233Q}	Babst *et al.*, 1997
pBW778	pRS414::*HA-ENTH1*	Baggett *et al.*, 2003
pBW910	pRS416::*End3*	Crnkovich, unpublished

Live-cell fluorescence microscopy

In brief, images were obtained at 30°C using an inverted microscope (Axiovert 200; Carl Zeiss) equipped with a Sensicam (Cooke), an X-Cite 120 PC fluorescence illumination system, and a 100×, 1.4 NA Plan-Apochromat objective lens. Within a given experiment, images were acquired using identical exposure conditions; subsequently, brightness and contrast adjustments were applied equally to all images.

Media and growth conditions

Standard yeast extract/peptone medium with 2% dextrose (YPD) was used for growth of yeast under rich conditions. For ammonium-rich conditions or plasmid maintenance, standard yeast nitrogen base (YNB) medium; containing 38mM ammonium sulfate, 2% dextrose, and appropriate amino acids and nutrients; was used. All yeast were grown at 30°C. For counter-selection growth assays, cells were grown on minimal agar medium containing 4.31 μM 5-FOA for selection against *URA3* or 3.22 μM 5-FAA for selection against *TRP1*.

References

Aguilar RC, Watson HA, Wendland B (2003) The yeast Epsin Ent1 is recruited to membranes through multiple independent interactions. *J Biol Chem* **278:** 10737-43

Aguilar RC, Watson HA, Wendland B (2006) The yeast Epsin Ent1 is recruited to membranes through multiple independent interactions. *J Biol Chem* **278:** 10737-43

Allen RD, Schroeder CC, Fok AK (1992) Endosomal system of Paramecium: coated pits to early endosomes. *J Cell Sci* **101:** 449-61

Apel AR, Hoban K, Chuartzman S, Tonikian R, Sidhu S, Schuldiner M, Wendland B, Prosser D (2017) Syp1 regulates the clathrin-mediated and clathrin-independent endocytosis of multiple cargo proteins through a novel sorting motif. *Mol Biol Cell* **28:** 2434-2448

Azmi I, Davies B, Dimaano C, Payne J, Eckert D, Babst M, Katzmann DJ (2006) Recycling of ESCRTs by the AAA-ATPase Vps4 is regulated by a conserved VSL region in Vta1. *J Cell Biol* **172:** 705-17

Babst M, Sato TK, Banta LM, Emr SD (1997) Endosomal transport function in yeast requires a novel AAA-type ATPase, Vps4p. *EMBO J* **16:** 1820-31

Babst M, Wendland B, Estepa EJ, Emr SD (1998) The Vps4p AAA ATPase regulates membrane association of a Vps protein complex required for normal endosome function. *EMBO J* **17:** 2982-93

Babst (2011) MVB vesicle formation: ESCRT-dependent, ESCRT-independent and everything in between. *Curr Opin Cell Biol* **23:** 452-7

Bender A, Pringle JR (1991) Use of a screen for synthetic lethal and multicopy suppressee mutants to identify two new genes involved in morphogenesis in Saccharomyces cerevisiae. *Mol Cell Biol* **11:** 1295-305

Boeke JD, Trueheart J, Natsoulis G, Fink GR (1987) 5-Fluoroorotic acid as a selective agent in yeast molecular genetics. *Methods Enzymol* **154:** 164-75

Cenciarelli C, Hou D, Hsu KC, Rellahan BL, Wiest DL, Smith HT, Fried VA, Weissman AM (1992) Activation-induced ubiquitination of the T cell antigen receptor. *Science* **257:** 795-7

Christ L, Raiborg C, Wenzel EM, Campsteijn C, Stenmark H (2017) Cellular Functions and Molecular Mechanisms of the ESCRT Membrane-Scission Machinery. *Trends Biochem Sci* **42:** 42-56

Cowles CR, Odorizzi G, Payne GS, Emr SD (1997) The AP-3 adaptor complex is essential for cargo-selective transport to the yeast vacuole. *Cell* **91:** 109-18

Dorfman BZ (1969) The isolation of adenylosuccinate synthetase mutants in yeast by selection for constitutive behavior in pigmented strains. *Genetics* **(2):** 377-89

Dunn, K. W., T. E. McGraw, and F. R. Maxfield (1989) Interactive fractionation of recycling receptors from lysosomally destined ligands in an early sorting endosome. *J Cell Biol* **109:** 3303-3314

Engqvist-Goldstein AEY, Drubin DG (2003) Actin assembly and endocytosis: From yeast to mammals. *Annual Review of Cell and Developmental Biology* **19:** 287-332

Farrell KB, Grossman C, Di Pietro SM (2015) New Regulators of Clathrin-Mediated Endocytosis Identified in Saccharomyces cerevisiae by Systematic Quantitative Fluorescence Microscopy. *Genetics* **201:** 1061-70

Felder S, Miller K, Moehren G, Ullrich A, Schlessinger J, Hopkins CR (1990) Kinase activity controls the sorting of the epidermal growth factor receptor within the multivesicular body. *Cell* **61:** 623-34

Futter CE, Pearse A, Hewlett LJ, Hopkins CR (1996) Multivesicular endosomes containing internalized EGF-EGF receptor complexes mature and then fuse directly with lysosomes. *J Cell Biol* **132:** 1011-23

Goldstein AL, McCusker JH (1999) Three new dominant drug resistance cassettes for gene disruption in Saccharomyces cerevisiae. *Yeast* **15:** 1541-53

Goode BL, Eskin JA, Wendland B (2015) Actin and endocytosis in budding yeast. *Genetics* **199:** 315-58

Gruenberg J, Maxfield FR (1995) Membrane transport in the endocytic pathway. *Curr Opin Cell Biol* **7:** 552-63

Isnard AD, Thomas D, Surdin-Kerjan Y (1996) The study of methionine uptake in Saccharomyces cerevisiae reveals a new family of amino acid permeases. *J Mol Biol* **262:** 473-84

Jones EW and Fink GR (1982) Regulation of amino acid and nucleotide biosynthesis in yeast, 181-299. *In* J. N. Strathern, J. R. Broach, and E. W. Jones (ed.), The molecular biology of the yeast *Saccharomyces*: metabolism and gene expression. Cold Spring Harbor Laboratory Press, Cold Spring Harbor, N.Y.

Kaksonen M, Sun Y, Drubin DG (2003) A pathway for association of receptors, adaptors, and actin during endocytic internalization. *Cell* **115:** 475-87

Kaksonen M, Toret CP, Drubin DG (2005) A modular design for the clathrin- and actin-mediated endocytosis machinery. *Cell* **123:** 305-320

Katzmann DJ1, Babst M, Emr SD (2001) Ubiquitin-dependent sorting into the multivesicular body pathway requires the function of a conserved endosomal protein sorting complex, ESCRT-I. *Cell* **106:** 145-55

Longtine MS, McKenzie A III, Demarini DJ, Shah NG, Wach A, Brachat A, Philippsen P, Pringle JR (1998) Additional modules for versatile and economical PCR-based gene deletion and modification in Saccharomyces cerevisiae. *Yeast* **14:** 953-961

Maldonado-Báez L, Dores MR, Perkins EM, Drivas TG, Hicke L, Wendland B (2008) Interaction between Epsin/Yap180 adaptors and the scaffolds Ede1/Pan1 is required for endocytosis. *Mol Biol Cell* **19:** 2936-48

Marini AM, Soussi-Boudekou S, Vissers S, Andre B (1997) A family of ammonium transporters in Saccharomyces cerevisiae. *Mol Cell Biol* **17:** 4282-93

Mayor, S., J. F. Presley, and F. R. Maxfield (1993) Sorting of membrane components from endosomes and subsequent recycling to the cell surface occurs by a bulk flow process. *J Cell Biol* **121:** 1257-1269

Nishimura K, Fukagawa T, Takisawa H, Kakimoto T, Kanemaki M (2009) An auxin-based degron system for the rapid depletion of proteins in nonplant cells. *Nat Methods* **6:** 917-922

Prosser DC, Whitworth K, Wendland B (2010) Quantitative analysis of endocytosis with cytoplasmic pHluorin chimeras. *Traffic* **11:** 1141-50

Prosser DC, Drivas TG, Maldonado-Báez L, Wendland B (2011) Existence of a novel clathrin-independent endocytic pathway in yeast that depends on Rho1 and formin. *J Cell Biol* **195:** 657-71

Prosser DC, Wrasman K, Woodard TK, O'Donnell AF, Wendland B (2016) Applications of pHluorin for Quantitative, Kinetic and High-throughput Analysis of Endocytosis in Budding Yeast. *J Vis Exp* (116) doi: 10.3791/54587

Raths S, Rohrer J, Crausaz F, Riezman H (1993) end3 and end4: two mutants defective in receptor-mediated and fluid-phase endocytosis in Saccharomyces cerevisiae. *J Cell Biology* **120:** 55-65

Raymond CK, Howald-Stevenson I, Vater CA, Stevens TH (1992) Morphological classification of the yeast vacuolar protein sorting mutants: evidence for a prevacuolar compartment in class E vps mutants. *Mol Biol Cell* **3:** 1389-402

Reider A, Wendland B (2011) Endocytic adaptors--social networking at the plasma membrane. *J Cell Sci* **124:** 1613-1622

Robinson JS, Klionsky DJ, Banta LM, Emr SD (1988) Protein sorting in Saccharomyces cerevisiae: isolation of mutants defective in the delivery and processing of multiple vacuolar hydrolases. *Mol Cell Biol* **8:** 4936-48

Roman H (1956) Studies of gene mutation in *Saccharomyces. Cold Spring Harb Symp Quant Biol* **21:** 175-85

Rothman JH, Howald I, Stevens TH (1989) Characterization of genes required for protein sorting and vacuolar function in the yeast Saccharomyces cerevisiae. *EMBO J* 8: 2057-65

Shaw JD, Hama H, Sohrabi F, DeWald DB, Wendland B (2003) PtdIns(3,5)P2 is required for delivery of endocytic cargo into the multivesicular body. *Traffic* **4:** 479-490

Schnall R, Mannhaupt G, Stucka R, Tauer R, Ehnle S, Schwarzlose C, Vetter I, Feldmann H (1994) Identification of a set of yeast genes coding for a novel family of putative ATPases with high similarity to constituents of the 26S protease complex. *Yeast* **10:** 1141-55

Stoorvogel, W., G. J. Strous, H. J. Geuze, V. Oorschot, and A. L. Schwartz (1991) Late endosomes derive from early endosomes by maturation. *Cell* **65:** 417-427

Stuchell-Brereton MD, Skalicky JJ, Kieffer C, Karren MA, Ghaffarian S, Sundquist WI (2007) ESCRT-III recognition by VPS4 ATPases. *Nature* **449:** 740-4

Tang HY, Munn A, Cai M (1997) EH domain proteins Pan1p and End3p are components of a complex that plays a dual role in organization of the cortical actin cytoskeleton and endocytosis in Saccharomyces cerevisiae. *Mol Cell Biol* **17:** 4294-304

Tang HY, Xu J, Cai M (2000) Pan1p, End3p, and S1a1p, three yeast proteins required for normal cortical actin cytoskeleton organization, associate with each other and play essential roles in cell wall morphogenesis. *Mol Cell Biol* **20:** 12-25

Taylor MJ, Perrais D, Merrifield CJ (2011) A high precision survey of the molecular dynamics of mammalian clathrin-mediated endocytosis. *PLoS Biol* **9:** e1000604

Toyn JH, Gunyuzlu PL, White WH, Thompson LA, Hollis GF (2000) A counterselection for the tryptophan pathway in yeast: 5-fluoroanthranilic acid resistance. *Yeast* **16:** 553-60

van der Sluijs, P., M. Hull, P. Webster, P. Male, B. Goud, and I. Mellman (1992) The small GTP-binding protein rab4 controls an early sorting event on the endocytic pathway. *Cell* **70:** 729-740

Wang P, Zhang Y, Li H, Chieu HK, Munn AL, Yang H (2005) AAA ATPases regulate membrane association of yeast oxysterol binding proteins and sterol metabolism. *EMBO J* **24:** 2989-99

Wendland B, Steece KE, Emr SD (1999) Yeast epsins contain an essential N-terminal ENTH domain, bind clathrin and are required for endocytosis. *EMBO J* **18:** 4383-93

Wiederkehr A, Avaro S, Prescianotto-Baschong C, Haguenauer-Tsapis R, Riezman H (2000) The F-box protein Rcy1p is involved in endocytic membrane traffic and recycling out of an early endosome in Saccharomyces cerevisiae. *J Cell Biol* **149:** 397-410

Yeo SC, Xu L, Ren J, Boulton VJ, Wagle MD, Liu C, Ren G, Wong P, Zahn R, Sasajala P, Yang H, Piper RC, Munn AL (2003) Vps20p and Vta1p interact with Vps4p and function in multivesicular body sorting and endosomal transport in Saccharomyces cerevisiae. *J Cell Sci* **116:** 3957-70

CHAPTER 4

Concluding Remarks

Abstract

Endocytosis is an immensely complex process. The data presented in this dissertation elucidate the workings and importance of some components of the endocytic machinery. Together, these factors act to traffic damaged molecules, or those that are no longer needed, from the cell surface, thereby allowing for effective responses to environmental changes and stresses. Here, we discuss the results described in this dissertation, the conclusions that can be made from these results, and their significance to the endocytosis field, as well as potential future directions for these projects based on this new information. We also consider the future of membrane trafficking research in general, from the questions that still remain to the methods that will be required to address them.

Summary of findings, conclusions, and contributions

Syp1 cargo trafficking

      The identification of additional Syp1 cargos, the ammonium permease, Mep3, and di-/tripeptide transporter, Ptr2, is one of the most important results presented here. The fact that these cargos are involved in the uptake of molecules important for cell growth and division indicates that Syp1 helps to regulate these processes. More specifically, Mep3 being a cargo of this adaptor suggests that Syp1 aids in controlling the concentration of ammonium within the cell. In addition to Mep3 and Ptr2, eight other candidate cargos of Syp1 were identified in the initial screen performed by our collaborator, and it is possible that one or more of these additional candidate cargos represent genuine cargos of Syp1. Perhaps the conditions used by our lab during confirmation of the candidates simply do not induce internalization of the protein; these cargos may only behave as a Syp1 cargo in response to specific growth conditions or temperatures, for example. Alternatively, overexpression of Syp1 may be required to cause of visible change in cargo trafficking, as is the case for Mid2.

      The first novel finding presented in this thesis is that the Syp1 μHD binds to its cargo protein, Mid2, via a DxY motif. Most of the candidate Syp1 cargos also contain this motif, and those that do not have DxY motifs possess biochemically similar amino acid motifs, such as ExY or DxΦ. This further indicates that, under the appropriate conditions, Syp1 may indeed direct the endocytosis of these proteins. Intriguingly, the newly identified Syp1 cargos, Mep3 and Ptr2, possess DxY motifs as well. Mep3 proved to be a highly useful *in vivo* tool for testing the role of DxY motifs in cargo trafficking. We demonstrated that Mep3 is not trafficked into the cell as efficiently without the DxY

motif, and that the rescue of Mep3 internalization upon reintroduction of this motif is Syp1-dependent. Together with our binding assays, these results confirm that Syp1 recognizes DxY motifs. This knowledge improves our ability to identify additional candidate Syp1 targets by searching for DxY motifs in other cargo proteins. Moreover, after a study suggested that Snc1 localization changes in the absence of Syp1 (Burston *et al.*, 2009), Snc1 binding to the μHD was tested due to the fact that a DxY motif is present within the Snc1 cytoplasmic tail. v-SNAREs are an essential component of clathrin-coated pits and vesicles, without which the formed vesicle would be unable to recognize its target compartment within the cell. Evidence that Syp1 contributes to Snc1 trafficking *in vivo* reveals this adaptor to be important for targeting an endocytic vesicle to the appropriate intracellular compartment after scission from the PM.

The connection between Syp1-mediated cargo trafficking and the ammonium concentration in growth medium was also intriguing. Our data established that Mep3 is internalized from the PM for delivery to vacuoles in a Syp1-dependent manner after a switch from rich growth conditions to minimal medium, in which the ammonium concentration is high. Syp1, therefore, plays an integral role in regulating the amount of ammonium within the cell. These results also demonstrate that trafficking of Mep3, a protein with homologues in mammalian cells (Heitman and Agar, 2000), can result from the treatment of budding yeast with ammonium, making it a promising tool for detailed studies of Syp1-cargo interactions. In addition to the upregulation of Mep3 internalization, results from other experiments revealed that the amount of Syp1 at endocytic sites is elevated when the extracellular ammonium concentration is high. This increase of Syp1 at endocytic patches is greater than that observed for another early-

acting protein involved in CME, Ede1, and occurs despite the amount of total Syp1 protein within the cell remaining unchanged. This implies that recruitment of Syp1 to sites of CME is specifically upregulated in response to increased ammonium concentration. Perhaps the presence of additional adaptors at endocytic patches is similarly induced by environmental conditions, with adaptors potentially playing unique roles in adjusting the composition of the PM in response to fluctuating levels of specific nutrients, like Mup1 internalization after increased methionine concentration (Prosser *et al.*, 2016).

In addition to searching for new Syp1 cargos and sorting motifs, we also examined if Syp1-mediated trafficking occurs via CME. This has never been tested, and Syp1 interacts physically with a component of Rho1-dependent CIE, Mid2 (Reider *et al.*, 2009; Prosser *et al.*, 2011). The four known Syp1 cargos all appeared to be primarily internalized via CME. Mid2, Snc1, and Mep3 localized almost entirely to the PM in CME-deficient cells, not only demonstrating that Syp1-mediated endocytosis of these three cargos occurs via CME, but also confirming that Syp1 traffics cargo via this pathway. Ptr2 also exhibited significant buildup at the PM in a CME mutant strain; however, there was evidence of Ptr2 trafficking to the vacuole within many of these cells as well, suggesting that an additional pathway may internalize Ptr2. Indeed, the loss of Bni1, an essential element of Rho1-dependent CIE (Prosser *et al.*, 2011), from cells increased the concentration of Ptr2 at the PM, confirming that this CIE pathway contributes significantly and observably to Ptr2 endocytosis under standard conditions. Ptr2 is the first protein in budding yeast shown to be a dual cargo of both CME and Rho1-dependent CIE.

Having confirmed that Ptr2 is a cargo of the CIE pathway as well as CME, we sought to demonstrate that the CIE component of Ptr2 trafficking is Syp1-dependent. Results of a live-cell, time-lapse microscopy experiment observing cortical actin patches suggested that, though the overexpression of Syp1 does not rescue defects associated with actin dynamics in a strain with disrupted CME (Bénédetti *et al.*, 1994), high-copy Syp1 is able to improve the endocytosis of Ptr2 under these conditions. This finding, combined with other results, suggested that Syp1 acts to promote the internalization of Ptr2 not only by CME, but via Rho1-dependent CIE as well. Therefore, Ptr2 may also become an important tool for studying the cellular decision-making involved in cargo trafficking by multiple endocytic mechanisms. Together, these findings reveal Syp1 to be an adaptor that recognizes multiple cargos through DxY motifs, mediating internalization through either CME or Rho1-dependent CIE, with the loss of Syp1 leading to the specific buildup of its cargos at the PM (Figure 4-1).

Interaction between Vps4 and endocytic adaptors

In another series of experiments described here, we sought to understand an observed negative genetic interaction between our adaptor mutant strain and Vps4. A colony-sectoring assay allowed for the identification of mutations that are lethal in the absence of the Yap180s and majority of the epsins (Maldonado-Báez *et al.*, 2008), producing a requirement of full-length *ENT1* for viability. Results from the sequencing of *VPS4* in these strains revealed mutations, including a frame-shift mutation at residue 8 that introduces a stop codon at residue 11, as well as a missense mutation, D283V. We were surprised to identify Vps4 in our screen for synthetic lethality with the adaptor
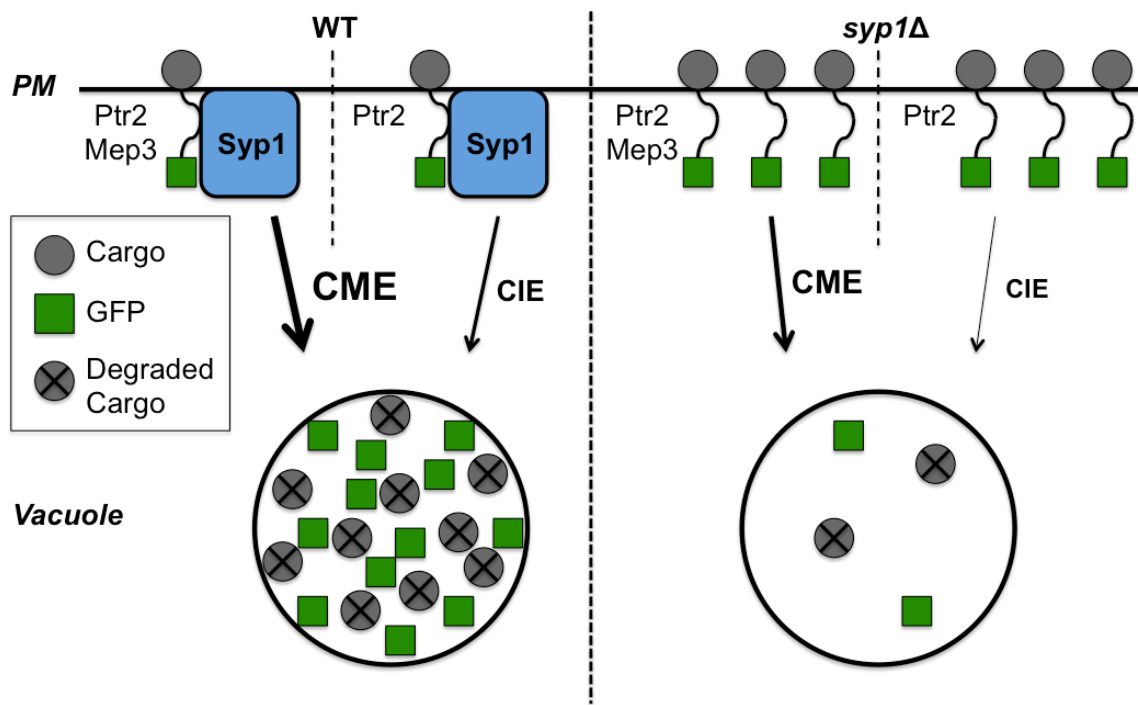
Figure 4-1. Model of Syp1 role in cargo trafficking via CME and Rho1-dependent CIE.

mutant background. Vps4 has been demonstrated to function at MVBs and compartments downstream along the endocytic path to the vacuoles (Robinson *et al.*, 1988; Rothman *et al.*, 1989; Babst *et al.*, 1997). This finding indicates that membrane trafficking events occurring away from the PM may, nonetheless, become essential for cells in which CME has been compromised.

Having determined that Vps4 is essential in adaptor mutant cells, we next aimed to identify the cause of the synthetic lethality. Due to the fact that cargo internalization is severely hindered in adaptor mutants (Maldonado-Báez *et al.*, 2008), we hypothesized that Vps4 also affects this process; the compounding of this phenotype might be the cause of the negative interaction. Indeed, when observing the localization of the GFP-tagged Ste3 protein in the absence of Vps4, we observed an increase in the concentration of Ste3 at the PM relative to WT cells. Additional experiments utilized a catalytically inactive form of Vps4, E233Q, revealing that the ESCRT complex disassembly function of Vps4 is required for normal trafficking of Ste3 away from the PM, as well as for the viability of adaptor mutant cells. Mep3 also accumulated above WT levels at the cell surface in *vps4Δ* cells. The idea that Vps4 activity affects the composition of the PM, and that this is a result of the inability of the cell to disassemble ESCRT complexes, is supported by these findings. The inviability of adaptor mutants expressing catalytically inactive Vps4[E233Q] also demonstrates that the synthetic lethality between Vps4 and the adaptor mutant strain is directly tied to Vps4 ESCRT disassembly activity, not another function of the AAA (Davies *et al.*, 2010). However, the number of cellular processes that Vps4 and other ESCRT proteins are associated with continues to grow (Christ *et al.*, 2017). Whether inviability results from the loss of Vps4 ESCRT disassembly activity at the

surface of MVBs, specifically, as opposed to at the PM or other area within the cell, remains unconfirmed.

Findings from our studies examining cargo trafficking in *vps4* mutants lead us to question whether the buildup of protein cargos at the PM that occurs without Vps4 is a result of enhanced endocytic recycling. In the absence of Vps4, cargos accumulate in compartments adjacent to vacuoles, as occurs in all E-Class vacuolar protein-sorting mutants (Raymond *et al.*, 1992), and we postulated that endocytic recycling of protein cargos might be upregulated in these cells, which are unable to efficiently degrade material via endocytosis to the vacuole lumen. Our data indicate that blocking endocytic recycling in a strain without Vps4 causes Ste3 to localize primarily to diffuse compartments within the cell and not the PM. This suggests that upregulation of endocytic recycling might be the source of cargo accumulation at the PM in a *vps4Δ*.

Without the formation of MVBs, cargos accumulate in Class-E compartments. These compartments may become saturated with internalized cargo that is unable to be sufficiently degraded. It is possible that the cell responds to the intracellular accumulation of cargo in vacuolar protein sorting mutants by redirecting protein and lipids back to the PM through recycling endosomes, since the yeast PM is able to accommodate concentrations of protein cargos that are well above the concentration observed in WT yeast. For example, the amount of Ste3 protein at the PM of the adaptor mutant is drastically higher than when these adaptors are present, yet the cells remain viable (Maldonado-Báez *et al.*, 2008; Prosser *et al.*, 2011). Therefore, the PM might act as a sink for cargos that cannot be tolerated or processed within E-class compartments of vacuolar protein sorting mutants, such as *vps4Δ* strain. However, the synthetic lethality

between Vps4 and the adaptor mutant strain, combined with the enhanced endocytic recycling observed in the absence of Vps4, could indicate that there is an upper limit to the amount of material the PM can handle. Without the four adaptor proteins, cargos nonspecifically accumulate at the PM, and it is possible that, without efficient degradation downstream, recycling of internalized material in a strain that also lacks Vps4 leads to overloading of the PM (Figure 4-2).

Nonetheless, there are other possible explanations for the genetic interaction between loss of both endocytic adaptors and Vps4. For instance, Vps4 has also been shown to play a role in sterol synthesis (Wang et al., 2005), and this function could potentially become indispensable in a CME-deficient strain. Additionally, findings in the study that first identified Vps4, which was then designated End13, were consistent with normal cargo internalization proficiency (Munn and Riezman, 1994). The researchers investigated α-factor internalization in the *vps4* mutant strain and observed only a subtle reduction in the trafficking of this mating pheromone into the cell. However, if increased cargo localization to the PM in the absence of Vps4 is indeed a result of enhanced endocytic recycling, one might expect a ligand such as α-factor to be internalized normally, even if the trafficking of its receptor is altered after removal from the PM. One thing is certain: revealing the reason for the inviability of adaptor mutant cells without functional Vps4 will be an exciting focus of future work.

We also found that negative genetic interactions with Vps4 are not specific to the adaptor mutant strain; the loss of End3 is also synthetic lethal with a *vps4Δ* strain. Therefore, it is possible that additional, perhaps even most, mutations that generally disrupt cargo trafficking from the PM will be similarly inviable in the absence of Vps4.
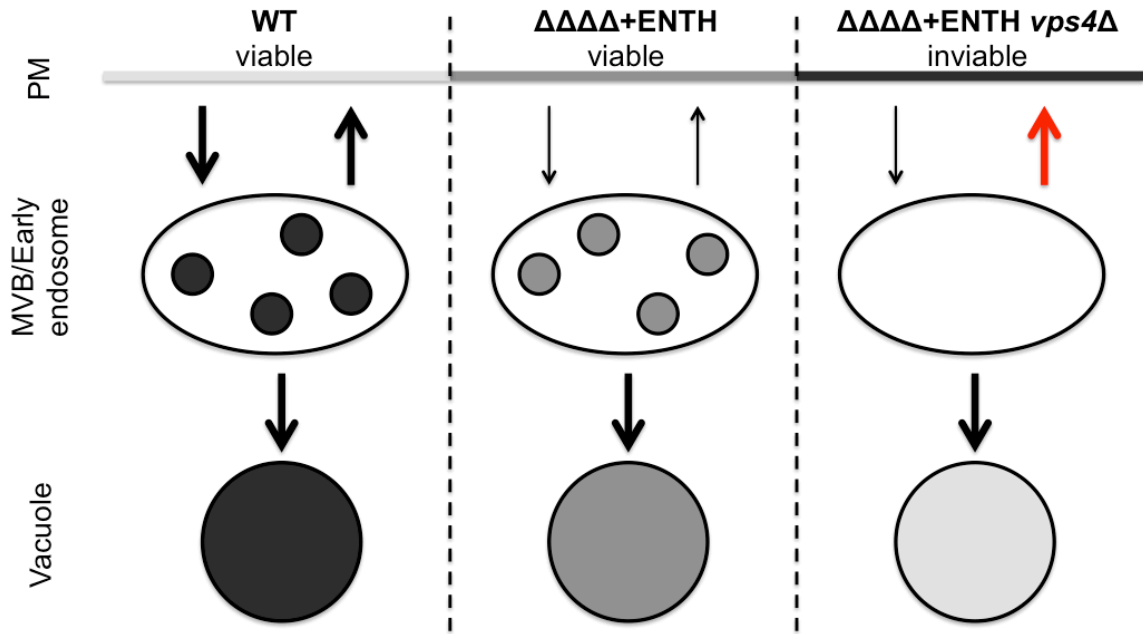
Figure 4-2. Model of cause for synthetic lethality between *vps4* and adaptor mutants. Arrows from PM to MVB/Early endosome, and from MVB/Early endosome to Vacuole indicate movement into the cell along the endocytic pathway. Arrows from the MVB/Early endosome to the PM indicate endocytic recycling. In this working model, the red arrow represents the recycling of endocytic cargo to the PM, which might be the cause of cell inviability through overloading of the PM with cargo.

For instance, the deletion of clathrin under these conditions may produce a synthetic lethal phenotype. The results of additional tests with other endocytic factors necessary for the proper functioning of CME will help to determine if this is true. Similarly, Vps4 does not appear to be the only component of the ESCRT machinery that is necessary for viability of the CME mutant; we identified the deletion of *VPS24* to interact negatively with the adaptor mutant background as well.

Interestingly, Vps24 is not associated with ESCRT disassembly like Vps4, but is instead part of the ESCRT-III complex responsible for the major membrane remodeling that occurs during ESCRT assembly (Babst *et al*., 1998). This provides another piece of evidence to support the idea that the ability of the cell to efficiently generate MVBs is the activity that becomes essential in endocytosis mutants. However, we also determined that not all proteins associated with ESCRT complexes are necessary for the viability of adaptor mutants; Vta1 is not essential for viability of the adaptor mutant despite being a binding partner of Vps4. Therefore, it is possible that only mutation of ESCRT-related genes that sufficiently hinder the movement of cargo-containing vesicles into the lumen of endocytic compartments will be lethal to CME mutants.

One of the most unexpected findings from the synthetic lethal screen is that mutants from many complementation groups other than the one from which Vps4 was identified also exhibited vacuolar protein sorting defects when we observed GFP-CPS localization and assayed CPY secretion. It is conceivable that protein trafficking between other compartments, such as the early endosome and Golgi, for instance, becomes crucially important when endocytosis at the PM is interrupted. Though additional experiments will be required to test these hypotheses, it is evident from our results that

cells lacking the ability to internalize material via CME are more sensitive to additional

mutations affecting vacuolar protein sorting, highlighting the importance of the endocytic

machinery.

References

Babst M, Sato TK, Banta LM, Emr SD (1997) Endosomal transport function in yeast requires a novel AAA-type ATPase, Vps4p. *EMBO J* **16:** 1820-31

Babst M, Wendland B, Estepa EJ, Emr SD (1998) The Vps4p AAA ATPase regulates membrane association of a Vps protein complex required for normal endosome function. *EMBO J* **17:** 2982-93

Bénédetti H, Raths S, Crausaz F, Riezman H (1994) The END3 gene encodes a protein that is required for the internalization step of endocytosis and for actin cytoskeleton organization in yeast. *Mol Biol Cell* **5:** 1023-37

Burston HE, Maldonado-Báez L, Davey M, Montpetit B, Schluter C, Wendland B, Conibear E (2009) Regulators of yeast endocytosis identified by systematic quantitative analysis. *J Cell Biol* **185:** 1097-1110

Christ L, Raiborg C, Wenzel EM, Campsteijn C, Stenmark H (2017) Cellular Functions and Molecular Mechanisms of the ESCRT Membrane-Scission Machinery. *Trends Biochem Sci* **42:** 42-56

Davies BA, Azmi IF, Payne J, Shestakova A, Horazdovsky BF, Babst M, Katzmann DJ (2010) Coordination of substrate binding and ATP hydrolysis in Vps4-mediated ESCRT-III disassembly. *Mol Biol Cell* **21:** 3396-408

Heitman J and Agre P (2000) A new face of the Rhesus antigen. *Nature Genetics* **26:** 258-259

Maldonado-Báez L, Dores MR, Perkins EM, Drivas TG, Hicke L, Wendland B (2008) Interaction between Epsin/Yap180 adaptors and the scaffolds Ede1/Pan1 is required for endocytosis. *Mol Biol Cell* **19:** 2936-48

Munn AL1, Riezman H (1994) Endocytosis is required for the growth of vacuolar H(+)-ATPase-defective yeast: identification of six new END genes. *J Cell Biol* **127:** 373-86

Prosser DC, Drivas TG, Maldonado-Báez L, Wendland B (2011) Existence of a novel clathrin-independent endocytic pathway in yeast that depends on Rho1 and formin. *J Cell Biol* **195:** 657-71

Prosser DC, Wrasman K, Woodard TK, O'Donnell AF, Wendland B (2016) Applications of pHluorin for Quantitative, Kinetic and High-throughput Analysis of Endocytosis in Budding Yeast. *J Vis Exp* **116** doi: 10.3791/54587

Raymond CK, Howald-Stevenson I, Vater CA, Stevens TH (1992) Morphological classification of the yeast vacuolar protein sorting mutants: evidence for a prevacuolar compartment in class E vps mutants. *Mol Biol Cell* **3:** 1389-402

Reider A, Barker SL, Mishra SK, Im YJ, Maldonado-Báez L, Hurley JH, Traub LM, Wendland B (2009) Syp1 is a conserved endocytic adaptor that contains domains involved in cargo selection and membrane tubulation. *Embo J* **28:** 3103-3116

Robinson JS, Klionsky DJ, Banta LM, Emr SD (1988) Protein sorting in Saccharomyces cerevisiae: isolation of mutants defective in the delivery and processing of multiple vacuolar hydrolases. *Mol Cell Biol* **8:** 4936-48

Rothman JH, Howald I, Stevens TH (1989) Characterization of genes required for protein sorting and vacuolar function in the yeast Saccharomyces cerevisiae. *EMBO J* 8: 2057-65

Wang P, Zhang Y, Li H, Chieu HK, Munn AL, Yang H (2005) AAA ATPases regulate membrane association of yeast oxysterol binding proteins and sterol metabolism. *EMBO J* **24:** 2989-99

APPENDICES

Appendix I

High-copy Tus1 restores viability of adaptor mutants possessing synthetic lethal alleles

Introduction

In addition to the work on Vps4, the colony-sectoring screen for synthetic lethal alleles in the adaptor mutant background has also yielded other interesting results. This short piece details results obtained from the study of mutants in Complementation Group 6, which demonstrate that the presence of a plasmid containing a portion of the gene for Tus1, a guanine nucleotide exchange factor (GEF) for Rho1 (Schmelzle *et al*., 2002), can allow the cells to grow without full-length Ent1. Here, we present evidence that Tus1 can indeed rescue the viability of a strain from this complementation group. Our findings also indicate that, when overexpressed, Tus1 can restore the viability of synthetic lethal mutants from other complementation groups, as well as rescue cargo trafficking in adaptor mutants.

Results

After transforming Complementation Group 6 mutants with genomic library, as
for Group 3 (Figure 3-2A), we next aimed to identify the plasmid-borne genes that
rescued the synthetic lethality. After isolating and sequencing plasmids from a number of
colonies, we found that one contained a fragment of the gene encoding the N-terminal
end of Tus1, the Rho1 GEF (Figure AI-1A). However, a prediction regarding domain
organization in Tus1, made using the simple modular architecture research tool
(SMART) (Schultz et al., 1998; Letunic *et al.*, 2015), indicates that the portion of this
protein that would be expressed from this plasmid contains just two conserved, proline-
rich regions and not the GEF domain (Figure AI-1A). Therefore, we tested the ability of
full-length Tus1 to rescue the Ent1 requirement of synthetic lethal mutants in this
complementation group. Encouragingly, mutants transformed with Tus1 were able to
shed the original Tus1-containg library plasmid and produce slow-growing colonies on
medium containing 5-FAA, unlike untransformed cells (Figure AI-1B). The outcome of
this experiment suggests that Tus1 can indeed rescue the inviability of this mutant.

Two additional GEFs for Rho1, Rom1 and Rom2 (Ozaki *et al.*, 1996; Byrne and
Wolfe, 2005), have been confirmed to upregulate the Rho1-dependent clathrin-
independent endocytic (CIE) pathway in budding yeast (Prosser *et al.*, 2011). Thus, we
transformed adaptor mutant cells expressing Ste3-GFP with a high-copy Tus1 plasmid to
determine if overexpression of this Rho1 GEF can replicate previously published results
in which Rom1 restores the internalization of Ste3 in cells lacking endocytic adaptors.
Whereas adaptor mutants with full-length Ent1 exhibited Ste3-GFP localization

163

A

B
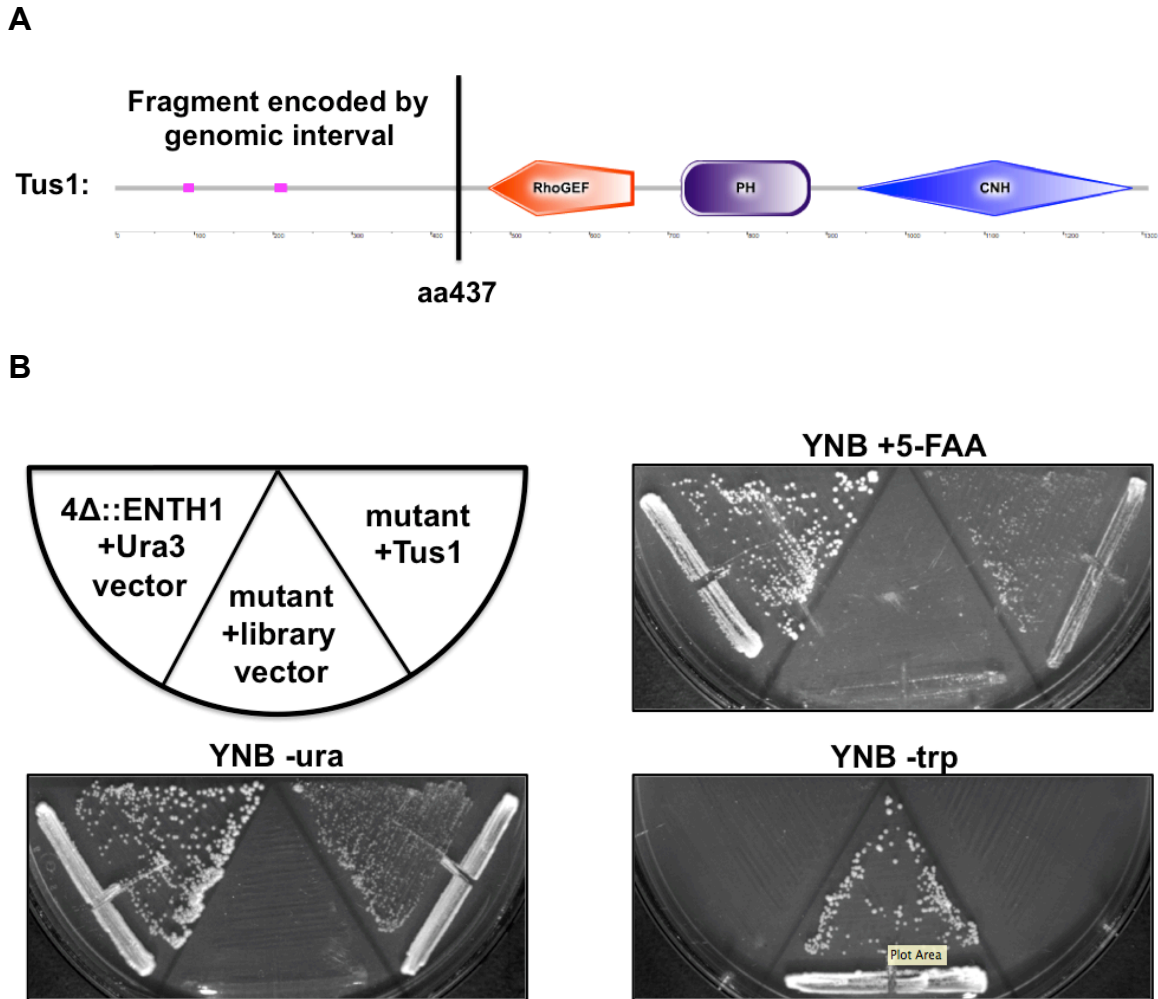
Figure AI-1. Tus1 rescues growth of a synthetic lethal mutant. (A) Diagram of Tus1 protein, including predicted domains, generated using the simple modular architecture research tool (SMART) protein domain predictor (Schultz et al., 1998; Letunic *et al.*, 2015). Pink indicates conserved, poly-proline region. (B) Assay in which a synthetic lethal mutant was transformed with a Ura3-Tus1 plasmid and tested for growth on 5-FAA. Adaptor mutant cells transformed with an empty Ura3 vector and the synthetic lethal mutant possessing the rescuing library plasmid were also included, acting as a positive and negative control for growth in the presence of 5-FAA, respectively.

comparable to WT, the fluorescent cargo accumulated at the PM in mutant cells with only the ENTH domain, as expected (Figure AI-2A). However, Ste3-GFP trafficking into the cell was largely rescued when Tus1 was overexpressed. These findings were corroborated by quantification of fluorescent signal from similar cells that express pHluorin-fused Ste3 instead of GFP (Figure AI-2A). Interestingly, this rescue may in fact be due to upregulation of the Rho1-dependent CIE pathway. Unlike adaptor mutant cells that lack Bnr1, the loss of Bni1 inhibits Tus1 restoration of Ste3 endocytosis (Figure AI-2B); Bni1 is a yeast formin that is required for functioning of this CIE mechanism (Kohno *et al*., 1996; Prosser *et al*., 2011). Therefore, Tus1 may be another Rho1 GEF that functions in yeast CIE.

Having verified that Tus1 can rescue Ste3 trafficking in adaptor mutants when overexpressed, we next sought to establish whether high-copy Tus1 can restore the viability of mutants in other complementation groups without full-length Ent1. To do this we again utilized a Tus1 overexpression plasmid, transforming cells from Groups 5 and 7. When Tus1 expression was enhanced, mutants from both groups generated slow-forming colonies on medium containing 5-FAA (Figure AI-3, A and B). In this experiment, 5-FAA counter-selects against the rescuing plasmid the cells obtained during the genomic library transformation (Figure 3-2A). The ability of high-copy Tus1 to rescue the viability of mutants from multiple complementation groups supports the hypothesis that this GEF can regulate Rho1-dependent CIE activity.

Figure AI-2. High-copy Tus1 rescues Ste3 internalization in adaptor mutants. (A) WT and adaptor mutant cells with either full-length Ent1 or only an ENTH domain expressing Ste3-GFP were transformed with either an empty or Tus1-expressing high-copy plasmid and grown on rich medium prior to imaging by fluorescence microscopy. Scale bar, 2 μm. Intensity of Ste3-pHluorin was quantified for each condition; intensity values were corrected for cell size and expressed in arbitrary units (a.u.) (error bars indicate mean ± SEM; **, $P < 0.01$; ***, $P < 0.001$; ****, $P < 0.0001$ compared to WT). (B) Adaptor mutant cells also lacking either Bnr1 or Bni1 and expressing Ste3-GFP were transformed with a high-copy Tus1 plasmid and grown on rich medium prior to imaging by fluorescence microscopy. Intensity of Ste3-pHluorin was quantified for each condition; intensity values were corrected for cell size and expressed in arbitrary units (a.u.) (error bars indicate mean ± SEM; ****, $P < 0.0001$ compared to WT).

Figure on following page.
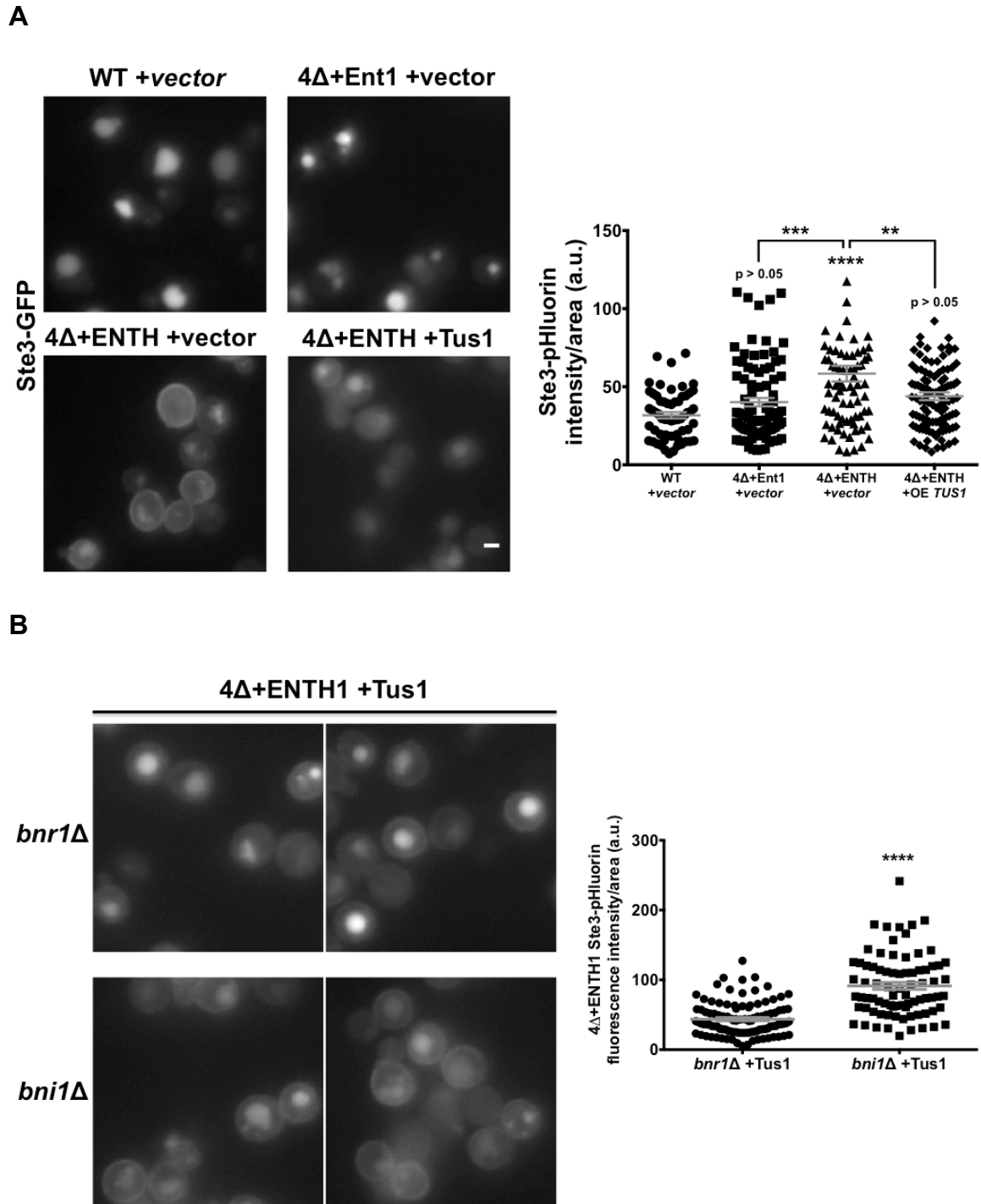
Figure AI-2. High-copy Tus1 rescues Ste3 internalization in adaptor mutants.
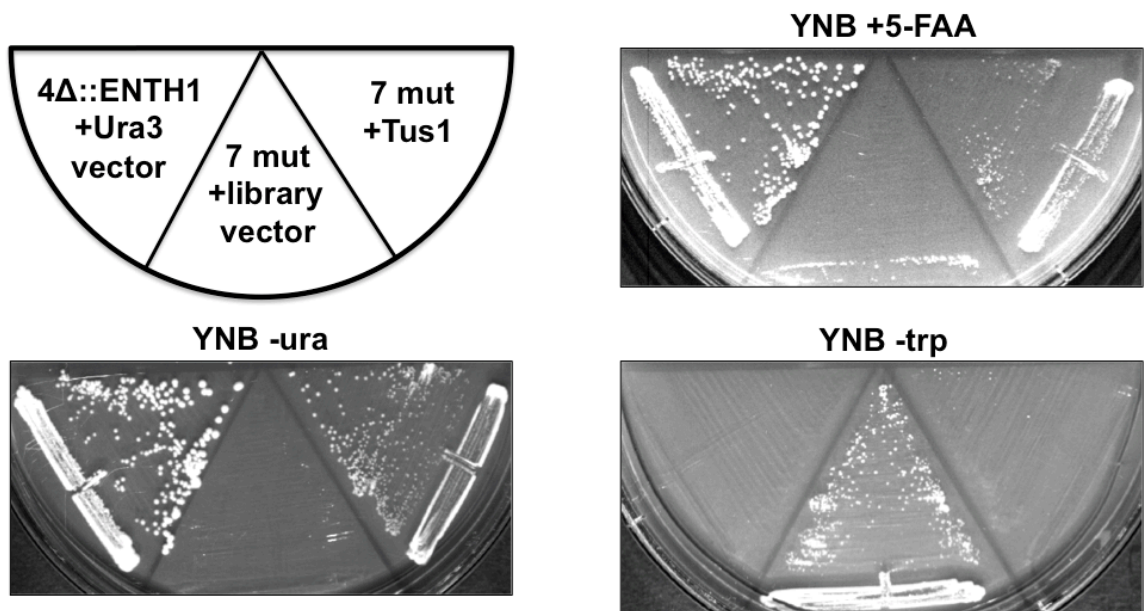
Figure AI-3. Cells overexpressing Tus1 do not require full-length Ent1 for viability. (A) Assay in which a synthetic lethal mutant was transformed with a high-copy Ura3-Tus1 plasmid and tested for growth on 5-FAA. Adaptor mutant cells transformed with an empty Ura3 vector and the synthetic lethal mutant possessing the rescuing library plasmid were also included, acting as a positive and negative control for growth in the presence of 5-FAA, respectively. (B) Assay in which a synthetic lethal mutant was transformed with a high-copy Ura3-Tus1 plasmid and tested for growth on 5-FAA. Adaptor mutant cells transformed with an empty Ura3 vector and the synthetic lethal mutant possessing the rescuing library plasmid were also included, acting as a positive and negative control for growth in the presence of 5-FAA, respectively.

Figure on following page.

A
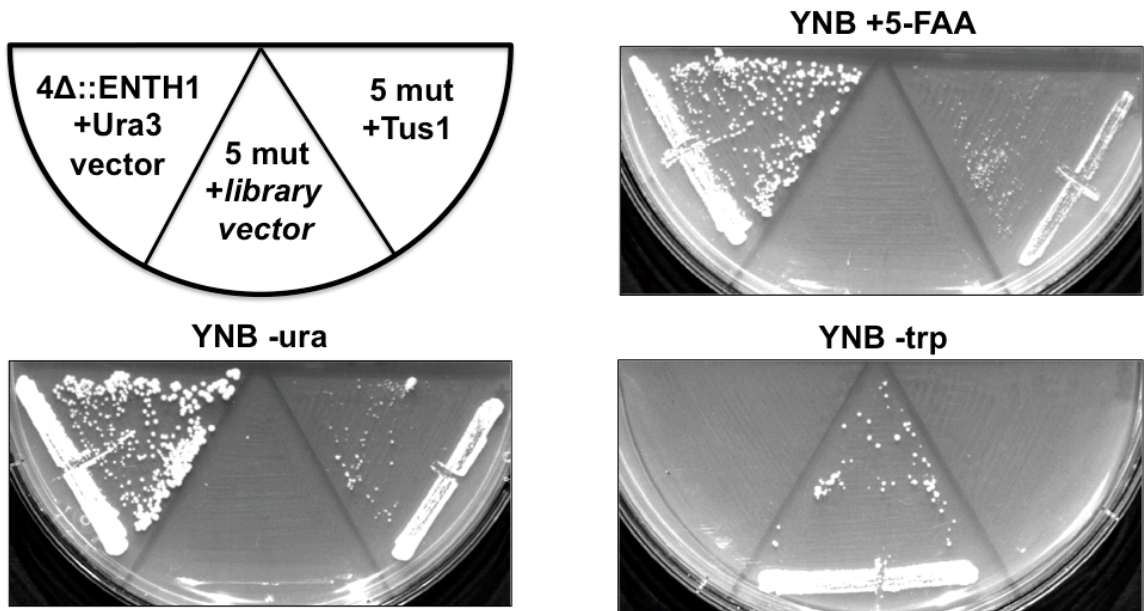
B

Figure AI-3. Cells overexpressing Tus1 do not require full-length Ent1 for viability.

Discussion

The data presented here suggest that Tus1 can rescue viability of mutagenized cells that lack endocytic adaptor proteins, but whether the loss of Tus1 is actually synthetic lethal with the adaptor mutant background remains unclear. One reason for this is that the *TUS1* fragment present on the single plasmid able to restore viability of the mutant in this complementation group expresses none of the Tus1 functional domains, including the RhoGEF domain. Perhaps this region of Tus1 is mutated in the synthetic lethal strain, leading to inviability without full-length Ent1, and the WT copy of the gene allows for rescue of its function as anticipated. Perhaps this Tus1 region is necessary for activation of the GEF. However, another possibility is that the *TUS1* N-terminus is not mutated in this strain, but an importance of this segment of the protein to Rho1-dependent CIE functioning allows for the extra copy of the gene fragment to rescue viability of the mutant cells. This region of Tus1 may be important for interactions with other proteins, for example, potentially being responsible even for bringing the Tus1 RhoGEF domain to Rho1. Enhanced recruitment of such proteins via the Tus1 N-terminus may sufficiently upregulate the CIE pathway to allow for rescue of synthetic lethal mutant viability. Sequencing the *TUS1* gene in these synthetic lethal mutants will provide greater clarity. In the future, it will be interesting to determine whether such dosage compensation is the source of rescued viability by Tus1, or if this gene indeed possesses a negative genetic relationship with the adaptor mutants.

It will also be exciting to verify Tus1 involvement in Rho1-dependent CIE. The preliminary findings included here indicate that Tus1 can restore the trafficking of Ste3-GFP in adaptor mutant cells to a near-WT level when overexpressed, and this appears to

be dependent on CIE; when a formin that is essential for the functioning of this pathway is deleted from the genome, the ability of Tus1 to improve Ste3 trafficking was abolished. A definitive experiment will combine the two experiments presented in Figure AI-2 and allow for direct comparison of Tus1-rescued adaptor mutants to those that also lack one of the two formins, Bnr1 or Bni1. Nonetheless, findings from growth assays with other synthetic lethal mutants that overexpress Tus1 support initial Ste3 imaging results (Figure AI-3). The capability of high-copy Tus1 to allow synthetic lethal mutants from multiple other complementation groups to grow without full-length Ent1 also suggests that Tus1 may be involved in an endocytic mechanism. Therefore, this GEF is a promising target for further research of Rho1-dependent CIE.

Appendix II

Loss of Pkc1 results in relocalization of the CME machinery

Introduction

Clathrin-mediated endocytosis (CME) occurs in a highly polarized fashion, with endocytic patches forming more commonly in the bud and neck of dividing cells. During the initiation of an endocytic event, adaptor proteins localize to the plasma membrane (PM) in a punctate fashion when observed by microscopy. One of the first adaptors to arrive at sites of endocytosis is Syp1 (Reider *et al*., 2009). Like most proteins associated with CME, Syp1 is found at endocytic patches, which predominantly occur within buds, but Syp1 also localizes to the bud tip and neck (Reider *et al*. 2009). A recent study demonstrated that the deletion of *PKC1*, a gene encoding the budding yeast protein kinase C homologue (Levin *et al*., 1990), causes Syp1 localization to the bud neck, specifically, to become even more pronounced than in WT cells (Merlini et al., 2015). However, it remains unknown how the loss of Pkc1 from cells affects the localization of other endocytic proteins. Due to the role of Syp1 in the initiation of CME events, is the positioning of later-arriving endocytic proteins affected by the absence of Pkc1 kinase activity as well? In this brief report, we present evidence that relocalization in a *pkc1Δ* is not specific to Syp1, but is true of the late-coat protein, Pan1, as well. In addition to this commonality, we also discuss the implications of differences between the endocytic patch phenotypes of Syp1 and Pan1 in a *pkc1* mutant.

Results

To test the role of Pkc1 in the polarization of endocytic proteins, we first aimed to generate a *pkc1Δ* strain. In the absence of Pkc1 activity, cells require osmotic support for viability; the addition of 1M sorbitol to media has been shown to rescue the viability and growth of Pkc1 mutants (Levin and Bartlett-Heubusch, 1992). After isolating cells for which our results suggested that *PKC1* had been deleted, we tested the ability to grow in the absence and presence of sorbitol to confirm that our *pkc1Δ* strain requires osmotic stabilization as well. Whereas no growth occurred on rich medium alone, the addition of sorbitol allowed the cells to grow and colonies to form (Figure AII-1). This corroborates results suggesting that *PKC1* was successfully deleted from the genome of these cells.

Having verified the loss of Pkc1, we used this strain to produce *pkc1* mutant cells that expressed fluorescently tagged proteins associated with CME. Our initial goal was to replicate published results indicating that Syp1 localization to the bud neck becomes more pronounced in yeast that lack Pkc1 (Merlini *et al*., 2015); thus, we imaged live WT and *pkc1Δ* strains expressing Syp1-GFP by fluorescence microscopy. As anticipated, Syp1-GFP localized primarily to endocytic patches within the bud and to the bud neck during cell division (Figure AII-2). Similarly, yeast without Pkc1 also exhibited bud neck-localization of Syp1-GFP, but the intensity of the fluorescent signal from this region appeared brighter. Therefore, our data corroborated previous findings. Moreover, an enhanced fluorescent signal was a general Syp1 phenotype in cells lacking the *PKC1* gene. Syp1-GFP cortical punctae were generally brighter in the mutant compared to WT, particularly within the mother cells.
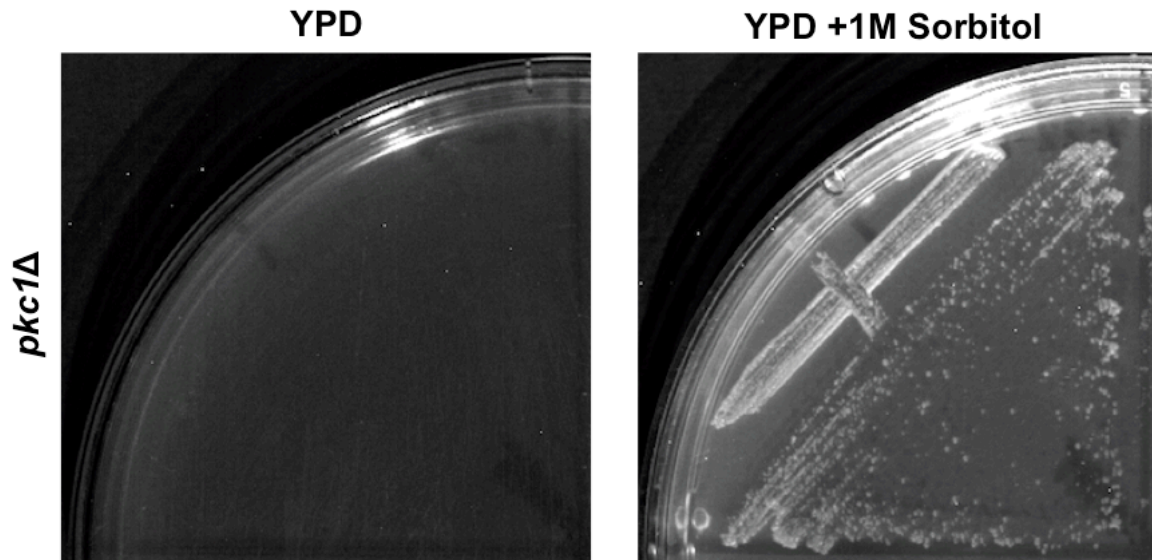
Figure AII-1. Cells cannot grow without osmotic support in the absence of Pkc1. A

pkc1Δ strain was tested for growth on rich medium (YPD) and rich medium with 1M

sorbitol.
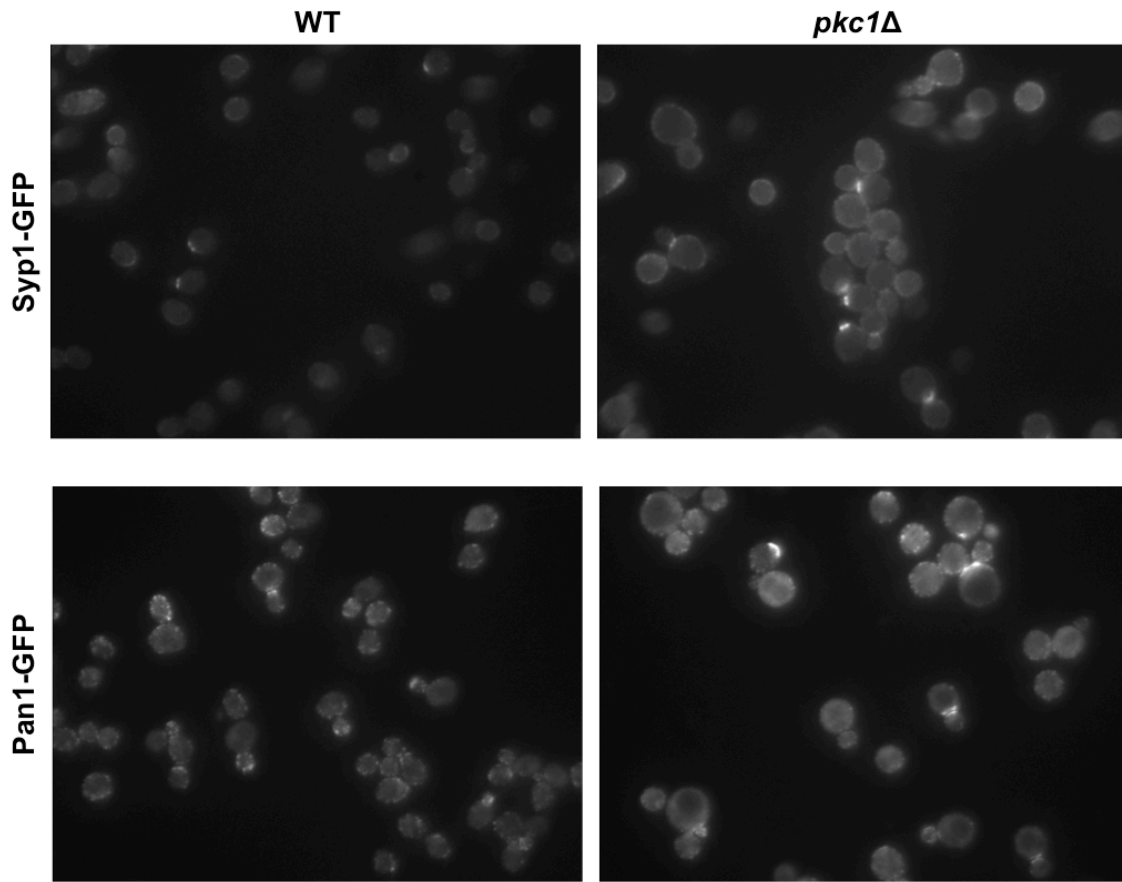
Figure AII-2. Pan1 is relocalized in *pck1*Δ cells in addition to Syp1. WT and *pck1*Δ cells expressing either Syp1-GFP or Pan1-GFP were grown on rich medium containing 1M sorbitol and imaging via live-cell fluorescence microscopy.

In addition to Syp1, we investigated the localization of another CME protein, Pan1. Unlike the early-arriving Syp1 protein, Pan1 is a member of the endocytic late coat and is essential for cell viability (Wendland *et al*., 1996; Tang *et al*., 1997; Wendland and Emr, 1998). After engineering cells that lack Pkc1 to express a Pan1-GFP chimera, we imaged this strain alongside WT yeast expressing Pan1-GFP. As is true for most components of the CME machinery, Pan1-GFP was observed at cortical patches, predominantly within the buds of dividing cells (Figure AII-2). However, Pan1-GFP was observed at the bud neck to a greater extent in the *pkc1*Δ strain when compared to protein localization in WT cells, comparable to results of experiments with Syp1. This result indicates that the bud neck localization of Pan1, like Syp1, is enhanced in *pkc1*Δ cells, and suggests that this may be a general endocytic phenotype in the absence of Pkc1. One difference was observed though: unlike the imaging results for Syp1, Panl-GFP patches at the cell surface were generally fainter and fewer in number in the *pkc1* mutants, indicating that the impact of *PKC1* deletion on these endocytic proteins is not entirely the same.

Discussion

In this brief report, we confirm that Syp1 localization to the neck of dividing yeast increases relative to WT cells when *PKC1* is deleted from the genome. Results of these experiments also demonstrate that Syp1 concentration at endocytic cortical patches is higher without Pkc1 functioning, indicating that Syp1 is either recruited to, and/or retained at, sites of CME to a greater extent in *pkc1Δ* cells. A high-throughput affinity-capture mass spectrometry study predicted that Pkc1 interacts physically with Syp1 (Breitkreutz *et al*., 2010); though this remains unconfirmed, perhaps Syp1 is a target of this kinase, and Pkc1-mediated phosphorylation of Syp1 is required for its dissociation from an endocytic site prior to vesicle scission. Other adaptors have also been implicated in Pkc1 phosphorylation, with Apm4 having been demonstrated to physically interact with Pkc1 (Chapa-y-Lazo and Ayscough, 2014). A physical interaction with Pkc1 was also predicted for Sla2 by a high-throughput, two-hybrid screen (Wang *et al*., 2012). Additionally, proteins like End3 and Sla1, which arrive later to endocytic sites and have been predicted to bind Pkc1 (Wang *et al*., 2012, Tonikian et al., 2009; Breitkreutz *et al*., 2010), may be targets of this kinase as well. Future studies may investigate the potential role of Pkc1 in regulating not only the presence of Syp1 at CME patches, but of other adaptors and other types of factors associated with these sites as well.

The late-coat constituent, Pan1, also largely relocalized to the bud neck when *PKC1* was deleted, indicating that this *pkc1* mutant phenotype is not specific to Syp1, or even to the early coat; instead, increased polarization may be a common phenotype of endocytic proteins in the absence of Pkc1. It is possible that the altered Syp1 positioning leads to the relocalization of other factors associated with CME by enhancing recruitment

to the bud neck, leading other endocytic proteins to exhibit the same phenotype. There were fewer Pan1-GFP punctae at the cell-surface in the *pkc1Δ* strain, and the fluorescent signal from patches that were present was less intense than in WT cells. This could be another indicator that CME events occur to a greater extent at the bud neck in *pkc1* mutants. However, Syp1-GFP patches at the cell surface appeared brighter in the mutants, contrasting the phenotype observed for Pan1. Maybe endocytic sites at the PM are initiated in the absence of Pkc1, but are unable to efficiently recruit late coat proteins, such as Pan1. This would indicate a regulatory role for Pkc1 in transitions that allow for CME to progress, perhaps through phosphorylation of Syp1 or other early-coat components, which then allows for the recruitment of later-arriving proteins.

Pkc1 is quickly becoming a promising candidate for helping to answer questions about how the cell regulates the positioning of endocytic sites, and we may come to find that this kinase is important for better understanding CME in general.

Appendices Materials and Methods

<u>Strains and plasmids</u>

A complete list of strains and plasmids used in this study can be found in Table A-1 and Table A-2, respectively. Strains were constructed using PCR-based genomic integration as described previously (Longtine *et al*., 1998; Goldstein and McCusker, 1999; Nishimura *et al*., 2009). For genomic integration of GFP or pHluorin, we designed primers using the F2 and R1 plasmid-specific sequences (Longtine *et al*., 1998). Transformations were performed according to standard procedures using the lithium acetate method, and integrations were confirmed by colony PCR and/or Western immunoblotting (data not shown).

<u>Live-cell fluorescence microscopy</u>

In brief, images were obtained at 30°C using an inverted microscope (Axiovert 200; Carl Zeiss) equipped with a Sensicam (Cooke), an X-Cite 120 PC fluorescence illumination system, and a 100×, 1.4 NA Plan-Apochromat objective lens. Within a given experiment, images were acquired using identical exposure conditions; subsequently, brightness and contrast adjustments were applied equally to all images.

For quantification of fluorescence intensity, background subtraction was performed using ImageJ, and integrated density was measured for a minimum of 50 cells per condition. All integrated density values were then corrected for cell size. Fluorescence intensity measurements were performed for all cells in a minimum of two separate fields per experimental group. Statistical analysis was performed using Prism

Table A-1. Strains used in the appendices.

Strain	Genotype	Source
BWY2858	*MATα leu2-3,112 ura3-52 his3-Δ200 trp1-Δ901 suc2-Δ9 lys2-801; GAL Ste3-GFP::KAN*	Prosser *et al.*, 2010
BWY5679	*MATα leu2-3,112 ura3-52 his3-Δ200 trp1-Δ901 suc2-Δ9 lys2-801; GAL ent1::LEU2 ent2::HIS3 yap1801::HIS3 yap1802::LEU2 Ste3-GFP::KAN +pBW768*	Maldonado-Báez *et al.*, 2008
BWY3399	*MATα leu2-3,112 ura3-52 his3-Δ200 trp1-Δ901 suc2-Δ9 lys2-801; GAL ent1::LEU2 ent2::HIS3 yap1801::HIS3 yap1802::LEU2 Ste3-GFP::KAN +pBW778*	Maldonado-Báez *et al.*, 2008
BWY3322	*MATα leu2-3,112 ura3-52 his3-Δ200 trp1-Δ901 suc2-Δ9 lys2-801; GAL ent1::LEU2 ent2::HIS3 yap1801::HIS3 yap1802::LEU2 Ste3-GFP::KAN bnr1::NAT +pBW778*	Prosser *et al.*, 2011
BWY3033	*MATα leu2-3,112 ura3-52 his3-Δ200 trp1-Δ901 suc2-Δ9 lys2-801; GAL ent1::LEU2 ent2::HIS3 yap1801::HIS3 yap1802::LEU2 Ste3-GFP::KAN bni1::NAT +pBW778*	Prosser *et al.*, 2011
BWY6660	*MATa leu2-3,112 ura3-52 his3-Δ200 trp1-Δ901 suc2-Δ9 lys2-801; GAL pkc1::NAT*	This study
BWY3534	*MATα leu2-3,112 ura3-52 his3-Δ200 trp1-Δ901 suc2-Δ9 lys2-801; GAL Syp1-GFP::KAN*	Reider *et al.*, 2009
BWY6678	*MATα leu2-3,112 ura3-52 his3-Δ200 trp1-Δ901 suc2-Δ9 lys2-801; GAL pkc1::NAT Syp1-GFP::KAN*	This study
BWY2459	*MATa leu2-3,112 ura3-52 his3-Δ200 trp1-Δ901 suc2-Δ9 lys2-801; GAL Pan1-GFP::KAN*	Barker et al., 2007
BWY6679	*MATa leu2-3,112 ura3-52 his3-Δ200 trp1-Δ901 suc2-Δ9 lys2-801; GAL pkc1::NAT Pan1-GFP::KAN*	This study
BWY2995	*MATα leu2-3,112 ura3-52 his3-Δ200 trp1-Δ901 suc2-Δ9 lys2-801; GAL Ste3-pHluorin::KAN*	Prosser *et al.*, 2010
BWY3036	*MATα leu2-3,112 ura3-52 his3-Δ200 trp1-Δ901 suc2-Δ9 lys2-801; GAL ent1::LEU2 ent2::HIS3 yap1801::HIS3 yap1802::LEU2 Ste3-pHluorin::KAN +pBW768*	Prosser *et al.*, 2011
BWY3037	*MATα leu2-3,112 ura3-52 his3-Δ200 trp1-Δ901 suc2-Δ9 lys2-801; GAL ent1::LEU2 ent2::HIS3 yap1801::HIS3 yap1802::LEU2 Ste3-pHluorin::KAN +pBW778*	Prosser *et al.*, 2011
BWY3588	*MATα leu2-3,112 ura3-52 his3-Δ200 trp1-Δ901 suc2-Δ9 lys2-801; GAL ent1::LEU2 ent2::HIS3 yap1801::HIS3 yap1802::LEU2 Ste3-pHluorin::KAN bnr1::NAT +pBW778*	Prosser *et al.*, 2011
BWY3584	*MATα leu2-3,112 ura3-52 his3-Δ200 trp1-Δ901 suc2-Δ9 lys2-801; GAL ent1::LEU2 ent2::HIS3 yap1801::HIS3 yap1802::LEU2 Ste3-pHluorin::KAN bni1::NAT +pBW778*	Prosser *et al.*, 2011

Table A-2. Plasmids used in the appendices.

Plasmid	Details	Source
pRS416	CEN, *URA3*	Laboratory plasmid
39NP_B8	P5472	Ho *et al.*, 2009
pBW2484	pRS426::*TUS1*	This study
pBW768	pRS414::*Ent1*	Aguilar *et al.*, 2006
pBW778	pRS414::*ENTH1*	Baggett *et al.*, 2003

(GraphPad); either Welch's unequal variances *t*-test or one-way ANOVA with Tukey's correction was used.

Media and growth conditions

Standard yeast extract/peptone medium with 2% dextrose (YPD) was used for growth of yeast under rich conditions. For ammonium-rich conditions or plasmid maintenance, standard yeast nitrogen base (YNB) medium; containing 38mM ammonium sulfate, 2% dextrose, and appropriate amino acids and nutrients; was used. All yeast were grown at 30°C. For counter-selection growth assays, cells were grown on minimal agar medium containing 3.22 μM 5-FAA for selection against *TRP1*. For growth with osmotic support, sorbitol (Fisher) was added to rich, YPD medium to a final concentration of 1M.

Appendices References

Aguilar RC, Longhi SA, Shaw JD, Yeh LY, Kim S, Schon A, Freire E, Hsu A, McCormick WK, Wastson HA, Wendland B (2006) Epsin N-terminal homology domains perform an essential function regulating Cdc42 through binding Cdc42 GTPase-activating proteins. *Proc Natl Acad Sci* **103:** 4116-21

Baggett JJ, D'Aquino KE, Wendland B (2003) The sla2p talin domain plays a role in endocytosis in *Saccharomyces cerevisiae*. *Genetics* **165:** 1661-74

Barker SL, Lee L, Pierce BD, Maldonado-Baez, Drubin DG, Wendland B (2007) Interaction of the endocytic scaffold protein Pan1 with the type I myosins contributes to the late stages of endocytosis. *Mol Biol Cell* **18:** 2893-903

Breitkreutz A, Choi H, Sharom JR, Boucher L, Neduva V, Larsen B, Lin ZY, Breitkreutz BJ, Stark C, Liu G, Ahn J, Dewar-Darch D, Reguly T, Tang X, Almeida R, Qin ZS, Pawson T, Gingras AC, Nesvizhskii AI, Tyers M (2010) A global protein kinase and phosphatase interaction network in yeast. *Science* **328:** 1043-6

Chapa-Y-Lazo B, Ayscough KR (2014) Apm4, the mu subunit of yeast AP-2 interacts with Pkc1, and mutation of the Pkc1 consensus phosphorylation site Thr176 inhibits AP-2 recruitment to endocytic sites. *Commun Integr Biol* **7:** e28522

Goldstein AL, McCusker JH (1999) Three new dominant drug resistance cassettes for gene disruption in Saccharomyces cerevisiae. *Yeast* **15:** 1541-53

Ho CH, Magtanong L, Barker SL, Gresham D, Nishimura S, Natarajan P, Koh JLY, Porter J, Gray CA, Andersen RJ, Giaever G, Nislow C, Andrews B, Botstein D, Graham TR, Yoshida M, Boone C. A molecular barcoded yeast ORF library enables mode-of-action analysis of bioactive compounds. *Nat Biotechnol* **27:** 369-77

Kohno H, Tanaka K, Mino A, Umikawa M, Imamura H, Fujiwara T, Fujita Y, Hotta K, Qadota H, Watanabe T, Ohya Y, Takai Y (1996) Bni1p implicated in cytoskeletal control is a putative target of Rho1p small GTP binding protein in Saccharomyces cerevisiae. *EMBO J* **15:** 6060-8

Letunic I, Doerks T, Bork P (2015) SMART: recent updates, new developments and status in 2015. *Nucleic Acids Res* **43** (database issue)**:** D257-60

Levin DE, Fields FO, Kunisawa R, Bishop JM, and Thorner J (1990) *Cell* **62:** 213-224

Levin DE, Bartlett-Heubusch E (1992) Mutants in the S. cerevisiae PKC1 gene display a cell cycle-specific osmotic stability defect. *J Cell Biol* **116:** 1221-9

Longtine MS, McKenzie A III, Demarini DJ, Shah NG, Wach A, Brachat A, Philippsen P, Pringle JR (1998) Additional modules for versatile and economical PCR-based gene deletion and modification in Saccharomyces cerevisiae. *Yeast* **14:** 953-961

Maldonado-Báez L, Dores MR, Perkins EM, Drivas TG, Hicke L, Wendland B (2008) Interaction between Epsin/Yap180 adaptors and the scaffolds Ede1/Pan1 is required for endocytosis. *Mol Biol Cell* **19:** 2936-48

Merlini L, Bolognesi A, Juanes MA, Vandermoere F, Courtellemont T, Pascolutti R, Séveno M, Barral Y, Piatti S (2015) Rho1- and Pkc1-dependent phosphorylation of the F-BAR protein Syp1 contributes to septin ring assembly. *Mol Biol Cell* **26:** 3245-62

Nishimura K, Fukagawa T, Takisawa H, Kakimoto T, Kanemaki M (2009) An auxin-based degron system for the rapid depletion of proteins in nonplant cells. *Nat Methods* **6:** 917-922

Ozaki K, Tanaka K, Imamura H, Hihara T, Kameyama T, Nonaka H, Hirano H, Matsuura Y, Takai Y (1996) Rom1p and Rom2p are GDP/GTP exchange proteins (GEPs) for the Rho1p small GTP binding protein in Saccharomyces cerevisiae. *EMBO J* **15:** 2196-207

Prosser DC, Whitworth K, Wendland B (2010) Quantitative analysis of endocytosis with cytoplasmic pHluorin chimeras. *Traffic* **11:** 1141-50

Prosser DC, Drivas TG, Maldonado-Báez L, Wendland B (2011) Existence of a novel clathrin-independent endocytic pathway in yeast that depends on Rho1 and formin. *J Cell Biology* **195:** 657-71

Reider A, Barker SL, Mishra SK, Im YJ, Maldonado-Baez L, Hurley JH, Traub LM, Wendland B (2009) Syp1 is a conserved endocytic adaptor that contains domains involved in cargo selection and membrane tubulation. *Embo J* **28:** 3103-3116

Schmelzle T, Helliwell SB, Hall MN (2002) Yeast protein kinases and the RHO1 exchange factor TUS1 are novel components of the cell integrity pathway in yeast. *Mol Cell Biol* **22:** 1329-39

Schultz J, Milpetz F, Bork P, Ponting CP (1998) SMART, a simple modular architecture research tool: identification of signaling domains. *Proc Natl Acad Sci* **95:** 5857-5864

Tang HY, Munn A, Cai M (1997) EH domain proteins Pan1p and End3p are components of a complex that plays a dual role in organization of the cortical actin cytoskeleton and endocytosis in Saccharomyces cerevisiae. *Mol Cell Biol* **17:** 4294-304

Tonikian R, Xin X, Toret CP, Gfeller D, Landgraf C, Panni S, Paoluzi S, Castagnoli L, Currell B, Seshagiri S, Yu H, Winsor B, Vidal M, Gerstein MB, Bader GD, Volkmer

R, Cesareni G, Drubin DG, Kim PM, Sidhu SS, Boone C (2009) Bayesian modeling of the yeast SH3 domain interactome predicts spatiotemporal dynamics of endocytosis proteins. *PLoS Biol* **7:** e1000218

Wang Y1, Zhang X, Zhang H, Lu Y, Huang H, Dong X, Chen J, Dong J, Yang X, Hang H, Jiang T (2012) Coiled-coil networking shapes cell molecular machinery. *Mol Biol Cell* **23:** 3911-22

Wendland B, McCaffery JM, Xiao Q, Emr SD (1996) A novel fluorescence-activated cell sorter-based screen for yeast endocytosis mutants identifies a yeast homologue of mammalian eps15 *J Cell Biol* **135:** 1485-500

Wendland B, Emr SD (1998) Pan1p, yeast eps15, functions as a multivalent adaptor that coordinates protein-protein interactions essential for endocytosis. *J Cell Biol* **141:** 71-84

Byrne KP, Wolfe KH (2005) The Yeast Gene Order Browser: combining curated homology and syntenic context reveals gene fate in polyploid species. *Genome Res* **15:** 1456-61

CURRICULUM VITAE

KYLE T. HOBAN
khoban2@jhu.edu

Biology Department
Johns Hopkins University
3400 N Charles St, UTL Building, Room 374
Baltimore, MD 21218

738 Macon St
Baltimore, MD 21224
(215) 696 - 7079
DOB: October 24, 1988; Allentown, PA

CURRENT POSITION: Graduate student in Wendland Lab; Johns Hopkins University

EDUCATION

Doctor of Philosophy   Expected Fall 2017
Cell, Molecular, Developmental Biology and Biophysics Program
Johns Hopkins University
> Proposed dissertation title: *Characterizing the role of adaptor proteins in endocytosis*

Bachelor of Arts   May 2011
Biological Sciences
University of Delaware
> Minors: Biochemistry and Chemistry

RESEARCH

Graduate Research   2012-Present
Biology Department, Johns Hopkins University
Graduate Student; Advisor: Beverly Wendland, PhD
> Investigated the mechanism of protein cargo recognition and trafficking by the endocytic adaptor, Syp1, in budding yeast; current work aims to understand the cause of negative genetic interactions between mutants of Vps4 and clathrin-mediated endocytosis

Undergraduate Research, Research Assistantship   2010-2011
BioImaging Center, Delaware Biotechnology Institute
Undergraduate Researcher; Advisor: Jeffrey Caplan, PhD
> Studied the role of stromules, tubular projections emanating from chloroplasts, in *N. benthamiana* immune responses

PUBLICATIONS

Hoban K, Lux S, Poprawski J, Zhang Y, Prosser DP, Norris C, Wendland B (In preparation) Vps4 is required for viability of clathrin-mediated endocytosis mutants and cargo trafficking from the plasma membrane.

PUBLICATIONS (continued)

Reider Apel A*, **Hoban K***, Chuartzman S, Tonikian R, Sidhu S, Schuldiner M, Wendland B, Prosser D. (2017) Syp1 regulates the clathrin-mediated and clathrin-independent endocytosis of multiple cargo proteins through a novel sorting motif. *Mol Biol Cell*. 28(18): 2434-2448.
*Co-first authors, listed alphabetically

Caplan JL, Kumar AS, Park E, Padmanabhan MS, **Hoban K**, Modla S, Czymmek K, Dinesh-Kumar SP. (2015) Chloroplast Stromules Function during Innate Immunity. *Dev Cell*. 34(1): 45-57.

INVITED PRESENTATIONS

Oral Presentation
Hoban K, Lux S, Poprawski J, Zhang Y, Prosser D, Norris C, Wendland B. (2016, December) *Vps4 is required for clathrin-mediated endocytosis mutant viability and cargo trafficking from the plasma membrane*. Microsymposium. American Society for Cell Biology Meeting, San Francisco, California.

Poster Presentation
Hoban K, Lux S, Poprawski J, Zhang Y, Prosser D, Norris C, Wendland B. (2016, December) *Vps4 is required for clathrin-mediated endocytosis mutant viability and cargo trafficking from the plasma membrane*. American Society for Cell Biology Meeting, San Francisco, California.
Hoban K, Reider Apel A, Chuartzman S, Schuldiner M, Wendland B. (2015, December) *Defining the adaptor function of endocytic protein Syp1*. American Society for Cell Biology Meeting, San Diego, California.
Hoban K, Reider Apel A, Chuartzman S, Schuldiner M, Wendland B. (2014, December) *Defining the adaptor function of endocytic protein Syp1*. American Society for Cell Biology Meeting, Philadelphia, Pennsylvania.

TEACHING & MENTORING

Teaching Assistant
Johns Hopkins University

Introduction to the Human Brain	Spring 2015, 2016, 2017
Developmental Biology Lab	Spring 2014
Genetics Lab	Fall 2013

University of Delaware

General Biology Laboratory	Fall 2010, Spring 2011

TEACHING & MENTORING (continued)

Lab Course Liaison and Teaching Assistant   Fall 2014, 2015, 2016, 2017
Johns Hopkins University
> Oversaw collaboration between Wendland Lab and Genetics Lab course, helping design two open-ended research projects for undergrads (one from 2014-16, the second in 2017)

Graduate Mentor   2014-2016
Johns Hopkins University
> Acted as primary mentor for two undergraduate students in the Wendland Lab

SKILLS

Cell biology: fluorescence microscopy, yeast biology & genetics
Biochemistry: protein expression, protein purification, Western blotting, protein binding
Molecular biology: cloning, DNA sequencing, genomic integration
Peer review: helped PhD advisor review several manuscripts
Presentation preparation and public speaking: presented eight scientific talks of varying length during PhD studies

HONORS & AWARDS

Johns Hopkins University
> Victor Corces Teaching Award, Genetics Lab   2013
> Anfinsen-Morgan Fellowship, CMDB Doctoral Program   2012

University of Delaware
> Honors Program Award   2011

UNIVERSITY & COMMUNITY SERVICE

Cofounder and Secretary, Homewood Researcher Safety Committee   2014-Present
Founder and Secretary, Biology Researcher Safety Committee   2015-Present
Mentor, STEM Achievement in Baltimore Elementary Schools   2015-2017
Judge, Mount Royal Elementary/Middle School Science Fair   2015

PROFESSIONAL ASSOCIATIONS

American Society for Cell Biology, Member   2014-Present

OTHER PROFESSIONAL EXPERIENCE

Research Assistant
> BioImaging Center, Delaware Biotechnology Institute   2011-2012
Emergency Department Scribe
> Scribe America   2011-2012

    PC Technician
        Versalign, Inc.   2008-2011

REFERENCES

Beverly Wendland, PhD
James B. Knapp Dean, Krieger School of Arts & Sciences
Professor, Department of Biology
Johns Hopkins University
(410) 516 - 4065 | bwendland@jhu.edu

Derek Prosser, PhD
Assistant Professor, Department of Biology
Virginia Commonwealth University
(804) 827-8596 | dprosser@vcu.edu

Carolyn Norris, PhD
Senior Lecturer, Department of Biology
Johns Hopkins University
(410) 516 - 8288 | carolyn.norris@gmail.com

Maurice Bessman, PhD
Professor Emeritus, Department of Biology
Johns Hopkins University
(410) 516 - 7776 | zoot@jhu.edu

Daniel Kuespert, PhD
Homewood Laboratory Safety Advocate
Johns Hopkins University
(410) 516 - 5525 | dkuespert@jhu.edu